

DYNAMIC PERFORMANCE OF WIND DRIVEN INDUCTION GENERATOR

*Thesis submitted in partial fulfillment of the requirements for the award of
degree of*

**Master of Engineering
in
Power Systems & Electric Drives**



Thapar University, Patiala

By:
Sahil Gupta
(Regn. No. - 80741019

Under the supervision of
Dr. Sanjay Kumar Jain
Assistant Professor, EIED

JULY 2009
ELECTRICAL & INSTRUMENTATION ENGINEERING DEPARTMENT
THAPAR UNIVERSITY
PATIALA – 147004

CERTIFICATE

I hereby certify that the work which is being presented in this thesis entitled “**Dynamic Performance of Wind Driven Induction Generator**” in partial fulfillment of the requirement for the award of the degree of Master of Engineering in *Power Systems & Electric Drives* submitted in Electrical & Instrumentation Engineering Department of Thapar University, Patiala, is an authentic record of my own work carried out under supervision of Dr. Sanjay Kumar Jain, Asst. Prof., EIED.

The matter presented in this thesis has not been submitted the award of any other degree of this or any other university.

Sahil Gupta
15 July 09
(Sahil Gupta)

It is certified that the above statement made by the student is correct to the best of our knowledge and belief.

Sanjay
15 July 09
Dr. Sanjay Kumar Jain

Assistant Professor, EIED
Thapar University, Patiala

S. Ghosh
15/7/09

Dr. Smarajit Ghosh

Professor & Head

Electrical & Instrumentation Engineering Department
Thapar University
Patiala

R. K. Sharma
16/7

Dr. R. K. Sharma

Dean of Academic Affairs

Thapar University
Patiala

ACKNOWLEDGEMENTS

I feel honored in expressing my profound sense of gratitude and indebtedness to **Dr. Sanjay Kumar Jain** , Assistant Professor, Electrical and Instrumentation Engineering Department, Thapar University, Patiala for his guidance, meticulous efforts, constructive criticism, inspiring encouragement, unflinching support and invaluable co-operation which enabled me to enrich my knowledge and reproduce it in the present form.

I also like to extend my gratefulness to **Dr. Smarajit Ghosh**, Professor and Head, Electrical and Instrumentation Engineering Department, Thapar University, Patiala for his perpetual encouragement, generous help and inspiring guidance. Thanks are also due to Dr. Yaduvir Singh, P.G. Coordinator, Electrical and Instrumentation Engineering Department, Thapar University.

Much appreciations is expressed to **Prof. Abhijit Mukherjee, Director, Thapar University, Prof. K.K. Raina, Deputy Director, Thapar University** and **Prof. R.K. Sharma, Dean of Academic Affairs** to provide me moral support to go ahead with my innovative M.E. Thesis work.

I am also very thankful to the entire faculty and staff members of Electrical and Instrumentation Engineering Department for their direct–indirect help, cooperation, love and affection, which made my stay at Thapar University memorable.

I wish to thank all my friends Devashish, Javed, Naveen and Saranjeet for their time to time suggestions and cooperation without which I would not have been able to complete my work.

Sahil Gupta
(80741019)

ABSTRACT

The increasing concern about various aspects of conventional generating units like depleting fossil fuels, environmental consideration and huge amount of money and time in implementing them have forced the research companies to exploit the renewable energy sources using small generating units. The wind energy which is fully renewable has a great potential and being exploited by many. Statistically, the share of wind energy in power sector is less; its share is nowadays growing at high rate. The generating schemes employ induction generators.

The work reported in this thesis focused on the dynamic analysis of wind driven cage induction generator. The performance has been studied for two cases namely direct grid connected induction generator and grid connected induction generator with local load and capacitor. For this, the d-q variable models in synchronous reference frame have been developed and performance is simulated by fourth order Runge Kutta integration method. The performance has been studied for change in various parameters like prime mover speed, transmission line resistance and reactance, change in reactive power compensation and load. The unpredictability of wind has been simulated by various functions. The change in wind speed leading to change in torque calculated using C_p -curve.

TABLE OF CONTENTS

	Page No.
<i>Certificate</i>	<i>i</i>
<i>Acknowledgement</i>	<i>ii</i>
<i>Abstract</i>	<i>iii</i>
<i>Table of contents</i>	<i>iv-vi</i>
<i>List of figures</i>	<i>vii-x</i>
CHAPTER-1 INTRODUCTION	1-5
1.1 OVERVIEW	1
1.2 LITERATURE REVIEW	2
1.3 OBJECTIVE OF THE WORK	4
1.4 ORGANIZATION OF THE THESIS	5
CHAPTER-2 WIND AS A SOURCE OF ELECTRIC POWER	6-23
2.1 INTRODUCTION	6
2.2 WIND DISTRIBUTION	7
2.2.1 THE IDEAL BRAKING AND BETZ LAW	9
2.3 PITCH AND STALL CONTROL OF WIND TURBINE	11
2.3.1 PITCH CONTROL	11
2.3.2 STALL CONTROL	11
2.4 WIND ENERGY CONVERSION SCHEME	12
2.4.1 DIRECT GRID CONNECTION	12
2.4.2 GRID OPERATION EMPLOYING POWER ELECTRONICS	13
2.5 WIND ENERGY STATISTICS	14
2.5.1 GLOBAL STATUS OF THE WIND ENERGY	14
2.5.2 WIND ENERGY IN INDIA	17
2.6 BENEFITS OF WIND POWER	19
2.6.1 ECONOMIC CONSIDERATION	19
2.6.2 SECURITY OF SUPPLY	19
2.6.3 ENVIRONMENTAL BENEFITS OF WIND POWER	20

2.6.4 JOBS	20
2.6.5 FULL RENEWABLE AND REDUCED HAZARDS	21
2.7 DIFFICULTIES WITH WIND POWER	21
2.7.1 VARIABILITY OF WIND	21
2.7.2 NOISE	22
2.8 CONCLUSION	22
CHAPTER-3 DYNAMIC MODEL OF WIND DRIVEN INDUCTION GENERATOR AND SIMULATION ALGORITHM	24-46
3.1 INTRODUCTION	24
3.2 STATIC COMPONENT MODELS	25
3.2.1 RESISTIVE ELEMENTS	26
3.2.2 INDUCTIVE ELEMENTS	27
3.2.3 CAPACITIVE ELEMENTS	28
3.3 INDUCTION MACHINE MODEL	29
3.3.1 INDUCTION MACHINE MODEL IN PHASE VARIABLES	29
3.3.2 GENERALIZED MODEL USING d-q VARIABLES	32
3.4 WIND TURBINE MODEL	37
3.5 DYNAMIC MODEL OF SYSTEMS AND ALGORITHM	38
3.5.1 INDUCTION GENERATOR CONNECTED TO GRID	39
3.5.2 ALGORITHM FOR GRID CONNECTED INDUCTION GENERATOR	
3.5.3 INDUCTION GENERATOR CONNECTED TO GRID WITH LOCAL LOAD AND SHUNT CAPACITOR	43
3.5.4 ALGORITHM FOR INDUCTION GENERATOR CONNECTED TO GRID WITH LOCAL LOAD AND CAPACITOR	46
CHAPTER-4 RESULTS AND DISCUSSIONS	47-78
4.1 DIRECT GRID CONNECTION OF INDUCTION	47
4.1.1 INDUCTION GENERATOR DRIVEN BY CONSTANT SPEED PRIME MOVER	47

4.1.2 INDUCTION GENERATOR DRIVEN BY WIND TURBINE	57
4.2 GRID CONNECTED INDUCTION GENERATOR WITH LOCAL LOAD AND CAPACITOR	68
4.2.1 INDUCTION GENERATOR DRIVEN BY CONSTANT SPEED PRIME MOVER INPUT	68
4.2.2 INDUCTION GENERATOR DRIVEN BY WIND TURBINE	73
CHAPTER -5 CONCLUSIONS AND SCOPE OF FUTURE WORK	79-80
5.1 CONCLUSIONS	79
5.2 SCOPE OF FUTURE WORK	80
REFERENCES	81-83
APPENDIX-A	84
APPENDIX-B	85-87

List of Figures

Figure No.	Caption	Page No.
Figure 2.1	Cross section of a rotor wing	7
Figure 2.2	Probability density of the Rayleigh distribution	8
Figure 2.3	Plot of (P/P_0) as a function of (V_2/V_1)	10
Figure 2.4	Direct grid connected wind energy conversion scheme	13
Figure 2.5	Variable speed system using cage induction generator	14
Figure 2.6	Global annual installed capacity	15
Figure 2.7	Global cumulative installed capacity	16
Figure 2.8	Annual growths in world wind market	16
Figure 2.9	Top 10 installed capacities in 2008	17
Figure 2.10	State wise percentage share in wind energy production	18
Figure 3.1	Transformation of static phase variables into d-q variables	25
Figure 3.2	Stator and rotor circuits of induction machine	30
Figure 3.3	Transformation of rotor phase variables into d-q variables	33
Figure 3.4	d-axis equivalent circuit of induction machine	36
Figure 3.5	q-axis equivalent circuit of induction machine	36
Figure 3.6	Induction generator connected to grid	39
Figure 3.7	Flow chart for digital simulation of grid connected induction machine	42
Figure 3.8	Schematic diagram of induction generator with local load and shunt capacitor	43
Figure 3.9	Flow chart for simulation of induction generator connected with local load	46
Figure 4.1	d-q axis currents during grid connection of induction generator	48
Figure 4.2	Stator currents of grid connected induction generator in phase variables	48

Figure 4.3	Speed-Time characteristics of grid connected induction generator	49
Figure 4.4	Torque-Time characteristics of grid connected induction generator	49
Figure 4.5	Torque-Speed characteristics of direct grid connected induction generator	50
Figure 4.6	Speed-Time characteristics of IG for different starting speeds	50
Figure 4.7	Torque-Time characteristics for GCIG with different starting speeds	51
Figure 4.8	Stator currents of grid connected IG for different starting speeds	51
Figure 4.9	Rotor currents of grid connected IG for different starting speeds	52
Figure 4.10	Stator currents of grid connected IG with different line resistance	53
Figure 4.11	Speed-Time characteristics of IG with different transmission line resistance	54
Figure 4.12	Torque-Time characteristics of IG with different transmission line resistance	54
Figure 4.13	Stator currents of IG with different transmission line reactance	55
Figure 4.14	Speed-Time characteristics of IG with different transmission line reactance	56
Figure 4.15	Torque-Time characteristics of IG for different transmission line reactance	56
Figure 4.16	C_p - plot for a wind turbine	57
Figure 4.17	wind speed function I	57
Figure 4.18	Stator and rotor Currents of wind driven IG with speed function I	58
Figure 4.19	Speed-Time characteristics of wind driven IG with speed function I	59
Figure 4.20	Torque-Time characteristics of wind driven IG with	59

	speed function I	
Figure 4.21	wind speed function II	60
Figure 4.22	Stator Currents of wind driven IG with speed function I	60
Figure 4.23	Rotor Currents of wind driven IG with speed function II	61
Figure 4.24	Speed-Time characteristics of wind driven IG with speed function II	61
Figure 4.25	Torque-Time characteristics of wind driven IG with speed function II	62
Figure 4.26	Speed-Time characteristics of wind driven IG different starting speeds	62
Figure 4.27	Torque-Time characteristics of wind driven IG with different starting speeds	63
Figure 4.28	Stator currents of wind driven IG with different starting speeds	63
Figure 4.29	Speed-Time characteristics of wind driven IG with different line resistance	64
Figure 4.30	Torque-Time characteristics of wind driven IG with different line resistance	65
Figure 4.31	Stator currents of wind driven IG with different line resistance	65
Figure 4.32	Speed-Time characteristics of wind driven IG with different line reactance	66
Figure 4.33	Torque-Time characteristics of wind driven IG with different line reactance	67
Figure 4.34	Stator currents of wind driven IG with different line reactance	67
Figure 4.35	Stator currents of grid connected IG with local load and capacitor	68
Figure 4.36	Rotor currents of grid connected IG with local load and capacitor	69
Figure 4.37	Load currents of grid connected IG with local load and capacitor	69
Figure 4.38	Transmission line currents of grid connected IG with	70

	local load and capacitor	
Figure 4.39	Voltage across capacitor of grid connected IG with local load and capacitor	70
Figure 4.40	Speed-Time characteristics of grid connected IG with local load and capacitor	71
Figure 4.41	Stator currents of IG with local load with different compensation	71
Figure 4.42	Transmission line currents with Stator currents of IG with local load with different compensation	72
Figure 4.43	Load current of IG with local load with different compensation	73
Figure 4.44	Capacitor voltages of IG with local load with different compensation	73
Figure 4.45	Stator current of wind driven IG with different compensation.	74
Figure 4.46	Transmission line currents of wind driven IG with different compensation	74
Figure 4.47	Load currents of wind driven IG with local load and different compensation.	75
Figure 4.48	Capacitor voltages of wind driven IG with local load and different compensation.	75
Figure 4.49	Speed-Time characteristics of wind driven IG with local load and different characteristics.	76
Figure 4.50	Stator current of wind driven IG with different load	77
Figure 4.51	Transmission line currents of wind driven IG with different load.	77
Figure 4.52	Load currents of wind driven IG with different load	77
Figure 4.53	Voltage across capacitor of wind driven IG with different load	78
Figure B.1	Free accelerating Torque-speed characteristics	82
Figure B.2	Free accelerating torque-time characteristics.	83
Figure B.3	Free accelerating speed-time characteristics	83
Figure B.4	Free accelerating d-q axis currents	84

CHAPTER 1

INTRODUCTION

1.1 OVERVIEW

Human efforts to utilize wind for energy have started in ancient times, when they used to sail the ships and boats. Later wind energy served the mankind by providing the energy for girding mills and water pumps. During its transformation from these crude and heavy devices to today's efficient and sophisticated machines, the technology went through various phases of development. In Holland, several decisive improvements were made on wind mills in the 16th century, leading to new types of mill, so called Dutch wind mill. The era of wind electric generators began close to 1900's. The first modern wind turbine, specifically designed for electricity generation was constructed in Denmark in 1890. The wind electric generators became commercially available in American market by 1925. The research on wind turbines started during 1950. However during this period electricity generated from wind costs 8-10 times more than that of fossil fuels. But oil crisis in 1970's forced the world to think about wind power generation and to work for cost efficient measures.

Wind power which has been proved as a potential source for generation of electricity with minimal environmental impact, is the fastest growing source for electric power generation and it is expected to remain so in future. Countries like Germany, United States of America, China and India have taken a lead in harnessing this nonpolluting and replenish able source of energy. In terms of economic value the wind energy sector has now become firmly installed as one of the important players in energy markets.

Harnessing wind energy for electric power generation is an area of research interest and at present, the emphasis is given to the cost effective utilization of energy resource for quality and reliable power supply. There are various techniques to harness this wind energy. The squirrel cage induction generator with its lower maintenance demands and simplified controls appeared to be a good solution for such applications. For its simplicity, robustness and small size per generated KW the induction generator is favored for wind power plants. For small power plants, squirrel cage induction generator has a

great economical appeal. A reactive power compensator is needed to reduce the reactive power demand.

1.2 LITERATURE REVIEW

Wind power which has been proved as a potential source for generation of electricity with minimal environmental impact. Countries like Germany, United States of America, China and India have taken a lead in harnessing this renewable energy [1]. India figures fifth among countries utilizing wind power. World wind energy is expected to be 190 GW worldwide by 2010 [2]. Despite constraints facing supply chains for wind turbines, the annual market for wind continued to increase at staggering rate of 29 % .In terms of economic value the wind energy sector has now become firmly installed as one of the important players in energy markets.

Musgrove [3] has presented the summary on wind energy and wind energy conversion systems. An overview of various types of wind turbines is also given. Wind turbine characteristics and aerodynamic forces on the wind turbine blade have been explained.

Recent technology advances in wind turbines, power electronics, and machine drives have made wind energy very competitive to fossil fuel power. Power electronics technology has gone through dynamic evolution in the last four decades from mercury arc converters to modern power semiconductor converters. The advent of solid-state variable-frequency inverters, various converter topologies, advanced PWM techniques and improved control and estimation methods gradually have resulted into high-performance ac drives of various types [4].

Yeh and Wang [5] have presented an approach based on Weibull distribution to find the capacity of wind turbine generators. Probability distribution of wind speed variation is represented by the Weibull distribution and relationships among mean wind speed.

Anderson, Richon and Campbell [6] have implemented an aerodynamic moment control by enclosing a pitch able section of the blade in an active control loop, using the external aerodynamic load as feedback variable. Muljadi and Butterfield [7] have

discussed the behavior of the wind turbine generator with pitch control capability under turbulent winds. Two methods to adjust the aerodynamic power were investigated: pitch control and generator load control.

Thiringer and Linders [8] have implemented a variable rotor speed control of a fixed-pitch wind Turbine using a special technique, in which operating point of the wind turbine is determined by using the measured rotor speed and power. Xingjia *et al.* [9] have proposed the active vibration control based on expert PID pitch control strategy. Experts PID controller combine the expert system and the PID controller.

Muller *et al.* [10] have presented a comparison of various generating systems used for wind energy conversion with the help of the power curves. Whereas Datta and Ranganathan [11] compared the fixed speed and variable speed wind energy conversion system using grid connected induction generator. The comparison has been done on the basis of major hardware components required, operating region and energy output with a defined wind function.

The control strategy of FESS to reduce the frequency variation proposed by Takahashi and Tamura [12] is based on adjustment of output of the main power plant in cooperation with the FESS depending on its energy charge level and direct frequency control.

The appropriate dynamic model is needed to study the behavior under dynamic or transient conditions. The d-q transformation is a transformation of coordinates from the three-phase stationary coordinate system to the $d-q$ rotating coordinate system. This transformation is made in two steps (1) A transformation from the three-phase stationary coordinate system to the two-phase, so called $\alpha-\beta$, stationary coordinate system. (2) A transformation from the $\alpha-\beta$ stationary coordinate system to the $d-q$ rotating coordinate system [13].

In transformation given by Park [14] the variables associated with the stator of synchronous machines are replaced with the variables associated with fictitious winding rotating with the rotor. We can say that stator variables are referred to a reference frame fixed in rotor. Brereton [15] applies Park transformation to induction machines and transformed the stator variable of induction machine to a frame of reference fixed in

rotor. In theory given by Stanley [16] the rotor variables in voltage equations of induction machine are transformed to variables associated with fictitious stationary winding. The speed of this reference frame is zero.

Hammons [17] has proposed a detailed induction generator model and analyzed the transient behavior of induction generator running at a speed close to synchronous speed when directly connected to electric distribution system.

Demoulias and Dokopoulos [19] have used simulation program to investigate the system behaviour of when wind turbine is disconnected from the grid under various circumstances. The transient behavior of a wind driven induction generator after its disconnection from the power grid has been investigated using experimental arrangement [20]. The cause of the capacitor failures is identified by finding the relationships between the voltage rise and the characteristics of the wind turbines using digital simulation [22].

Petru and Thiringer [23] have presented wind turbines modeling for power system studies and various parts of a wind turbine model, such as aerodynamic conversion, drive train, and generator representation, are analyzed.

Popa, Blaabjerg and Boldea [24] have proposed a method that allows an induction machine to run a turbine at its maximum power coefficient. The rotational speed is the controlled variable in proposed control strategy.

A generalized model of three phase induction model using MATLAB/SIMULINK has been presented by Shi *et al.* [25]. Electrical sub model, mechanical sub model and torque sub model has been described separately. Slootweg *et al.* [26] have represented a general model of variable speed generator wind turbines in power system simulations. Models of various subsystems like wind speed, rotor, rotor speed controller and generator have been presented.

The torsional response following incidence and clearance of severe supply system disturbances is investigated, when the rotor is stationary and when running at close to synchronous speed. The response is also checked during mal synchronization when excited by a controlled VAr source [27].

1.3 OBJECTIVE OF THE WORK

The objective of the present work is to study dynamic performance of wind driven grid connected induction generator by formulating appropriate mathematical models and study the effects of change in various parameters like prime mover speed, transmission line resistance and reactance, local load and capacitance.

1.4 ORGANIZATION OF THE THESIS

The thesis has been organized into five chapters. The present chapter summarizes the overview; work carried out by various researchers, authors' contribution and the outline of the thesis. The chapter 2 introduces the wind energy generation, various wind energy conversion systems employing cage induction generator presents the wind energy statistics. The Chapter 3 details the development of the dynamic model of wind driven induction generator model for direct grid connection and grid connection with local load and capacitor. The Chapter 4 details the results and discussions pertaining to dynamic behavior of grid connected wind driven induction generator under different system configurations. The effect of change in system conditions is studied and performance is compared with constant speed wind generation system. It also includes the free accelerating characteristics of induction machine. Finally, Chapter 5 summarizes the main findings and scope of future work.

CHAPTER 2

WIND AS SOURCE OF ELECTRIC POWER

2.1 INTRODUCTION

The history of wind power shows a general evolution from the use of simple, light devices driven by aerodynamic drag forces; to heavy, material-intensive drag devices; to the increased use of light, material-efficient aerodynamic lift devices in the modern era. Wind power has been used for centuries for different purposes such as: pumping water, propelling boats or grinding corn. Since the ancient times, Chinese and Babylonians were using wind energy for their agricultural use. After the world war II, the conventional large size power plants were set up. But the oil crisis in seventies made the world sit up and respond to the challenge by harness alternative resources. The remarkable contribution of wind power to the electricity supply started in the mid 1980s. Denmark was the first country in the world to erect wind turbines to harness wind power. The European countries took a lead in developing technology for harnessing the wind power.

Wind turbines extract the energy from the wind by transferring the thrusting force of the air passing through the turbine rotor into the rotor blades. There are two primary physical principles by which energy can be extracted from the wind; these are through the creation of either drag or lift force (or through a combination of the two). The cross section of rotor wing as shown in Fig. 2.1 will help understand these principles [3]. The wind passes over both surfaces of the airfoil shaped blade. As wind passes more rapidly over the longer (upper) side of the airfoil, creating a lower- pressure area above the airfoil. The pressure differential between top and bottom surfaces creates a thrust force, called aerodynamic lift.

In addition to lift force, a drag force perpendicular to the lift force impedes rotor rotation [3]. A prime objective in wind turbine design is for the blade to have a relatively high lift-to-drag ratio. This ratio can be varied along the length of the blade to optimize the turbine's energy output at various wind speeds. In an aircraft wing, this force causes the airfoil to rise, lifting the aircraft off the ground. Since the blades of a wind turbine are

constrained to move in a plane with the hub as its center, the lift force causes rotation about the hub. As a result, the lifting force is converted into a mechanical torque and this torque makes the shaft, as part of the turbine rotor, turn. The power in the shaft is used to produce electricity by coupling it with generator.

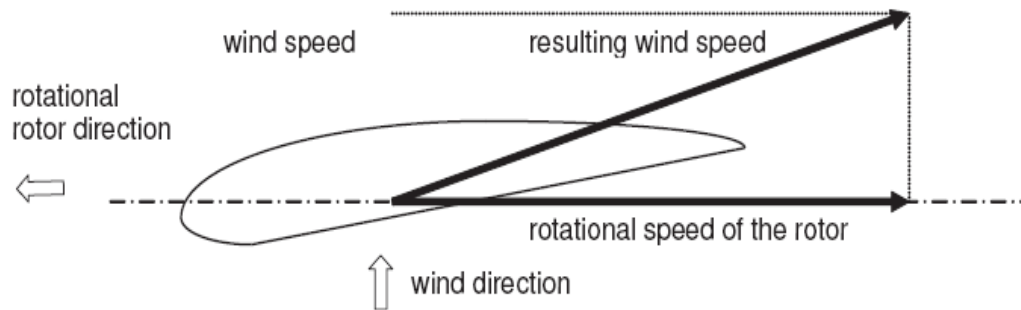


Figure 2.1 Cross section of a rotor wing

The basic features that characterize lift and drag are:

- Drag is in the direction of airflow
- Lift is perpendicular to the direction of airflow
- Generation of lift always causes a certain amount of drag to be developed
- With a good aerofoil, the lift produced can be more than thirty times greater than the drag.
- Lift devices are generally more efficient than drag devices

2.2 WIND DISTRIBUTION

The wind speed is described by most commonly used probability density function referred as Weibull function [5]. The Weibull distribution is expressed as-

$$f(w) = \frac{k}{c} \left(\frac{w}{c}\right)^{k-1} e^{-\left(\frac{w}{c}\right)^k} \quad (2.1)$$

where k is a shape parameter, c is a scale parameter and w is the wind speed. The average wind speed (or the expected wind speed) \bar{w} can be calculated as-

$$\bar{w} = \int_0^{\infty} w f(w) dw = \frac{c}{k} \left(\frac{1}{k}\right) \quad (2.2)$$

Where Γ is Euler's gamma function i.e.

$$\Gamma(z) = \int_0^{\infty} t^{z-1} e^{-t} dt \quad (2.3)$$

Weibull distribution is known as the Rayleigh distribution when shape parameter k equals 2. For the Rayleigh distribution, the scale factor c given the average wind speed and is calculated from eq. (2.1) and eq. (2.2) as-

$$C = \frac{2}{\sqrt{\pi}} \bar{w} \quad (2.4)$$

The wind speed probability density function of the Rayleigh distribution is plotted in Fig. 2.2. The average wind speeds in the Fig. are 8 m/s, 10 m/s, 12 m/s and 14 m/s.

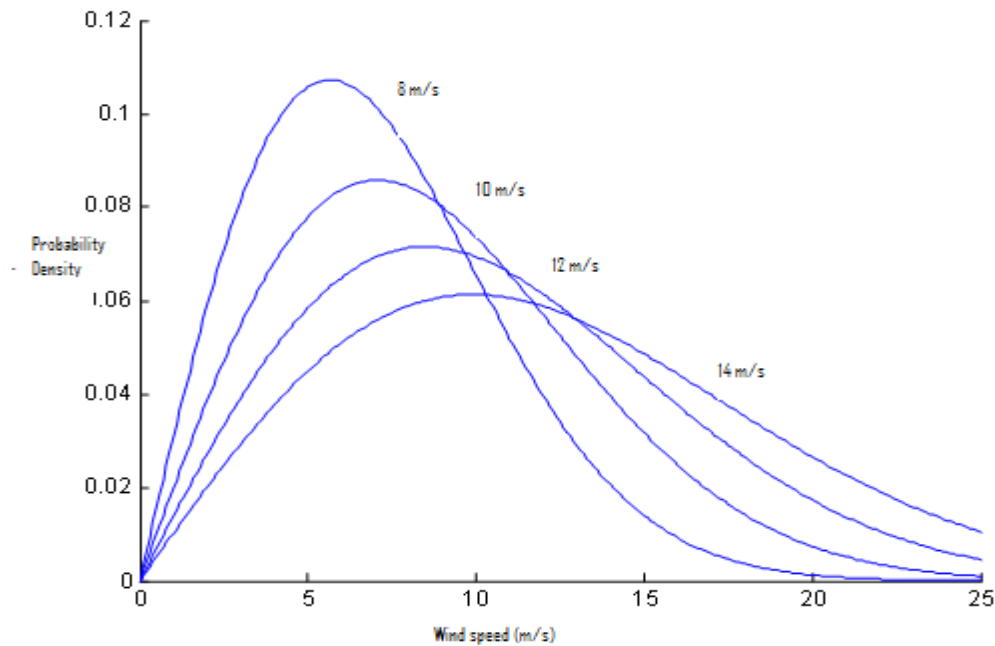


Figure 2.2 Probability density of the Rayleigh distribution.

2.2.1 THE IDEAL BRAKING AND BETZ LAW

Wind turbine extracts the energy from wind by slowing down the wind by blades. The more kinetic energy a wind turbine pulls out of the wind, the more the wind will be slowed down as it leaves the turbine. If all the energy from the wind is extracted, the air would move away with the speed zero, i.e. the air could not leave the turbine. In that case no energy could be extracted. In the other extreme case, the wind could pass through blades without being hindered at all. In this case we would likewise not have extracted any energy from the wind.

The wind energy can be converted into useful mechanical energy by applying braking between these two extreme cases. An ideal wind turbine would slow down the wind by 2/3 of its original speed. This can be explained by Betz law.

The Betz' law suggests that only 59% of the kinetic energy in the wind can be converted to mechanical energy using a wind turbine. This can be proved through the following steps-

Let the average wind speed through the rotor area is the undistributed wind speed before the wind turbine (V_1) and the wind speed after the passage through the rotor plane (V_2). So the average speed is $(V_1 + V_2)/2$

The mass of the air streaming through the rotor during one second is

$$m = \rho F \frac{(V_1 + V_2)}{2} \quad (2.5)$$

where

m: Mass per second,

ρ : Density of air,

F: Swept rotor area

According to Newton's second law the power extracted from the wind by the rotor is equal to the mass times the drop in the wind speed squared.

$$P = \left(\frac{1}{2}\right) \rho (V_1^2 - V_2^2) \quad (2.6)$$

Substituting eq. (2.5) into eq. (2.6) the power extracted from the wind can be calculated as-

$$P = (\rho/4) (V_1^2 - V_2^2) (V_1 + V_2) F \quad (2.7)$$

The total power in the undisturbed wind streaming through exactly the same area F , with no rotor blocking the wind is-

$$P_0 = (\rho/2) V_1^3 F \quad (2.8)$$

The ratio between the power we extract from the wind and the power in the undisturbed wind is then:

$$(P/P_0) = (1/2) (1 - (V_2/V_1)^2) (1 + (V_2/V_1)) \quad (2.9)$$

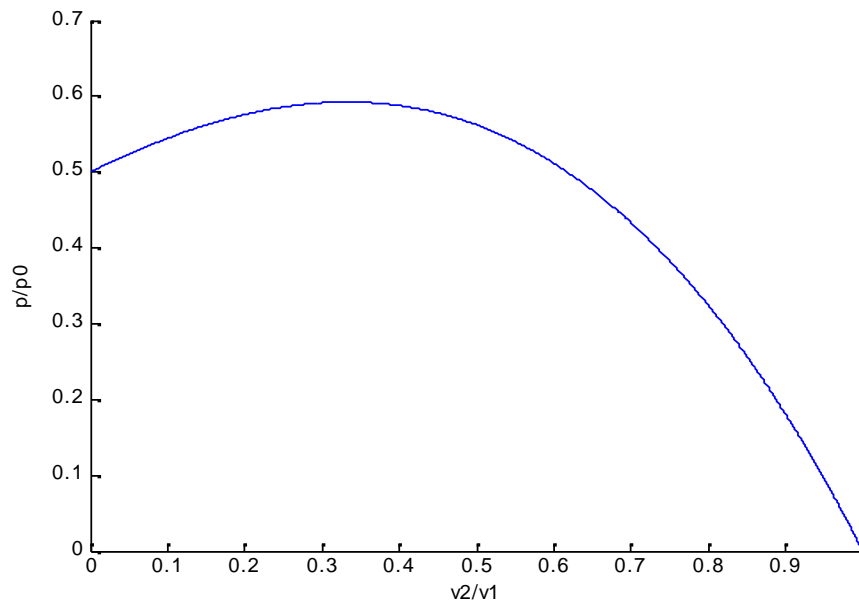


Figure 2.3 Plot of (P/P_0) as a function of (V_2/V_1)

Fig. 2.3 shows the plot of P/P_0 as a function of V_2/V_1 . It can be clearly observed that the function reaches its maximum for $V_2/V_1 = 1/3$ while the P/P_0 which proved that maximum power that can be extracted from the wind is 59% of the total power in the wind.

2.3 PITCH AND STALL CONTROL OF WIND TURBINE

An effective control system should be designed to control the output power of wind turbine to maximize their output. In case of stronger winds it becomes necessary to waste part of the excess energy of the wind in order to avoid damaging the wind turbine [6]. The wind turbines are designed to yield maximum output at wind speeds of 12-15 metres per second because the probability of this speed of wind is very high. It is not economical to design turbines that maximize their output at stronger winds because such strong winds are rare.

2.3.1 PITCH CONTROL

Pitch control is a method of controlling the speed of a wind turbine by varying the orientation or pitch of the blades [7]. On a pitch controlled wind turbine, the turbine's electronic controller checks the power output of the turbine several times per second. When the power output becomes too high, it sends a corrective signal to the blade pitch mechanism which immediately pitches (turns) the rotor blades slightly out of the wind. Conversely, the blades are turned back into the wind whenever the wind drops again.

In designing a pitch controlled wind turbine, it should be ensured that the rotor blades pitch varies exactly by the required amount. On a pitch controlled wind turbine, the computer will generally pitch the blades a few degrees every time the wind changes in order to keep the rotor blades at the optimum angle in order to maximize output for all wind speeds.

2.3.2 STALL CONTROL

Wind turbine stalling works by increasing the angle at which the relative wind strikes the blades (angle of attack), and it reduces the induced drag (drag associated with lift). Stalling increases automatically when the winds speed up. The rotor blade has been aerodynamically designed to ensure that the moment wind speed becomes too high [8]. stalling creates turbulence on the side of the rotor blade not facing the wind. This stall prevents the lifting force of the rotor blade from acting on the rotor. A rotor blade for a stall controlled wind turbine is twisted slightly along its longitudinal axis. This is partly

done in order to ensure that the rotor blade stalls gradually rather than abruptly when the wind speed reaches its critical value.

The basic advantage of stall control is that one avoids moving parts in the rotor itself, and a complex control system. On the other hand, stall control represents a very complex aerodynamic design problem, and related design challenges in the structural dynamics of the whole wind turbine, e.g. to avoid stall-induced vibrations. Nearly two thirds of the wind turbines currently being installed in the world are stall controlled.

2.4 WIND ENERGY CONVERSION SCHEMES

Several kinds of generator technologies have been developed and are in use today [4]. Broadly the generator may be working in stand alone or synchronized with grid. A short overview of grid connected wind generator topologies employing squirrel cage induction generator is presented. These topologies can be broadly classified on the basis of use of power electronic circuitry as-

- Direct grid connected operation.
- Grid operation employing power electronics.

2.4.1 DIRECT GRID CONNECTION

Induction generator is the prevalent choice for fixed speed wind energy systems because of its simplicity, robustness and relative low cost. This concept consists of a rotor connected to a squirrel cage induction generator through a gear box is shown in Fig. 2.4. The gear box is needed because the optimal rotor and generator speed ranges are different. This concept is known as Danish concept and many low power wind turbines build to date has been constructed according to this Danish concept [10]. The inductive circuit of squirrel cage induction generator consumes reactive power so to improve the power factor of whole system capacitors are often added to supply magnetizing current. The generator is directly grid coupled; therefore, speed variations are very small. Because the speed variations are very small the turbine is normally considered to operate at constant speed. Often the fixed speed wind turbine systems are provided with two fixed speeds. This is accomplished by using generators with adjustable pole winding

configuration. This will increase the aerodynamic capture as well as reduces the magnetizing losses of generator at low wind speeds.

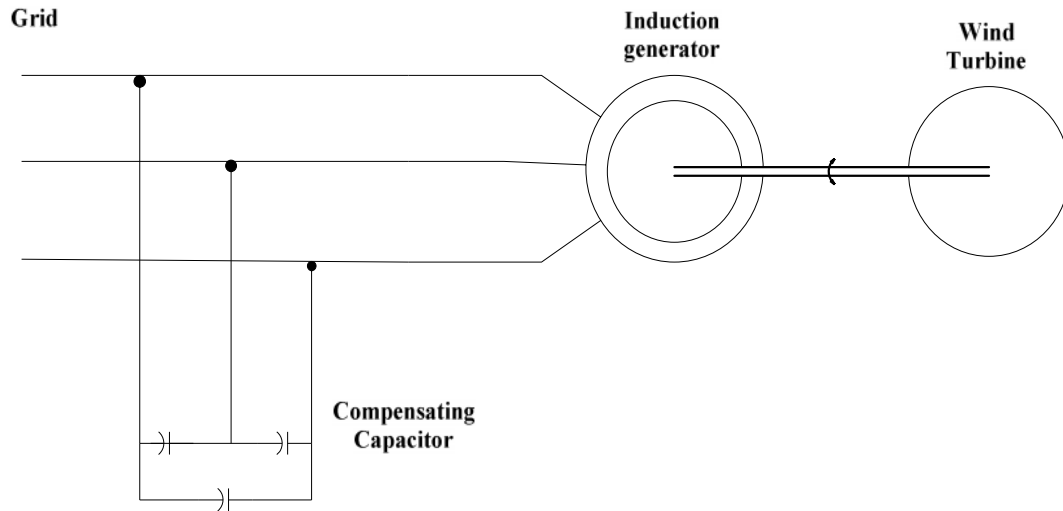


Figure 2.4 Direct grid connected wind energy conversion scheme

The performance of fixed-speed wind turbines very much depends on the characteristics of mechanical sub circuits e.g. pitch control time constants, main breaker maximum switching rate, etc. The response time of some of these mechanical circuits may be in the range of tens of milliseconds. As a result, each time a gust of wind hits the turbine, a fast and strong variation of electrical output power can be observed. When induction machines are operated using vector control techniques, fast dynamic response and accurate torque control are obtained.

2.4.2 GRID OPERATION EMPLOYING POWER ELECTRONICS

In this scheme induction generator is connected to grid through power electronics converter-inverter set. Schema of this scheme is given in Fig. 2.5. Converter changes variable frequency output of induction generator to constant dc and this dc is converted to constant frequency ac by firing angle control of converter inverter set [10-11]. The induction generator could be either cage bar rotor or wound rotor type. The gearbox is designed so that maximum rotor speed corresponds to rated speed of the generator. One

major advantage with this system is it's well developed and robust in control. Irrespective of this there are several disadvantages which are listed below [10].

- The power electronics equipment has to be designed for the full power rating of the generator which makes the system expensive.
- Inverter output filters and EMI filters are rated for full power rating, making filter design difficult and costly.
- Converter efficiency plays an important factor in total system efficiency over the entire operating range.

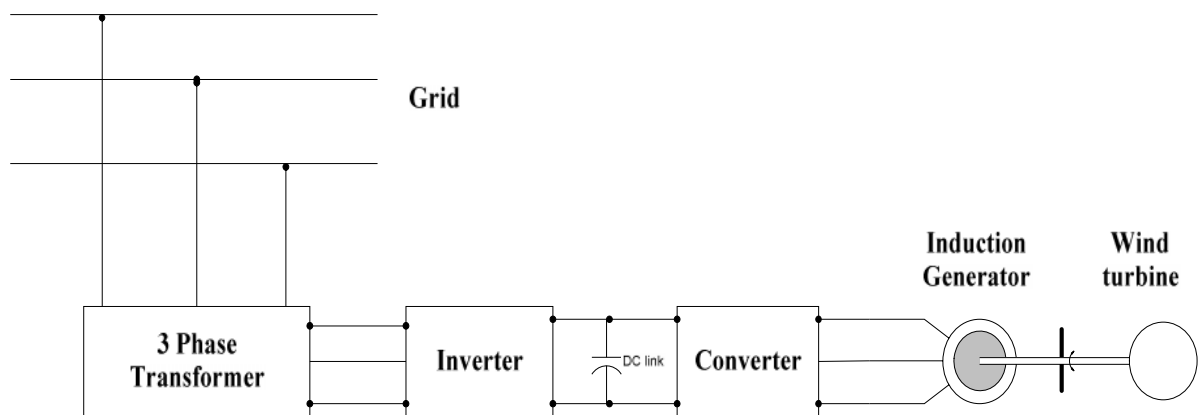


Figure 2.5 Variable speed system using cage induction generator

2.5 WIND ENERGY STATISTICS

The statistics demonstrating the global status of wind energy and status of wind energy in India are presented. These statistics have been summed with available data.

2.5.1 GLOBAL STATUS OF THE WIND ENERGY

Wind energy has continued the worldwide success story as the most dynamically growing energy source again in the year 2008. Since 2005, global wind installations more than doubled. In its best year yet, the market for new wind turbines showed a 42% increase with 27261 MW of new capacity in 2008. The global year wise new installed capacity is shown in Fig. 2.6. Since 1998 the wind energy has grown up by more than 25000 MW

from 2187 MW to 27261 MW. All wind turbines installed by the end of 2008 worldwide are generating 260 TWh per annum, equaling more than 1.5 % of the global electricity consumption [1]. The wind sector represented in 2008 a turnover of 40 billion. Based on accelerated development and further improved policies, a global capacity of more than 1500000 MW is possible by the year 2020. This development, led by the United States, Germany, Spain, China and India took the worldwide total to 121188 MW. This shows an increase of 29% compared with the 2007 market [2]. Fig. 2.7 and Fig. 2.8 show the cumulative installed capacity and the yearly world market growth respectively.

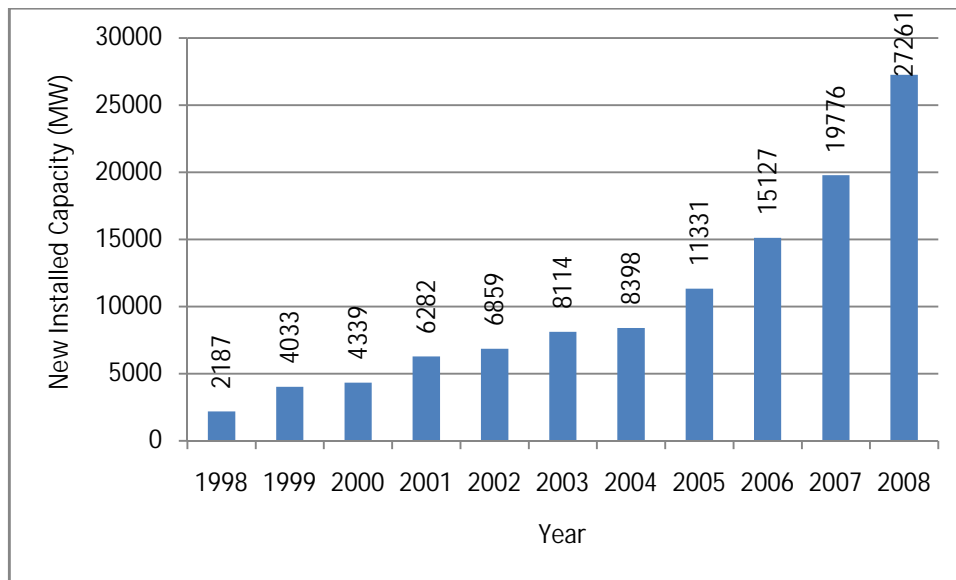


Figure 2.6 Global annual installed capacity

The top five countries in terms of total installed capacity at the end of 2008 were USA (25.17 GW), Germany (23.9 GW), Spain (16.74 GW), China (12.2 GW) and India (9.58 GW). In year 2008 USA takes over the global number one position from Germany and China getting ahead of India for the first time. Fig. 2.19 shows the total installed capacity of top wind producing countries. While Europe remains the leading market for wind energy, new European installations represented just 32.8 % of the global total, down from nearly 75% in 2004. For the first time in decades, more than half of the annual wind market was outside Europe and this trend is likely to continue.

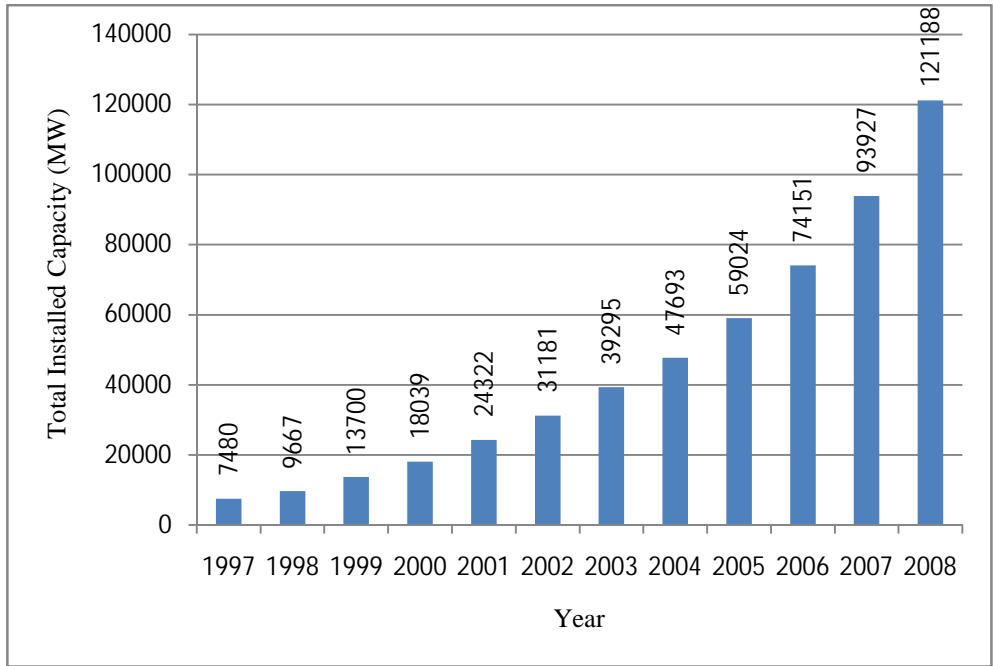


Figure 2.7 Global cumulative installed capacity

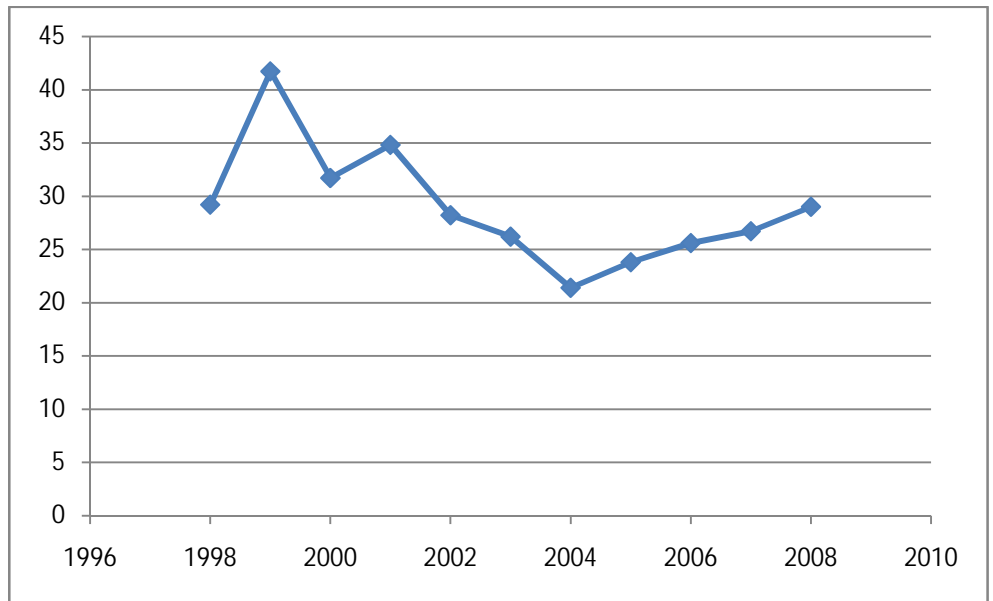


Figure 2.8 Annual growths in world wind market

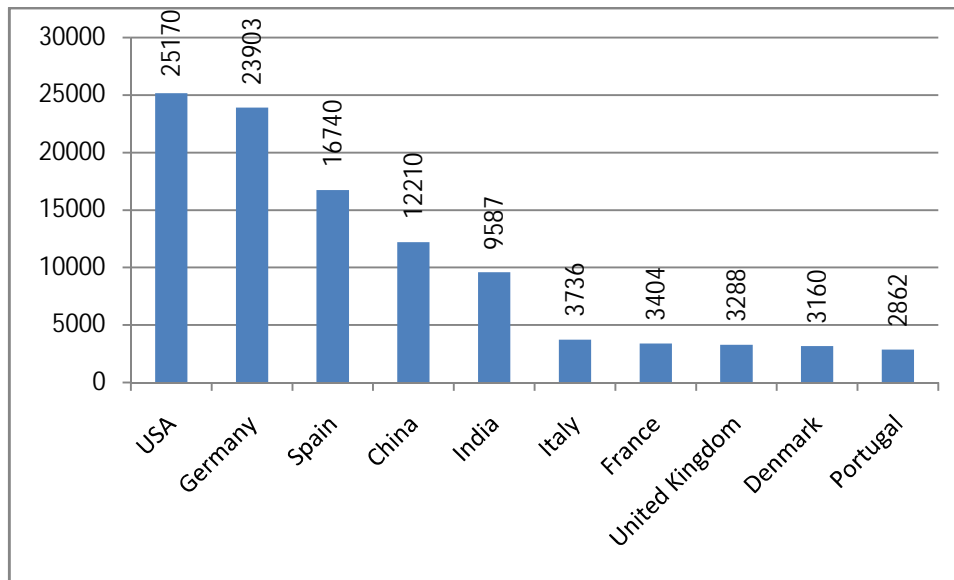


Figure 2.9 Top 10 installed capacities in 2008

2.5.2 WIND ENERGY IN INDIA

Wind energy is continuing strongly in India. India is at 5th position in harnessing the wind power for production of wind power with total installed capacity of 9521 MW. Future trends show that wind energy is continuing to grow strongly in India. The development of Indian wind power has so far been concentrated in a few regions, especially the southern state of Tamil Nadu, which accounts for more than half of all installations. This is beginning to change, with other states, including Maharashtra, Gujarat, Rajasthan and Karnataka, West Bengal, Madhya Pradesh and Andhra Pradesh starting to catch up. As a result wind farms can be seen under construction right across the country, from the coastal plains to the hilly hinterland and sandy deserts. Table 2.1 shows the state State-wise wind power installed capacity as on September 2008 and Fig. 2.12 shows the percentage contribution of each state in wind power generation. The Indian government is expecting an annual capacity addition of up to 2000 MW in the coming years. The Indian Ministry of New and Renewable Energy (MNRE) is working to create an attractive environment for the export, purchase, wheeling and banking of electricity generated by wind power projects. State Electricity Regulatory Commissions (SERC) are also promoting wind energy, through preferential tariffs and a minimum obligation on distribution companies to source a certain share of electricity from renewable energy. Ten

states have set up renewable purchase obligations, requiring utilities to source up to 10% of their power from renewable.

India has a solid domestic manufacturing base, including global player Suzlon, which accounts for over half of the market. In addition, other international companies have set up production facilities in India, including Vestas, Repower, Siemens, LM Glasfiber and Enercon.

Table 2.1 State wise wind power installed capacity in India

Sl. No.	State	Capacity in MW
1.	Andhra Pradesh	122.50
2.	Gujarat	1414.70
3.	Karnataka	1164.10
4.	Kerala	18.00
5.	Madhya Pradesh	187.70
6.	Maharashtra	1823.90
7.	Rajasthan	671.00
8.	Tamil Nadu	4115.80
9.	West Bengal	1.10
10.	Orissa	3.20
Total		9521.80

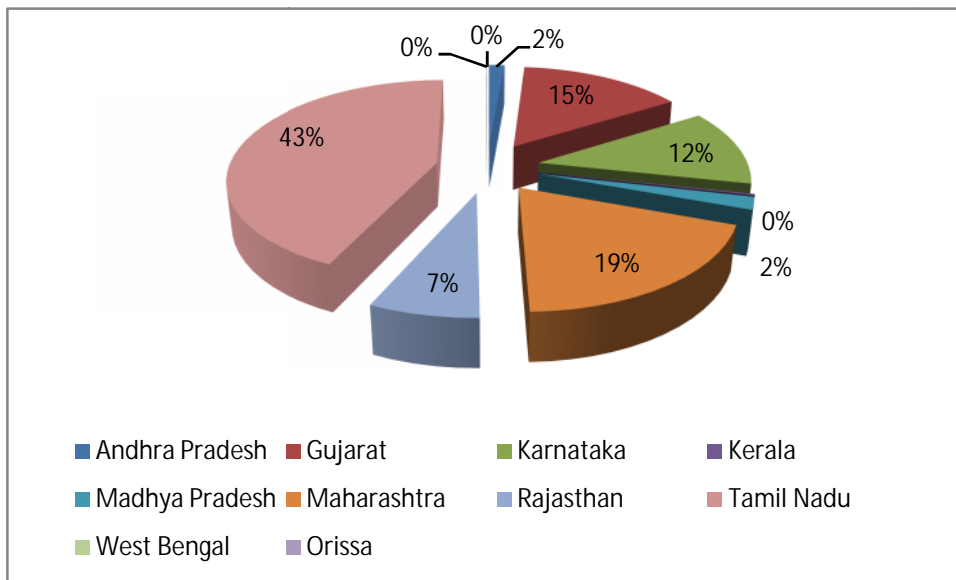


Figure 2.10 State wise percentage shares in wind energy production

2.6 BENEFITS OF WIND POWER

The growth of the market for wind energy is being driven by a number of factors, that include the context of energy supply and demand, the rising profile of environmental issues, like climate change and the impressive improvements in the technology itself. These factors have combined in many regions of the world to encourage political support for the industry's development. The benefits of wind power have been summed up under the following points-

2.6.1 ECONOMIC CONSIDERATION

The wind power is the least expensive of other forms of alternative energy and the electricity at the cost of around 5 cents per kWh can be generated. This cost is projected to decline even more as technology improves because most of the cost with wind power is initial investment and very little cost is needed to maintain it [1]. For conventional generation technologies, future price developments are a significant risk factor and if current trends are any indication, they are likely to continue rising into the unforeseeable future. Wind power is commercially attractive, especially when taking into account the price of carbon, which is a factor in a growing number of markets.

The wind power industry is revitalizing regional economies, providing quality jobs and expanding tax bases in rural regions struggling to keep their economies moving ahead in the face of the global flight to the cities. This is resulting into regional economic development as experienced in Tamil Nadu and Gujarat

2.6.2 SECURITY OF SUPPLY

As energy demand continues to increase, supplies of the main fossil fuels used in power generation, are becoming more expensive and more difficult to extract. Therefore, major economies of the world are increasingly relying on imported fuel at unpredictable cost, sometimes from regions of the world where conflict and political instability threaten the security of that supply [1].

In contrast to the uncertainties surrounding supplies of conventional fuels, and volatile prices, wind energy is a massive indigenous power source which is permanently available

in virtually every country. There are no fuel costs, no geo-political risk and no supply dependence on imported fuels from politically unstable regions. Every KWh generated by wind power has the potential to displace fossil fuel imports, improving both security of supply and the national balance of payments.

2.6.3 ENVIRONMENTAL BENEFITS OF WIND POWER

The dependency on electric energy is increasing day by day, consequently the need for more power plants. Today, most of the electricity is generated by burning fossil fuels, which emits the green house gases and other polluting gases like NO_x , SO_x results into climate change [2]. Climate change is now generally accepted to be the greatest environmental threat facing the world, and keeping our planet's temperature at sustainable levels has become one of the major concerns of policy makers. More wind energy generation will improve the environment.

Greenhouse gases like CO_x are produced naturally in our environment through volcanic activity and organic matter decomposition and by burning of fossil fuels to generate electricity. Using wind to generate electricity reduces CO_x emission. Sulphur dioxide and nitrogen oxide is a byproduct of burning fossil fuels. In the atmosphere it can react with other chemicals to form acidic compounds. These gases are the main components of the 'acid rain'. Acid rain threatens our lakes and forests by raising the level of acidity. At present power sector is the largest single source of emissions accounting for about 40% of CO_x and about 25% of overall emissions. This is costing billions in additional health costs and infrastructure damage. Wind power does not emit any climate change inducing carbon dioxide nor other air pollutants. The wind energy not only reduces the emission of green house gases it also has a positive effect on the quality of air we breathe.

2.6.4 JOBS

One fundamental advantage of wind energy is that it replaces expenditure on mostly imported fossil or nuclear energy resources by human capacities. Wind energy utilization creates many more jobs than centralized, non-renewable energy sources. The wind sector worldwide has become a major job generator: Within only three years, the wind sector worldwide almost doubled the number of jobs from 235000 in 2005 to 440000 in the year

2008. These 440000 employees in the wind sector worldwide, most of them highly skilled jobs, are contributing to the generation of 260 TWh of electricity. It is expected that wind energy will produce 540000 jobs in 2009 and 660000 jobs in 2010 [1].

2.6.5 FULLY RENEWABLE AND REDUCED HAZARDS

Wind energy does not deplete natural resources. Unlike fossil fuels that have a finite supply, Wind is renewed every day as the earth heats and cools. While it is true that wind energy supplies can come and go based on weather patterns, seasons and so forth, the overall renewable side of production is one of the benefits of wind energy production that make it very attractive. Approximately one pound of coal is saved by every kilowatt-hour generated by wind.

Production of fossil fuel and nuclear power can pose rather large safety hazards. A reduction of these is another one of the many benefits of wind energy production. The benefits of wind energy are rather extensive. Although it is difficult to fully replace the use of other sources of energy with the wind alone, this type of energy can greatly reduce reliance upon them.

2.7 DIFFICULTIES WITH WIND POWER

Despite of many benefits of wind power, there are some difficulties also in converting the wind energy into electric power. Various difficulties with wind power are also discussed herewith under the following headings.

2.7.1 VARIABILITY OF WIND

The main difficulty with wind energy is that wind is intermittent. Wind speeds vary with time of day, time of year, height above ground, and location on the earth's surface. Near the earth's surface, winds are usually greater during the middle of the day and decrease at night. Wind speeds also vary strongly with time of year. In the southern Great Plains, the winds are strongest in the spring and weakest in the summer (July and August). Utilities here are summer peaking, and hence need the most power when winds are the lowest and the least power when winds are highest. Due to this variability in wind , the power output

will be zero (or very small) for perhaps 10% of the time, rated for perhaps another 10% of the time, and at some intermediate value the remaining 80% of the time.

For a fixed speed system the turbulence of the wind will result in variation in power output. However, output fluctuations of wind generators cause network frequency variations in power systems [19]. This can decrease the power quality and then cause a restriction of wind farm installation, especially in an isolated power system. This means that some sort of storage is necessary to mitigate these power quality problems and to compensate variation in power. Following are the most commonly used storage systems.

- Flywheel storage. .
- Compressed air energy storage.
- Superconducting magnetic energy storage.
- Battery storage.

2.7.2 NOISE

The noise from the wind turbines is incredible. It sounded like airplanes or helicopters. New turbines may have quieter bearings and gears, but the huge magnetized generators cannot avoid producing a low-frequency hum and the problem of 100-foot rotor blades chopping through the air at over 100 mph also is insurmountable. Every time each rotor passes the tower, the compression of air produces a deep resonating thump. Only a gravelly "swishing" may be heard directly beneath the turbine, but farther away the resulting sound of several towers together has been described to be as loud as a motorcycle, like aircraft continually passing overhead. In mountainous areas the sound echoes over larger distances.

2.8 CONCLUSION

With the pace of development the demand of energy is growing rapidly. It has become impossible to meet this growing need of energy with conventional methods of generation because of depleting fossil fuel reserves and increasing crude oil prices. To sustain this pace of development it is necessary to search and develop non conventional sources of energy. Wind energy is a very good alternative to this problem. There is large potential of

wind energy in India and in rest of the world. Wind energy is cheaper than other renewable sources of energy like solar energy. After the payback period it is totally free of cost for rest of its operating period. Wind energy also gets attention because of the rising concern towards climate changes as wind is a clean source of energy. Wind energy also has some negative impacts and all of these negative aspects will only become worse if even a small part of the industry's plans for hundreds of thousands of towers becomes reality however, the negative impacts must of course be weighed against the benefits and these are negligible.

CHAPTER 3

DYNAMIC MODEL OF WIND DRIVEN INDUCTION GENERATOR AND SIMULATION ALGORITHM

3.1 INTRODUCTION

The steady state equivalent circuit is useful for studying the performance of the machine in steady state. This implies that all transients arising during load change and other transient condition are neglected. To study the effect of various transients like change in load, input etc, the dynamic model is needed. The need of dynamic model for wind driven induction generator is needed because the prime mover input does not remain constant. The prime mover input changes as the velocity of wind changes. This causes the transients in currents and electromagnetic torque produced, the transient performance can be calculated iteratively and therefore it require that dynamic model should reduce the computational effort to compute the performance quickly.

The dynamic behaviour of induction machine can be described with the help of differential equations the inductance terms in these equations are time varying and some of them are function of rotor speed, which increases the complexity of these differential equations. To reduce the computation effort to solve these equations, the variables are transferred to a frame of reference which rotates at an arbitrary angular velocity [18].

Reference frames are much like observer platforms, in that each of the platforms gives a unique view of the system at hand as well as a dramatic simplification of the system equations. For example, consider that, for the purposes of control it is desirable to have system variables as dc quantities, although the actual variables are sinusoidal. This can be accomplished by having a reference frame revolving at the same angular speed as that of sinusoidal variables. As the reference frames are moving at an angular speed equal to angular frequency of the sinusoidal supply, then the differential speed between them is reduced to zero, resulting in the sinusoidal being perceived as a dc signal from reference frames [21].

The d-q variables models derived by transforming phase variables model into d-q variable model with frame of reference rotating at arbitrary speed has the following advantages [18].

- The dynamic performance equations has constant inductances
- For balanced conditions, zero sequence quantities disappears
- The number of voltage equations is reduced
- The time-varying voltage equations become time-invariant ones

3.2 STATIC COMPONENT MODEL

The system equations can be obtained by developing the d-q variable model for static components such as resistance, inductor and capacitor. The transformation of static variables into corresponding d-q variables and vice-versa is given by eq. 3.1.

$$\left. \begin{aligned} f_{qd0s} &= K_s f_{abcs} \\ f_{abcs} &= K_s^{-1} f_{qd0s} \end{aligned} \right\} \quad (3.1)$$

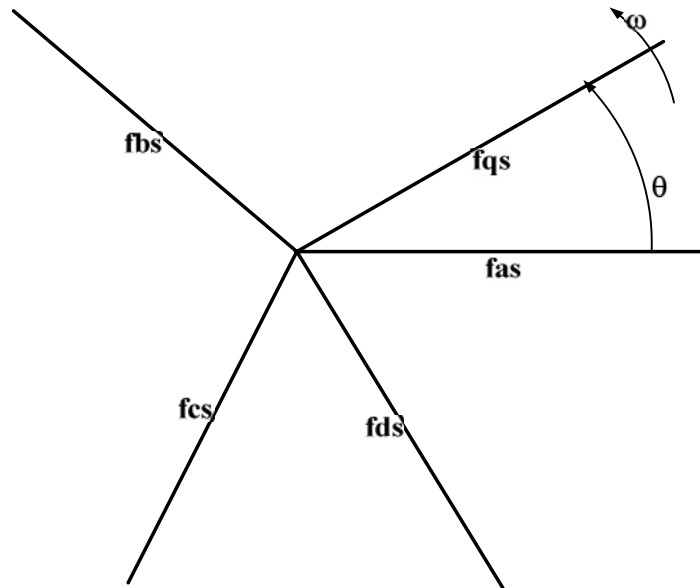


Figure 3.1 Transformation of static phase variables into d-q variables

Where K_s is matrix of transformation of stationary circuit elements, this can be obtained from the Fig. 3.1 by using trigonometric relationships. In Fig. 3.1 f_{as} , f_{bs} , f_{cs} are the three phase variables of stationary circuit and each have phase displaced by 120. The equations of transformation may be thought of as if the f_{qs} and f_{ds} are orthogonal to each other and rotating at an angular velocity of ω . f_{qs} is leading f_{as} by an angle θ . f_{ds} variables are not associated with reference frame but is arithmetically related to abc variables. Correspondingly when f_{as} , f_{bs} , f_{cs} are resolved into f_{qs} and f_{ds} .

$$f_{qs} = f_{as} \cos(\theta) + f_{bs} \cos(\theta - \frac{2\pi}{3}) + f_{cs} \cos(\theta + \frac{2\pi}{3}) \quad (3.2)$$

$$f_{ds} = f_{as} \sin(\theta) + f_{bs} \sin(\theta - \frac{2\pi}{3}) + f_{cs} \sin(\theta + \frac{2\pi}{3}) \quad (3.3)$$

So K_s can be defined as

$$K_s = \frac{2}{3} \begin{bmatrix} \cos(\theta) & \cos(\theta - \frac{2\pi}{3}) & \cos(\theta + \frac{2\pi}{3}) \\ \sin(\theta) & \sin(\theta - \frac{2\pi}{3}) & \sin(\theta + \frac{2\pi}{3}) \\ \frac{1}{2} & \frac{1}{2} & \frac{1}{2} \end{bmatrix} \quad (3.4)$$

$$K_s^{-1} = \begin{bmatrix} \cos(\theta) & \sin(\theta) & 1 \\ \cos(\theta - \frac{2\pi}{3}) & \sin(\theta - \frac{2\pi}{3}) & 1 \\ \cos(\theta + \frac{2\pi}{3}) & \sin(\theta + \frac{2\pi}{3}) & 1 \end{bmatrix} \quad (3.5)$$

and

$$\theta = \int_0^t \omega(\xi) d\xi + \theta(0) \quad (3.6)$$

The factor (2/3) is chosen so that the peak value of d-q axis currents becomes equal to peak value of stator current under sinusoidal conditions.

3.3.1 RESISTIVE ELEMENTS

From above concept of transformation the voltage current relationship for static elements can be transformed to arbitrary reference frame [21]. In phase variables the voltage equation for resistive element can be written as-

$$v_{abc s} = r_s i_{abc s} \quad (3.7)$$

By applying the transformation given in eq. (3.1)

$$v_{dq0s} = K_s r_s (K_s)^{-1} = r_s i_{dq0s} \quad (3.8)$$

Where r_s is diagonal matrix of stator winding resistance. Stator phase windings are designed to have same resistance. If phase resistances are unequal then resistance matrix associated with arbitrary frame of reference variables contains sinusoidal function of θ . If all nonzero elements of r_s matrix are equal then

$$K_s r_s (K_s)^{-1} = r_s \quad (3.9)$$

3.3.2 INDUCTIVE ELEMENTS

For three phase inductive circuit, the voltage equation can be written as-

$$v_{abc s} = p \lambda_{abc s} \quad (3.10)$$

By applying the transformation given in eq. (3.1)

$$v_{dq0s} = K_s p [(K_s)^{-1} \lambda_{dq0s}] \quad (3.11)$$

$$V_{dq0s} = K_s p [(K_s)^{-1}] \lambda_{dq0s} + K_s (K_s)^{-1} p \lambda_{dq0s} \quad (3.12)$$

$$K_s p [(K_s)^{-1}] = \begin{vmatrix} 0 & 1 & 0 \\ -1 & 0 & 0 \\ 0 & 0 & 0 \end{vmatrix} \quad (3.13)$$

Substitute eq. (3.13) in eq. (3.12)

$$v_{dq0s} = \lambda_{dqs} + p \lambda_{dq0s} \quad (3.14)$$

The first term in eq. (3.14) is referred as speed voltage with the speed being the angular velocity of the arbitrary reference frame. When reference frame is stationary, reference frame speed is zero so the speed voltages and the voltage equations for three phase

inductive circuit become familiar time rate of change of flux linkages. This is analogous to that reference frame is fixed where the circuit physically exists.

In case of magnetically linear system it has been customary to express the flux linkages as the product of inductance and current matrix before performing a change of variables [21]. For a linear circuit flux linkages can be expressed as

$$\lambda_{abc s} = L_s i_{abc s} \quad (3.15)$$

$$\lambda_{dq0 s} = K_s L_s (K_s)^{-1} i_{dq0 s} \quad (3.16)$$

$$K_s L_s (K_s)^{-1} = L_s \quad (3.17)$$

L_s is inductance matrix for three phase induction machine and is given as

$$L_s = \begin{bmatrix} L_{ls} + L_{ms} & \frac{-1}{2} L_{ms} & \frac{-1}{2} L_{ms} \\ \frac{-1}{2} L_{ms} & L_{ls} + L_{ms} & \frac{-1}{2} L_{ms} \\ \frac{-1}{2} L_{ms} & \frac{-1}{2} L_{ms} & L_{ls} + L_{ms} \end{bmatrix} \quad (3.18)$$

$$K_s L_s (K_s)^{-1} = \begin{bmatrix} L_s - L_m & 0 & 0 \\ 0 & L_s - L_m & 0 \\ 0 & 0 & L_s - L_m \end{bmatrix} \quad (3.19)$$

where

$$L_s = L_{ls} + L_{ms} \quad (3.20)$$

$$L_m = \frac{-1}{2} L_{ms} \quad (3.30)$$

3.3.3 CAPACITIVE ELEMENTS

For a three phase capacitive element the relation of current in phase variable is given by

$$i_{abc s} = p q_{abc s} \quad (3.21)$$

Apply the transformation given in eq. (3.1) to eq. (3.21)

$$i_{dq0 s} = K_s p [(K_s)^{-1} q_{dq0 s}] \quad (3.22)$$

$$i_{dq0s} = K_s p [(K_s)^{-1}] q_{dq0s} + K_s (K_s)^{-1} p [q_{dq0s}] \quad (3.23)$$

$$K_s p [(K_s)^{-1}] = \begin{bmatrix} 0 & 1 & 0 \\ -1 & 0 & 0 \\ 0 & 0 & 0 \end{bmatrix} \quad (3.24)$$

By using eq. (3.24) in eq. (3.23) yield the following result

$$i_{dq0s} = q_{dq0s} + p q_{dq0s} \quad (3.25)$$

$$(q_{dq0s})^T = [q_{ds} \quad -q_{qs} \quad 0] \quad (3.26)$$

3.3 INDUCTION MACHINE MODEL

The following assumptions are made to derive the model of induction machine [15].

- (i) The air gap is uniform.
- (ii) Balanced rotor and stator windings, with sinusoidally distributed mmf.

The induction machine model in reference frame can be obtained by first referring its model in phase variables. The induction machine equations have been developed in phase variables and then by applying the d-q transformation machine model in arbitrary reference frame.

3.3.1 INDUCTION MACHINE MODEL IN PHASE VARIABLES

Three phase induction machines have three phase windings both on stator and rotor. The phase windings are displaced in space by 120° electric degrees from each other. When stator is connected to supply, a rotating magnetic field of uniform strength and rotating at an angular speed equal to stator frequency is produced. This rotating magnetic field produces currents in short circuited rotor windings. According to Lenz law, the reaction is to counter the source of the current which produces a rotation. Depending on the shaft load the rotor will settle down to a speed ω_r .

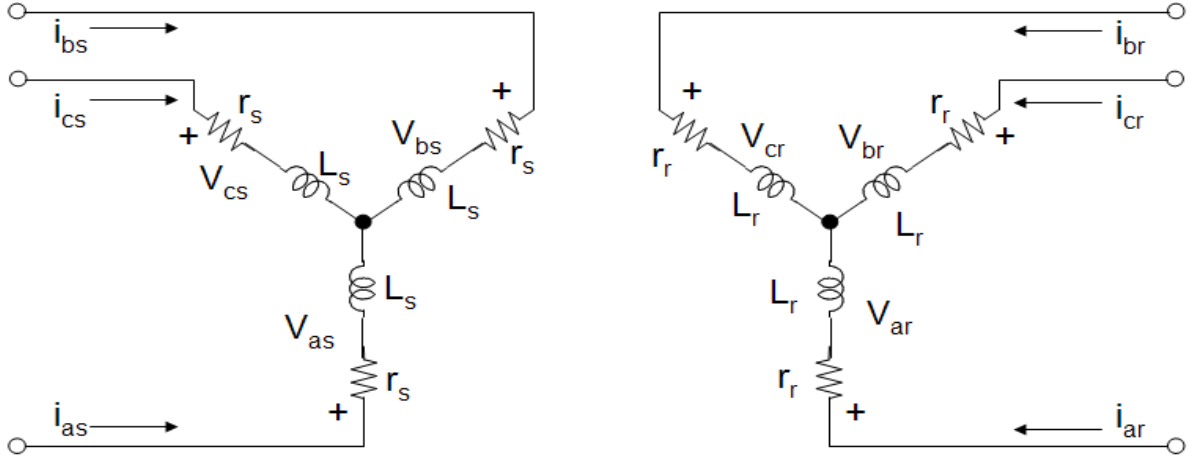


Figure 3.2 Stator and rotor circuits of induction machine

From the Fig. 3.2 of induction machine the voltage equations in machine variables can be expressed as

$$v_{abcs} = r_s i_{abcs} + p \lambda_{abcs} \quad (3.27)$$

$$v_{abcr} = r_r i_{abcr} + p \lambda_{abcr} \quad (3.28)$$

In magnetic linear system the flux can be represented as product of inductances and currents.

$$\begin{bmatrix} \lambda_{abcs} \\ \lambda_{abcr} \end{bmatrix} = \begin{bmatrix} L_s & L_{sr} \\ (L_{sr})^T & L_r \end{bmatrix} \begin{bmatrix} i_{abcs} \\ i_{abcr} \end{bmatrix} \quad (3.29)$$

The stator winding inductance L_s , rotor winding inductance L_r and mutual inductance L_{sr} are defined below.

$$L_s = \begin{bmatrix} L_{ls} + L_{ms} & \frac{-1}{2} L_{ms} & \frac{-1}{2} L_{ms} \\ \frac{-1}{2} L_{ms} & L_{ls} + L_{ms} & \frac{-1}{2} L_{ms} \\ \frac{-1}{2} L_{ms} & \frac{-1}{2} L_{ms} & L_{ls} + L_{ms} \end{bmatrix} \quad (3.30)$$

$$L_r = \begin{bmatrix} L_{lr} + L_{mr} & \frac{-1}{2} L_{mr} & \frac{-1}{2} L_{mr} \\ \frac{-1}{2} L_{mr} & L_{lr} + L_{mr} & \frac{-1}{2} L_{mr} \\ \frac{-1}{2} L_{mr} & \frac{-1}{2} L_{mr} & L_{lr} + L_{mr} \end{bmatrix} \quad (3.31)$$

The mutual inductance between stator and rotor is dependent on the rotor position i.e. speed of rotor. The value mutual inductance changes from zero to maximum value L_{sr} depending on the position of rotor.

$$L_{sr} = L_{sr} \begin{bmatrix} \cos(\theta_r) & \cos(\theta_r + \frac{2\pi}{3}) & \cos(\theta_r - \frac{2\pi}{3}) \\ \cos(\theta_r - \frac{2\pi}{3}) & \cos(\theta_r) & \cos(\theta_r + \frac{2\pi}{3}) \\ \cos(\theta_r + \frac{2\pi}{3}) & \cos(\theta_r - \frac{2\pi}{3}) & \cos(\theta_r) \end{bmatrix} \quad (3.32)$$

In above equations L_{ls} and L_{ms} are the stator winding leakage and magnetizing inductance respectively. For rotor winding L_{lr} and L_{mr} are leakage and magnetizing inductance respectively. L_{sr} is the amplitude of the mutual inductances between stator and rotor windings. For convenience all rotor variables are referred to stator winding by using turn ratio for expressing the voltage equations in machine variables.

$$\begin{aligned} i'_{abcr} &= \frac{N_r}{N_s} i_{abcr} \\ v'_{abcr} &= \frac{N_s}{N_r} v_{abcr} \\ \lambda'_{abcr} &= \frac{N_s}{N_r} \lambda_{abcr} \\ L_{ms} &= \frac{N_s}{N_r} L_{sr} \\ L'_{sr} &= \frac{N_s}{N_r} L_{sr} \end{aligned} \quad (3.33)$$

When rotor variables are referred to stator side the flux linkages and voltage equations referred to stator winding can be expressed as

$$\begin{bmatrix} \lambda_{abcs} \\ \lambda'_{abcr} \end{bmatrix} = \begin{bmatrix} L_s & L'_{sr} \\ (L'_{sr})^T & L_r \end{bmatrix} \begin{bmatrix} i_{abcs} \\ i'_{abcr} \end{bmatrix} \quad (3.34)$$

$$\begin{bmatrix} v_{abcs} \\ v'_{abcr} \end{bmatrix} = \begin{bmatrix} r_s + pL_s & pL'_{sr} \\ p(L'_{sr})^T & r'_r + pL_r \end{bmatrix} \begin{bmatrix} i_{abcs} \\ i'_{abcr} \end{bmatrix} \quad (3.35)$$

where

$$L'_{sr} = L_{ms} \begin{bmatrix} \cos(\theta_r) & \cos(\theta_r + \frac{2\pi}{3}) & \cos(\theta_r - \frac{2\pi}{3}) \\ \cos(\theta_r - \frac{2\pi}{3}) & \cos(\theta_r) & \cos(\theta_r + \frac{2\pi}{3}) \\ \cos(\theta_r + \frac{2\pi}{3}) & \cos(\theta_r - \frac{2\pi}{3}) & \cos(\theta_r) \end{bmatrix} \quad (3.36)$$

and

$$L'_r = \begin{bmatrix} L'_{lr} + L_{ms} & -\frac{1}{2}L_{ms} & -\frac{1}{2}L_{ms} \\ -\frac{1}{2}L_{ms} & L'_{lr} + L_{ms} & -\frac{1}{2}L_{ms} \\ -\frac{1}{2}L_{ms} & -\frac{1}{2}L_{ms} & L'_{lr} + L_{ms} \end{bmatrix} \quad (3.37)$$

In magnetic linear system the stored energy is the sum of the self inductances of each winding times one half the square of its current and all mutual inductances, each times the current the current in two windings coupled by the mutual inductance. Leakage inductances are not considered here because energy stored in these inductances does not contribute to the energy stored in magnetic circuit [21].

$$T_e = \left(\frac{P}{2}\right) (i_{abc})^T \frac{\partial}{\partial \theta_r} [L'_{sr}] i'_{abc} \quad (3.38)$$

$$T_e = -\left(\frac{P}{2}\right) L_{ms} \left\{ [i_{as}(i'_{ar} - \frac{1}{2}i'_{br} - \frac{1}{2}i'_{cr}) + i_{bs}(i'_{br} - \frac{1}{2}i'_{ar} - \frac{1}{2}i'_{cr}) + i_{cs}(i'_{cr} - \frac{1}{2}i'_{br} - \frac{1}{2}i'_{ar})] \sin\theta_r + \frac{\sqrt{3}}{2} [i_{as}(i'_{br} - i'_{cr}) + i_{bs}(i'_{cr} - i'_{ar}) + i_{cs}(i'_{ar} - i'_{br})] \cos\theta_r \right\} \quad (3.39)$$

The relation between torque and rotor speed is given by

$$p\omega_r = \left(\frac{P}{2J}\right) (T_e - T_L) \quad (3.40)$$

J is inertia of the rotor

T_L is load torque

3.3.2 GENERALIZED MODEL IN d-q VARIABLES

In developing the model of an induction it is worth noting the following aspects of its characteristics-

- The rotor has symmetrical structure. This makes the d and q axis equivalent circuits similar [15].
- The dynamics of rotor circuit is determined by slip.

- Rotor winding can be modelled by an equivalent three phase winding because shorted rotor windings produce a field with the same number of poles as produced by stator winding

In the analysis of three phase induction machine the transformation of rotor variables to the arbitrary reference frame is also desirable. The equations of transformation for rotor circuit variables are

$$\left. \begin{aligned} f_{qd0r} &= K_r f_{abcr} \\ f_{abcr} &= K_r^{-1} f_{qd0r} \end{aligned} \right\} \quad (3.41)$$

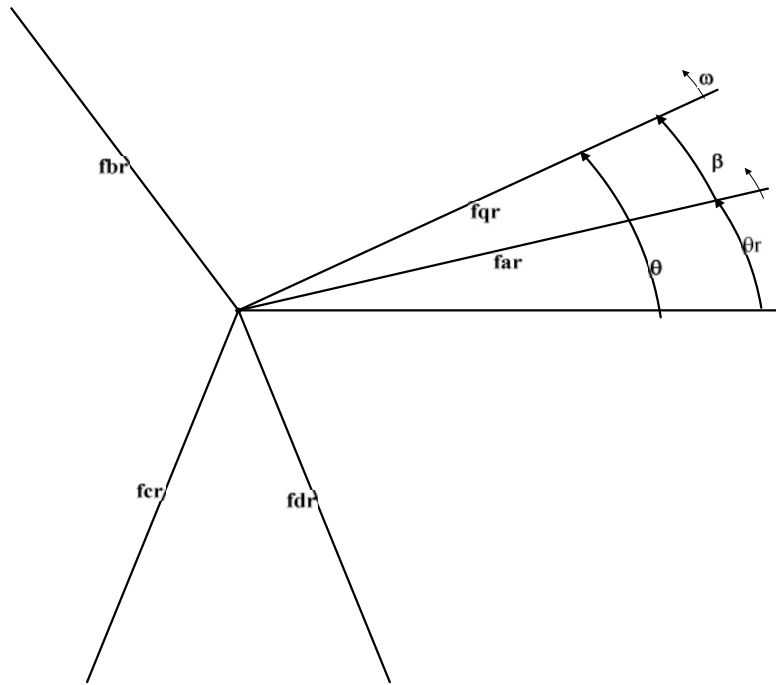


Figure 3.3 Transformation of rotor phase variables into d-q variables

K_r is matrix of transformation of stationary circuit elements, this can be obtained from the Fig. 3.3 by using trigonometric relationships. ω is used instead of θ because the rotor phase variables are rotating.

$$K_r = \frac{2}{3} \begin{bmatrix} \cos(\beta) & \cos(\beta - \frac{2}{3}) & \cos(\beta + \frac{2}{3}) \\ -\sin(\beta) & -\sin(\beta - \frac{2}{3}) & -\sin(\beta + \frac{2}{3}) \\ \frac{1}{2} & \frac{1}{2} & \frac{1}{2} \end{bmatrix} \quad (3.42)$$

$$K_r^{-1} = \begin{bmatrix} \cos(\beta) & -\sin(\beta) & 1 \\ \cos(\beta - \frac{2}{3}) & -\sin(\beta - \frac{2}{3}) & 1 \\ \cos(\beta + \frac{2}{3}) & -\sin(\beta + \frac{2}{3}) & 1 \end{bmatrix} \quad (3.43)$$

and

$$= -\theta_r \quad (3.44)$$

$$\theta_r = \int_0^t \omega_r(\xi) d\xi + \theta_r(0) \quad (3.45)$$

Application of transformation given in eq. (3.1) on the eq. (3.34) gives the following relation.

$$\begin{bmatrix} \lambda_{abcs} \\ \lambda'_{abc r} \end{bmatrix} = \begin{bmatrix} K_S L_S (K_S)^{-1} & K_S L'_{Sr} (K_r)^{-1} \\ K_r (L'_{Sr})^T (K_S)^{-1} & K_r L'_r (K_r)^{-1} \end{bmatrix} \begin{bmatrix} i_{abcs} \\ i'_{abc r} \end{bmatrix} \quad (3.46)$$

$$K_S L_S (K_S)^{-1} = \begin{bmatrix} L_{ls} + \frac{3}{2} L_{ms} & 0 & 0 \\ 0 & L_{ls} + \frac{3}{2} L_{ms} & 0 \\ 0 & 0 & L_{ls} \end{bmatrix} \quad (3.47)$$

$$K_r L'_r (K_r)^{-1} = \begin{bmatrix} L'_{Sr} + \frac{3}{2} L_{ms} & 0 & 0 \\ 0 & L'_{Sr} + \frac{3}{2} L_{ms} & 0 \\ 0 & 0 & L'_{Sr} \end{bmatrix} \quad (3.48)$$

$$K_r L'_{Sr} (K_r)^{-1} = K_r (L'_{Sr})^T (K_S)^{-1} = \begin{bmatrix} \frac{3}{2} L_{ms} & 0 & 0 \\ 0 & \frac{3}{2} L_{ms} & 0 \\ 0 & 0 & 0 \end{bmatrix} \quad (3.49)$$

$$L_m = \frac{3}{2} L_{ms} \quad (3.50)$$

Application of eq. (3.1) and eq. (3.41) on voltage equation in phase variables given in eq. (3.27) and eq. (3.28) will result in voltage equations in reference frame variables.

$$v_{dq0s} = r_s i_{dq0s} + \lambda_{qds} + p\lambda_{qs} \quad (3.51)$$

$$v'_{dq0r} = r'_r i'_{dq0r} + (-\omega_r) \lambda'_{qdr} + p\lambda'_{dq0r} \quad (3.52)$$

Eq. (3.51) and eq. (3.52) can be written in expanded form

$$\begin{aligned} v_{qs} &= r_s i_{qs} - \lambda_{ds} + p\lambda_{qs} \\ v_{ds} &= r_s i_{ds} - \lambda_{qs} + p\lambda_{ds} \\ v_{0s} &= r i_{0s} + p\lambda_{0s} \\ v_{qr} &= r_r i_{qr} - (-\omega_r) \lambda_{dr} + p\lambda_{qr} \\ v_{dr} &= r_r i_{dr} - (-\omega_r) \lambda_{qr} + p\lambda_{dr} \\ v_{0r} &= r_r i_{0r} + p\lambda_{0r} \end{aligned} \quad \left. \begin{array}{l} | \\ \vdots \\ | \\ | \\ \vdots \\ | \\ | \end{array} \right\} \quad (3.53)$$

In above equations superscript (') is omitted for the sake of simplicity and all rotor variables are referred to stator winding.

Where

$$\begin{aligned} \lambda_{qs} &= L_{ls} i_{qs} + L_m (i_{qs} + i_{qr}) \\ \lambda_{ds} &= L_{ls} i_{ds} + L_m (i_{ds} + i_{dr}) \\ \lambda_{0s} &= L_{ls} i_{0s} \\ \lambda_{qr} &= L_{lr} i_{qr} + L_m (i_{qs} + i_{qr}) \\ \lambda_{dr} &= L_{lr} i_{dr} + L_m (i_{ds} + i_{qr}) \\ \lambda_{0r} &= L_{lr} i_{0s} \end{aligned} \quad \left. \begin{array}{l} | \\ \vdots \\ | \\ | \\ \vdots \\ | \\ | \end{array} \right\} \quad (3.54)$$

On the basis of above discussion an equivalent circuit of induction machine in arbitrary reference frame can be drawn [16].

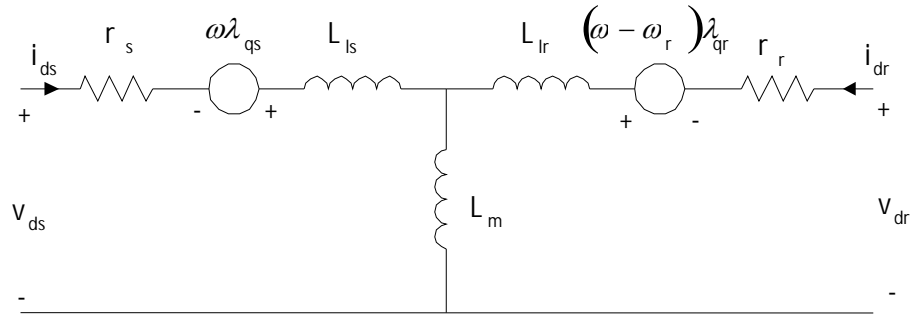


Figure 3.4 d-axis equivalent circuit of induction machine

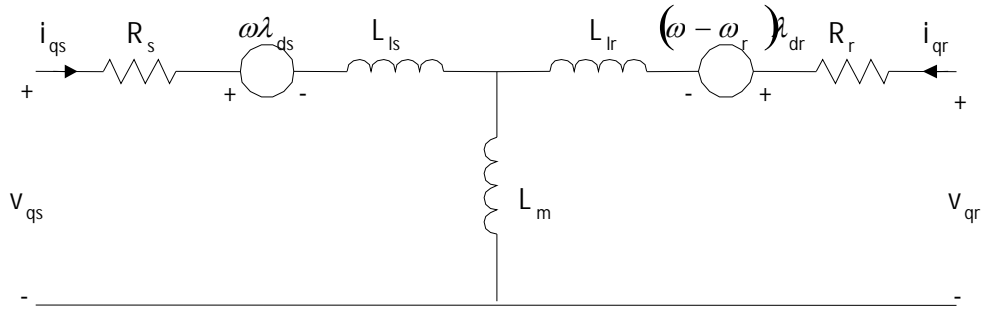


Figure 3.5 q-axis equivalent circuit of induction machine

In last section we have derived the expression of torque in machine variables and by applying transformation given in eq. (3.1) and eq. (3.41) to eq. (3.38) the expression of torque in arbitrary reference frame can be obtained.

$$T_e = \left(\frac{P}{2}\right) \left((K_s)^{-1} i_{dq0} \right)^T \frac{\partial}{\partial \theta_r} [L'_{sr}] (K_r)^{-1} i'_{dq0r} \quad (3.55)$$

The further manipulation will yield the relation of torque in terms of current and flux linkage

$$T_e = \left(\frac{3}{2}\right) \left(\frac{P}{2}\right) (i_{qs} i'_{dr} - i_{ds} i'_{qr}) \quad (3.56)$$

$$T_e = \left(\frac{3}{2}\right) \left(\frac{P}{2}\right) (\lambda_{ds} i_{qs} - \lambda_{qs} i_{ds}) \quad (3.57)$$

3.4 WIND TURBINE MODEL

A wind turbine is characterized by its power-speed characteristics. The wind turbine rotor, which extracts the energy from the wind and converts it into mechanical power, is a complex aerodynamic system [23-24]. For state of art modeling of the rotor using blade element theory have number of drawbacks. These drawbacks are listed below.

- Instead of only one wind speed signal, an array of wind speed signals has to be applied.
- Detailed information about the rotor geometry should be available.
- Computations become complicated and lengthy

To solve these problems, a simplified way of modeling the wind turbine rotor is normally used when the electrical behavior of the system is the main point of interest. An algebraic relation between wind speed and mechanical power extracted is assumed, which is described by the following equation:

$$P_m = 0.5 \cdot C_p(\lambda_i, \beta) \cdot \rho \cdot A \cdot v^3 \quad (3.58)$$

Where

P_m is the power extracted from the wind [W];

λ_i is tip speed ratio;

β is blade pitch angle;

ρ is the air density [Kg/m³];

A is the area covered by the wind turbine rotor blades [m²];

C_p is the power coefficient and is given by

$$C_p = 0.5176 \left(\frac{116}{\lambda_i} - 0.04 \beta - 5 \right) e^{\frac{-21}{\lambda_i}} + 0.0068 \quad (3.59)$$

Where

$$\lambda_t = \frac{1}{\frac{1}{\lambda + 0.08 \beta} - \frac{0.035}{\beta^3 + 1}} \quad (3.60)$$

And

$$= \frac{V}{v} = \frac{R \omega r}{v} \quad (3.61)$$

where

β is pitch angle

v is the wind speed [m/sec]

V is velocity of rotor tip [m/sec]

$r = 2$ f is the angular velocity [radians/sec]

f is frequency of rotation [Hz]

R is length of rotor blade.

3.5 DYNAMIC MODEL OF SYSTEMS

The dynamic behavior of grid connected induction generator is studied for the following to configurations.

1. Induction generator connected to grid.
2. Induction generator with local load and shunt capacitor connected to grid.

The dynamic models of these configurations are derived to simulate various transient conditions [19]. The grid is represented as a source of constant voltage and constant frequency i.e. an infinite bus. The transmission line is considered as transposed line and is represented as transposed line and is represented by a lumped resistance and inductance. The local load is also assumed to be constant impedance.

The dynamic models for the analysis of grid connected configuration under balanced terminal conditions are derived in d-q variables in synchronously rotating reference frame.

3.5.1 INDUCTION GENERATOR CONNECTED TO GRID

The schematic diagram of induction generator connected to infinite bus via a short transmission line is shown in Fig. 3.5. The schematic diagram is like two bus configuration in which local bus, to which generator is connected, is connected to an infinite bus through a transmission line [19]. The change in prime mover input to generator is reflected as the change in generated current and so the injected current to infinite bus through transmission line.

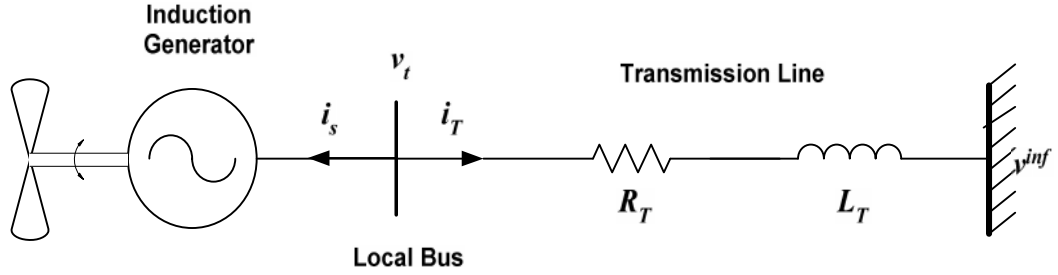


Figure 3.6 Induction generator connected to grid

The induction machine model in motoring mode is given by eq. (3.53) and eq. (3.54). Using these equations induction machine can be modelled as generator by changing the direction of stator current [18].

$$v_{qs} = -r_s i_{qs} + \omega_e (-L_{ls} i_{ds} + L_m (-i_{ds} + i_{dr})) + p (-L_{ls} i_{qs} + L_m (-i_{qs} + i_{qr})) \quad (3.62)$$

$$v_{ds} = -r_s i_{ds} - \omega_e (-L_{ls} i_{qs} + L_m (-i_{qs} + i_{qr})) + p (-L_{ls} i_{ds} + L_m (-i_{ds} + i_{dr})) \quad (3.63)$$

$$v_{qr} = r_r i_{qr} + (\omega_e - \omega_r) (L_{lr} i_{dr} + L_m (-i_{ds} + i_{dr})) + p (L_{lr} i_{qr} + L_m (-i_{qs} + i_{qr})) \quad (3.64)$$

$$v_{dr} = r_r i_{dr} - (\omega_e - \omega_r) (L_{lr} i_{qr} + L_m (-i_{qs} + i_{qr})) + p (L_{lr} i_{dr} + L_m (-i_{ds} + i_{dr})) \quad (3.65)$$

$$p\omega_r = \left(\frac{p}{2J}\right) (T_L - T_e) \quad (3.66)$$

In general these induction generator equations can be written in differential form as-

$$p[i] = [L]^{-1} \{[v] - [R][i] - [G][i]\} \quad (3.67)$$

where

$$v = [v_{qt} \quad v_{dt} \quad 0 \quad 0]^T \quad (3.68)$$

$$i^{sys} = [i_{qs} \quad i_{ds} \quad i_{qr} \quad i_{dr}]^T \quad (3.69)$$

$$L^{sys} = \begin{bmatrix} L_S & 0 & L_M & 0 \\ 0 & L_S & 0 & L_M \\ L_M & 0 & L_r & 0 \\ 0 & L_M & 0 & L_r \end{bmatrix} \quad (3.70)$$

$$G^{sys} = \begin{bmatrix} 0 & \omega_e L_S & 0 & \omega_e L_M \\ -\omega_e L_S & 0 & -\omega_e L_M & 0 \\ 0 & (\omega_e - \omega_r) L_M & 0 & (\omega_e - \omega_r) L_r \\ -(\omega_e - \omega_r) L_M & 0 & -(\omega_e - \omega_r) L_r & 0 \end{bmatrix} \quad (3.71)$$

A transmission line having impedance $Z_T (R_T + jX_T)$ and injecting current i_T into infinite bus is considered between the induction generator and infinite bus. The transmission line equations in synchronous reference frame are written as

$$\left. \begin{aligned} v_{qt} &= v_q^{inf} + R_T i_{qT} + \omega_s L_T i_{dT} + L_T p i_{qT} \\ v_{dt} &= v_d^{inf} + R_T i_{dT} - \omega_s L_T i_{qT} + L_T p i_{dT} \end{aligned} \right\} \quad (3.72)$$

The transmission line current i_T is related to stator current i_s as

$$i_T = -i_s \quad (3.73)$$

The generator bus voltage can be expressed in terms of infinite bus voltage by substituting eq. (3.72) and eq. (3.73) into eq. (3.67). This substitution yields the result as given in following expression.

$$p[i^{sys}] = [L^{sys}]^{-1} \{ [v^{sys}] - [R^{sys}][i^{sys}] - [G^{sys}][i^{sys}] \} \quad (3.74)$$

where

$$v^{sys} = [v_q^{inf} \quad v_d^{inf} \quad 0 \quad 0]^T \quad (3.75)$$

$$i^{sys} = [i_{qs} \quad i_{ds} \quad i_{qr} \quad i_{dr}]^T \quad (3.76)$$

$$L^{sys} = \begin{bmatrix} L_S + L_T & 0 & L_M & 0 \\ 0 & L_S + L_T & 0 & L_M \\ L_M & 0 & L_r & 0 \\ 0 & L_M & 0 & L_r \end{bmatrix} \quad (3.77)$$

$$G^{sys} = \begin{bmatrix} 0 & \omega_e(L_S + L_T) & 0 & \omega_e L_M \\ -\omega_e(L_S + L_T) & 0 & -\omega_e L_M & 0 \\ 0 & (\omega_e - \omega_r)L_M & 0 & (\omega_e - \omega_r)L_r \\ -(\omega_e - \omega_r)L_M & 0 & -(\omega_e - \omega_r)L_r & 0 \end{bmatrix} \quad (3.78)$$

From above discussion we can conclude that dynamic behavior of this configuration can be described by the differential equations corresponding to variables i_{qs} , i_{ds} , i_{qr} , i_{dr} , ω_r , i_{qT} , i_{dT} , v_{qt} , v_{dt} . These equations can be solved by Runge-Kutta method as give in Appendix A. The step by step algorithm is given below and corresponding flow chat for digital simulation is given in Fig. 3.7.

3.5.2 ALGORITHM FOR DIRECT GRID CONNECTED INDUCTION GENERATOR

1. Read induction machine parameters, grid voltage, short transmission line parameters, wind turbine parameters, wind velocity and time period (t_f) for simulation.
2. Initialize the time $t=0$.
3. Calculate the performance coefficient for wind turbine for varying wind velocity using eq. (3.59) and calculate wind turbine output power using eq. (3.58).
4. Find the voltages in d-q variables using transformation matrix given in eq. (3.1)
5. Find the dynamic model of induction generator in form of differential equations, when connected to grid through transmission line.
6. Solve these differential equations using forth order Runge-Kutta method and find rotor speed, current, flux linkages and torque.
7. Check whether find time is reached or not. If final time is not reached then increase the time by small step Δt and go to step 3 and repeat. Otherwise plot the results. if $t < t_f$

$$t = t + \Delta t$$

8. Stop

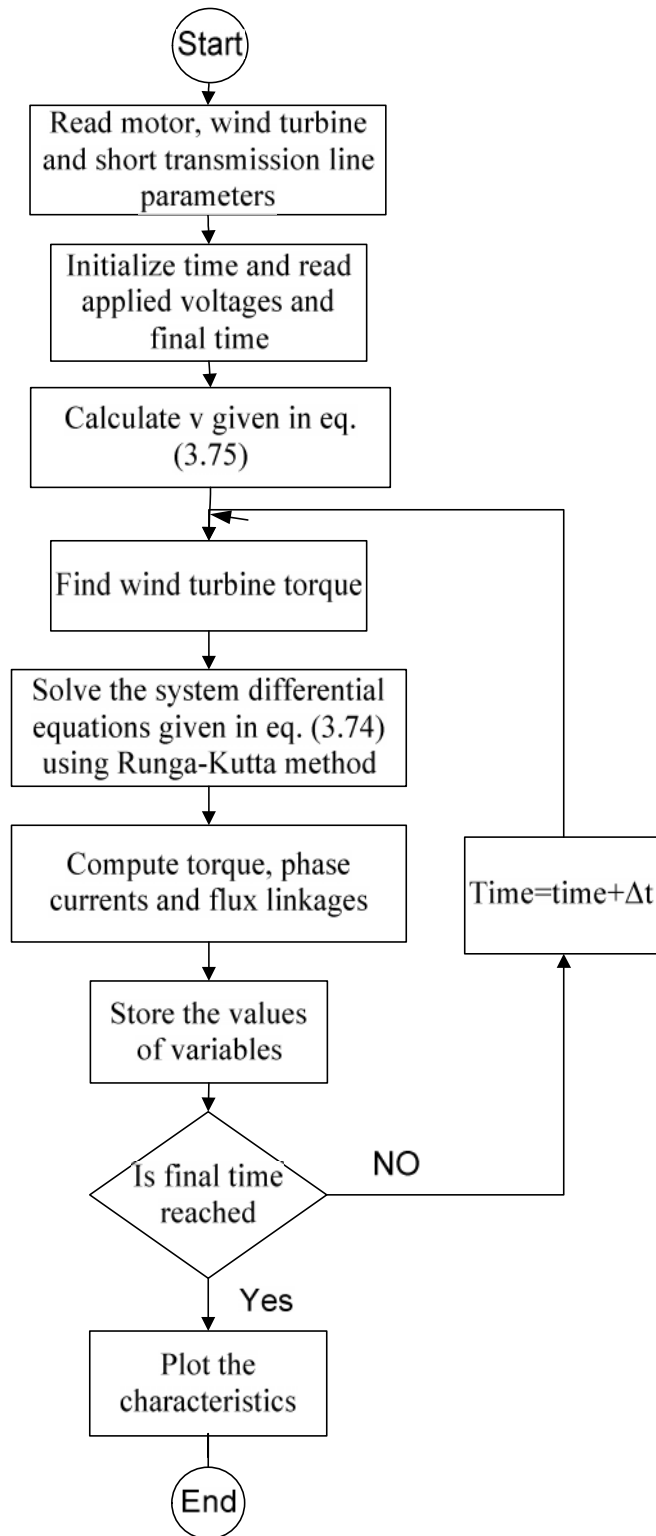


Figure 3.7 Flow chart for digital simulation of grid connected induction machine

3.5.3 DYNAMIC MODEL OF INDUCTION GENERATOR WITH LOCAL LOAD AND SHUNT CAPACITOR CONNECTED TO GRID

In last section we have discussed induction generator connected to grid without any load and capacitor. In this case induction generator variables have attained steady state values after small time. After this a local load and a capacitor is connected to local bus which is connected to infinite bus via a short transmission line. The schematic diagram of this configuration is shown in Fig. 3. The shunt capacitor will govern the local bus voltage, whereas in previous configuration, the local bus voltage is expressed in terms of infinite bus voltage and voltage drop across the transmission line. The performance of this configuration is affected by the change in load and shunt capacitor.

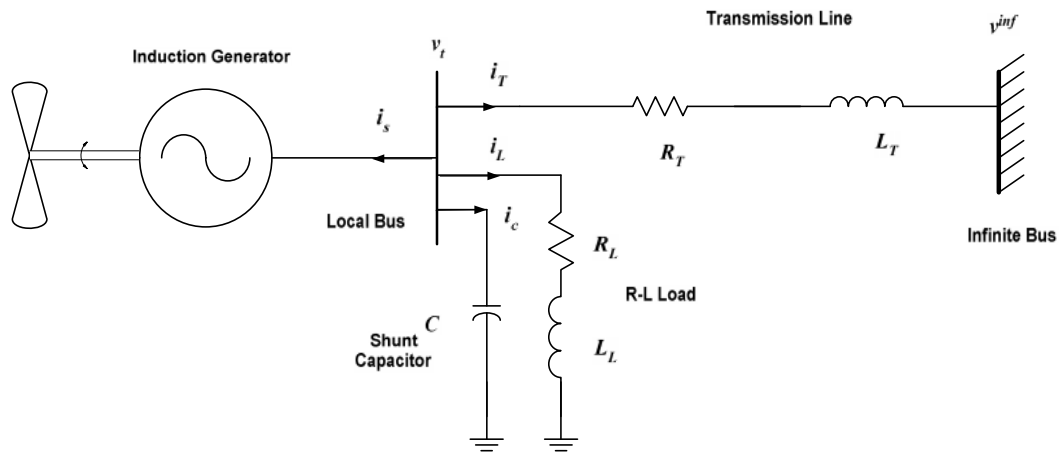


Figure 3.8 Schematic diagram of induction generator with local load and shunt capacitor

Equations of induction generator and transmission line are written as equation 3. The equations for constant impedance load $Z_L (R_L + jX_L)$ connected at local bus are

$$\left. \begin{aligned} v_{qt} &= R_L i_{qL} + \omega_e L_L i_{dL} + L_L p i_{qL} \\ v_{dt} &= R_L i_{dL} - \omega_e L_L i_{qL} + L_L p i_{dL} \end{aligned} \right\} \quad (3.79)$$

When capacitor is connected then the equations of capacitor currents in d-q variables can be written as-

$$i_{qc} = \omega_e C v_{dt} + C p v_{qt} \quad (3.81)$$

$$i_{dc} = \omega_e C v_{qt} + C p v_{dt} \quad (3.82)$$

Capacitor current can be expressed in terms of generator, load and transmission line currents

$$i_c = -(i_T + i_s + i_L) \quad (3.83)$$

The dynamic behavior of this configuration can be described by the differential equations corresponding to variables $i_{qs}, i_{ds}, i_{qr}, i_{dr}, \omega_r, i_{qT}, i_{dT}, i_{qL}, i_{dL}, v_q^{LB}, v_d^{LB}$. These equations are expressed in state variable form as

$$\begin{aligned} p[i] &= [L]^{-1} \{ [V] - [R][i] - [G][i] \} \\ p\omega_r &= \left(\frac{P}{2J} \right) (T_L - T_e) \\ pi_{qT} &= [v_{qt} - v_q^{inf} - R_T i_{qT} - \omega_s L_T i_{dT}] / L_T \\ pi_{dT} &= [v_{dt} - v_d^{inf} - R_T i_{dT} - \omega_s L_T i_{qT}] / L_T \\ pi_{qL} &= [v_{qt} - R_L i_{qL} - \omega_e L_L i_{dL}] / L_L \\ pi_{dL} &= [v_{dt} - R_L i_{dL} - \omega_e L_L i_{qL}] / L_L \\ pv_{qt} &= [i_{qc} - \omega_e C v_d^{LB}] / C \\ pv_{dt} &= [i_{dc} + \omega_e C v_q^{LB}] / C \end{aligned} \quad (3.84)$$

These differential equations are solved by Runge-Kutta fourth order method of integration given in Appendix A. The flow chart for digital simulation is shown in Fig. 3.9.

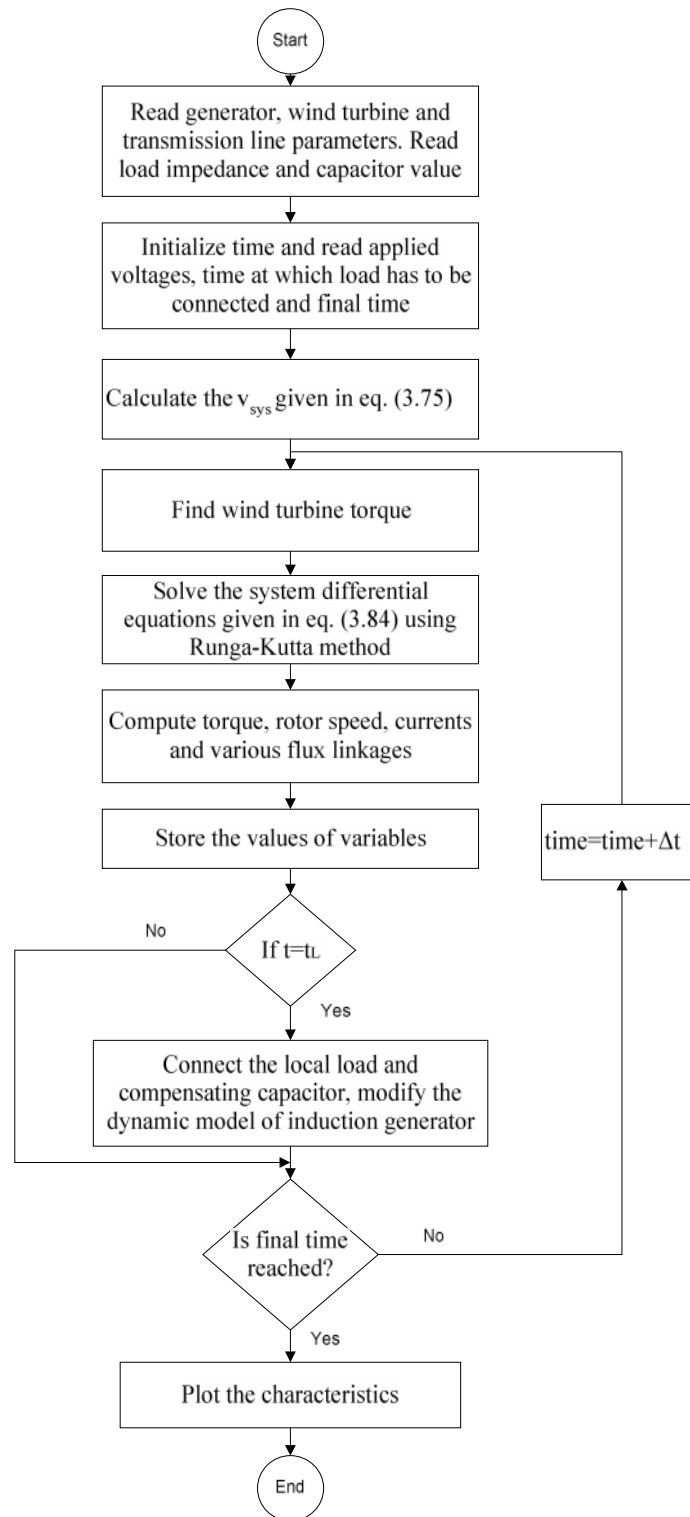


Figure 3.9 Flow chart for simulation of induction generator connected with local load

3.5.4 ALGORITHM FOR INDUCTION GENERATOR WITH LOCAL LOAD AND CAPACITOR

1. Read induction machine parameters, grid voltage, short transmission line parameters, local load impedance, compensating capacitor value, wind turbine parameters wind velocity, time when load has to connected (t_L) and time period (t_f) for simulation.
2. Initialize the time $t=0$
3. Find the voltages in d-q variables using transformation matrix given in eq. (3.1)
4. Find the dynamic model of induction generator in form of differential equations, when connected to grid through transmission line.
5. Calculate the performance coefficient for wind turbine for varying wind velocity using eq. (3.59) and calculate wind turbine output power using eq. (3.58).
6. Solve these differential equations using forth order Runge-Kutta method and find rotor speed, current, flux linkages and torque.
7. Check the time if $t=t_L$ then connect the local load and compensating capacitor otherwise go to step 9.
8. Modify the induction generator model equations according to new configuration and go to step 5.
9. Check whether final time is reached or not. If final time is not reached then increase the time by small step Δt and go to step 5 and repeat. Otherwise display the results.

if $t < t_f$

$t=t+\Delta t$

10. Stop

RESULTS AND DISCUSSIONS

The performance of the grid connected induction generator (IG) driven by constant speed prime mover and wind turbine has been studied. The wind turbine has been simulated by different speed time characteristics. The effects of various parameters like prime mover speed, transmission line parameters, compensation by shunt capacitors of different values, change in local load etc. have been studied. The study has been carried out on the 3 hp, 220V, 4 pole, 60 Hz, 3 phase induction machine [21] whose parameters are as $r_s=0.435$, $X_{ls}=0.754$, $X_M=26.13$, $X_{lr}=0.754$, $r_r=0.816$, $J=0.089$. The free accelerating characteristics of induction machine in motoring mode are shown in the Appendix-B, are matching with the characteristics given in [21].

4.1 DIRECT GRID CONNECTION OF INDUCTION GENERATOR

Induction generator is connected to grid through a short transmission line as shown in Fig.3.6. The induction generator can be driven by a constant speed prime mover or through wind turbine having unpredicted speed varying with time. The performance of induction generator is studied for change in initial speed, transmission line resistance and reactance.

4.1.1 INDUCTION GENERATOR DRIVEN BY CONSTANT SPEED PRIME MOVER

The induction generator (IG) driven at synchronous speed is connected to grid via a transmission line ($R_T=0.117$, $X_T=1.424$). The corresponding performance characteristics are shown in Fig. 4.1 to Fig. 4.5. At the grid connection, the transients are experienced in currents and torque which are settling down to steady value after 0.25 sec. These transients are shown in Fig. 4.1 indicating d-q axis currents of stator and rotor. The variation of stator currents in phase variables with time are shown in Fig. 4.2. The phase currents are the measurable parameters. In synchronous reference frame, these currents are the reflection of change in q-axis and d-axis stator current and not the speed of rotor.

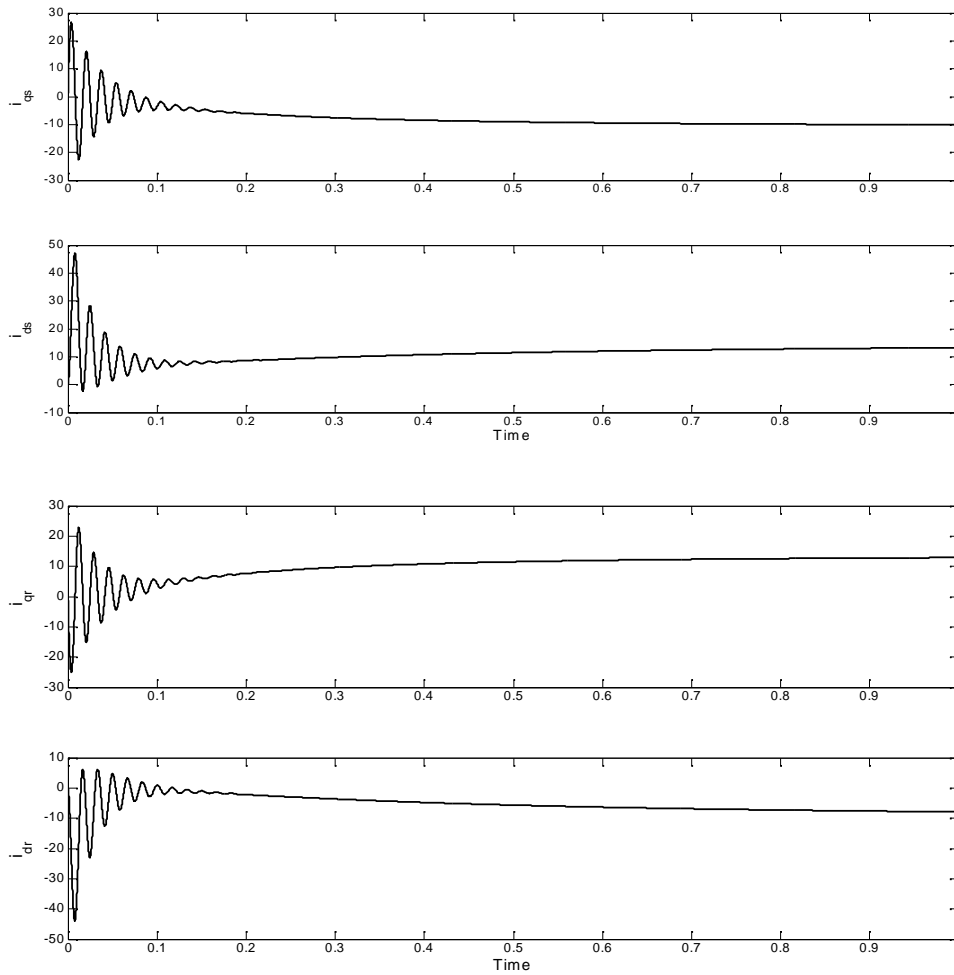


Figure 4.1 d-q axis currents during grid connection of induction generator

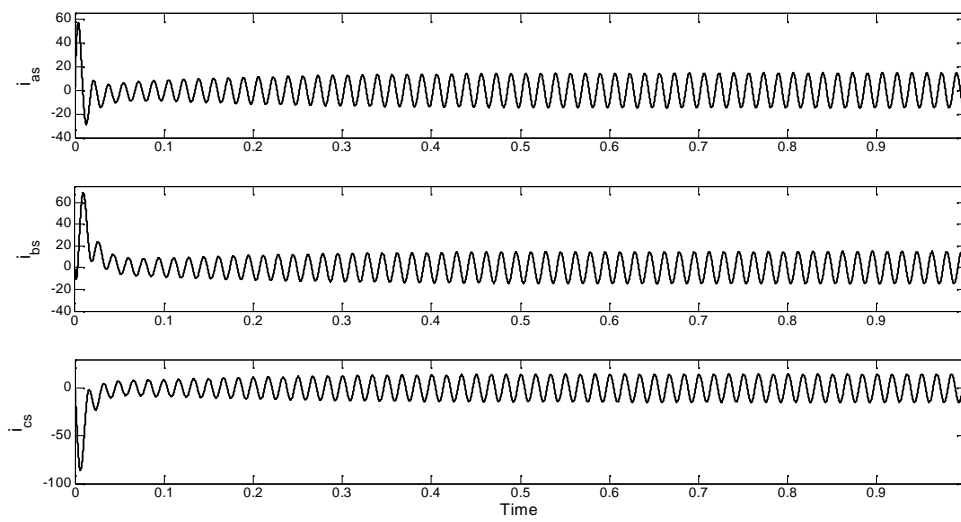


Figure 4.2 Stator currents of grid connected induction generator in phase variables

The speed time characteristics are shown in Fig.4.3. The speed drops slightly when generator is started and goes above synchronous speed because induction machine works as generator at super-synchronous speed. After a short time generator speed becomes constant. The torque and torque speed characteristics are shown in Fig. 4.4 and Fig. 4.5 respectively. After initial transients of less than 0.1 sec, torque approaches to 10 Nm due to the initial value of prime mover input torque is 10 Nm. These transients are due to the fact that induction generator draws magnetizing current from grid.

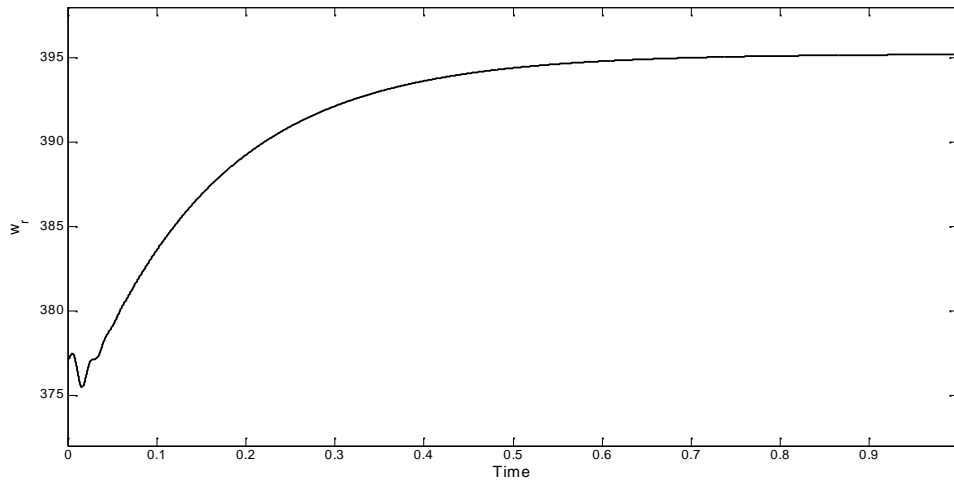


Figure 4.3 Speed-Time characteristics of grid connected induction generator

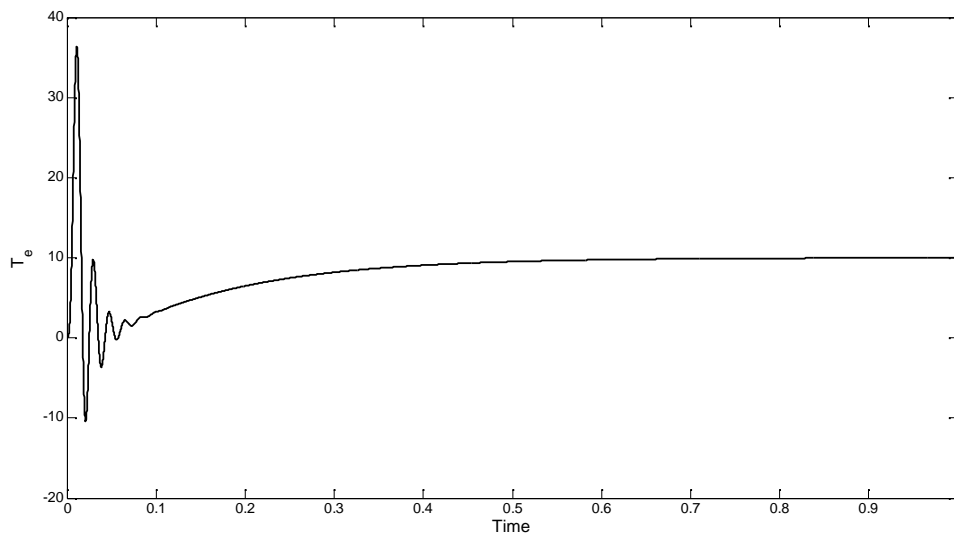


Figure 4.4 Torque-Time characteristics of grid connected induction generator

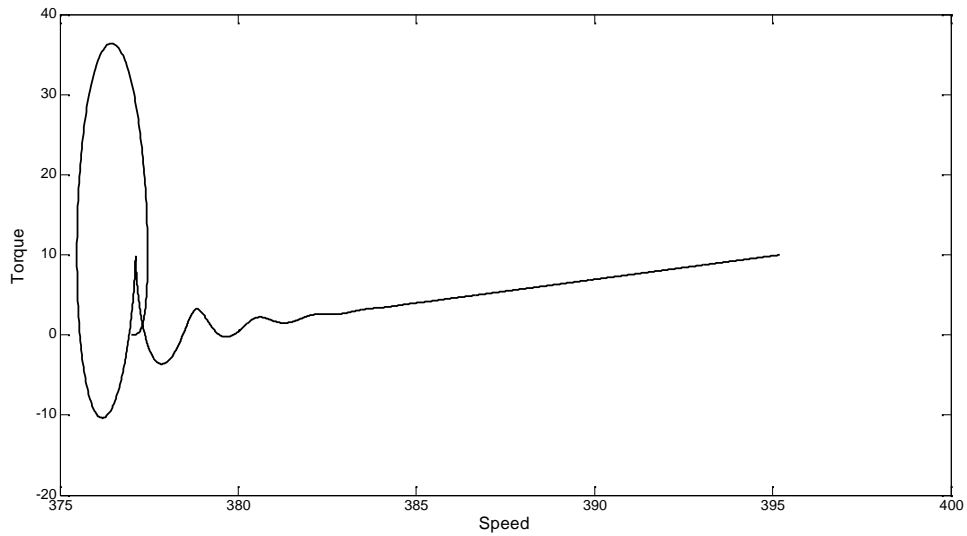


Figure 4.5 Torque-Speed characteristics of direct grid connected induction generator

(i) EFFECT OF CHANGE IN INITIAL SPEED

The transients during the connection of generator to grid are affected by the speed of prime mover. To observe the performance at different prime mover speed, generator is started at speed 5% below and 5% above the synchronous speed and variations in variables are compared with different speeds as shown in Fig. 4.6 to Fig. 4.9.

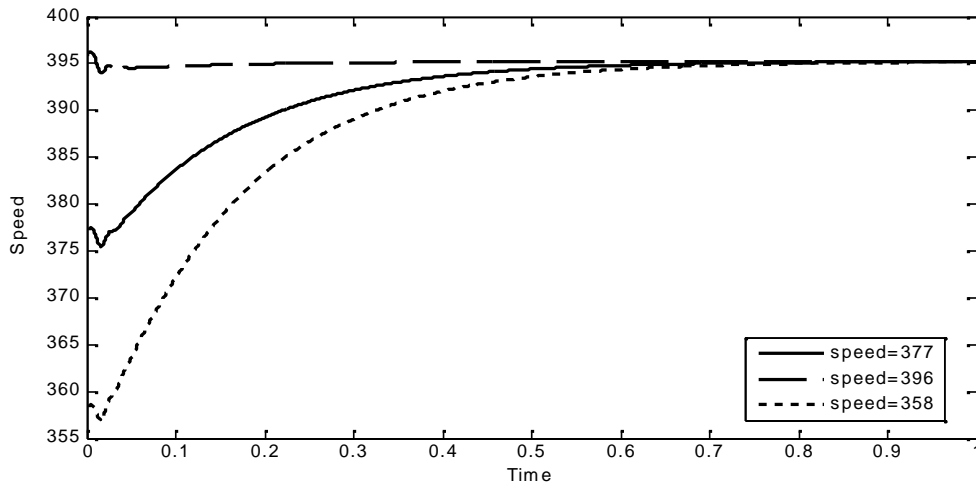


Figure 4.6 Speed-Time characteristics of IG for different starting speeds.

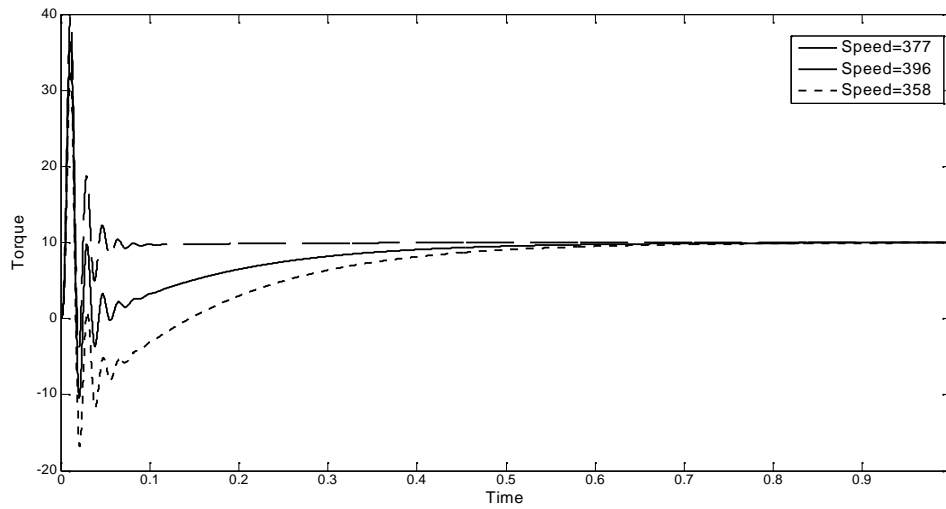


Figure 4.7 Torque-Time characteristics for GCIG with different starting speeds

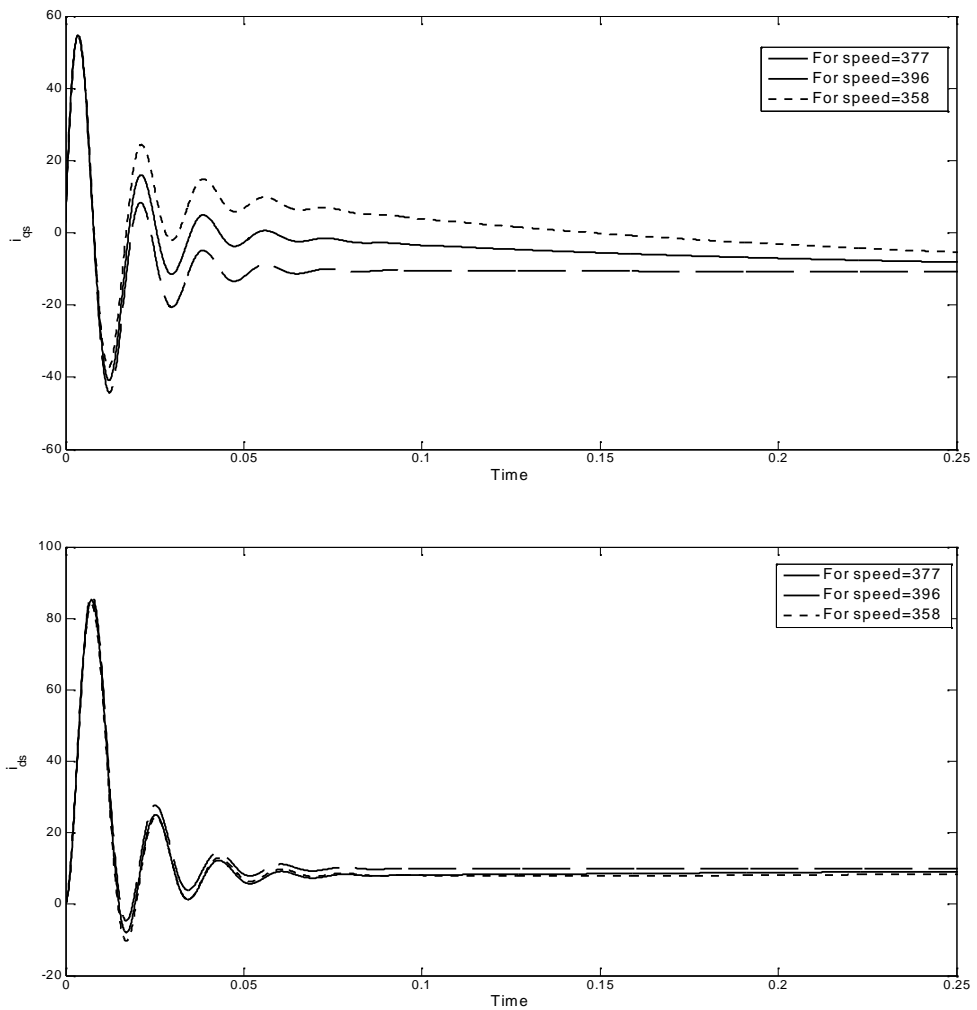


Figure 4.8 Stator currents of grid connected IG for different starting speeds

Fig. 4.6 shows speed-time characteristics of induction generator for different starting speeds. Though starting speed is different in all three cases yet generator attains a same steady speed. Generator when started with speed below synchronous speed, the torque developed is negative and after the generator picks up speed above synchronous speed it becomes positive. Steady value of torque is resulted as same irrespective of the initial speed. The torque-time characteristics are shown in Fig.4.7

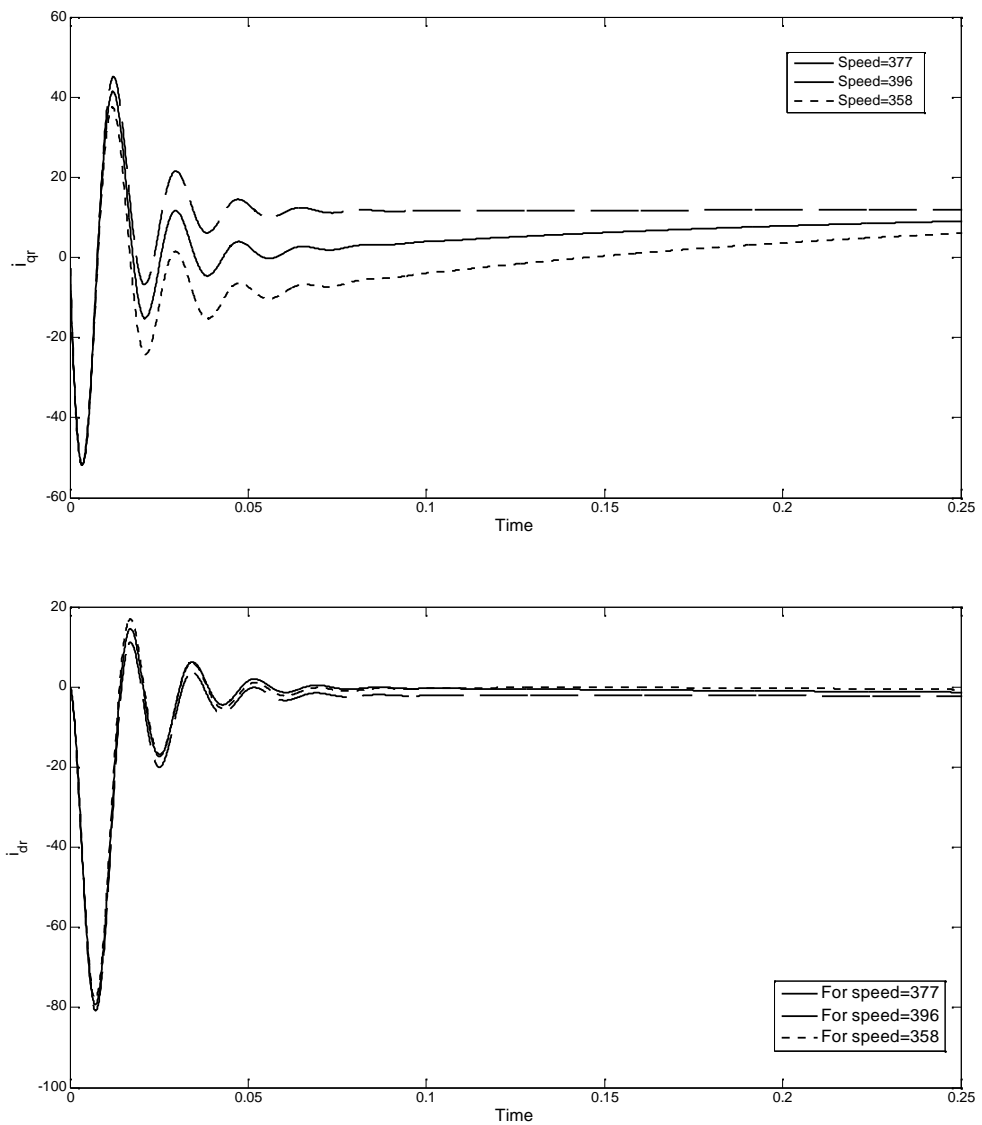


Figure 4.9 Rotor currents of grid connected IG for different starting speeds

The large transients are experienced in currents when generator is started with speed apart from the synchronous speed which has been damped out after transient time. The stator and rotor currents of IG are shown in Fig. 4.8 and Fig. 4.9 respectively.

(ii) CHANGE IN TRANSMISSION LINE PARAMETERS

The response of grid connected induction generator is dependent on the transmission line parameters. To study the effect of line parameters, the generator is run with different transmission line resistance and reactance and the response of system variables is compared with different values of resistance and reactance.

(a) EFFECT OF CHANGE IN TRANSMISSION LINE RESISTANCE

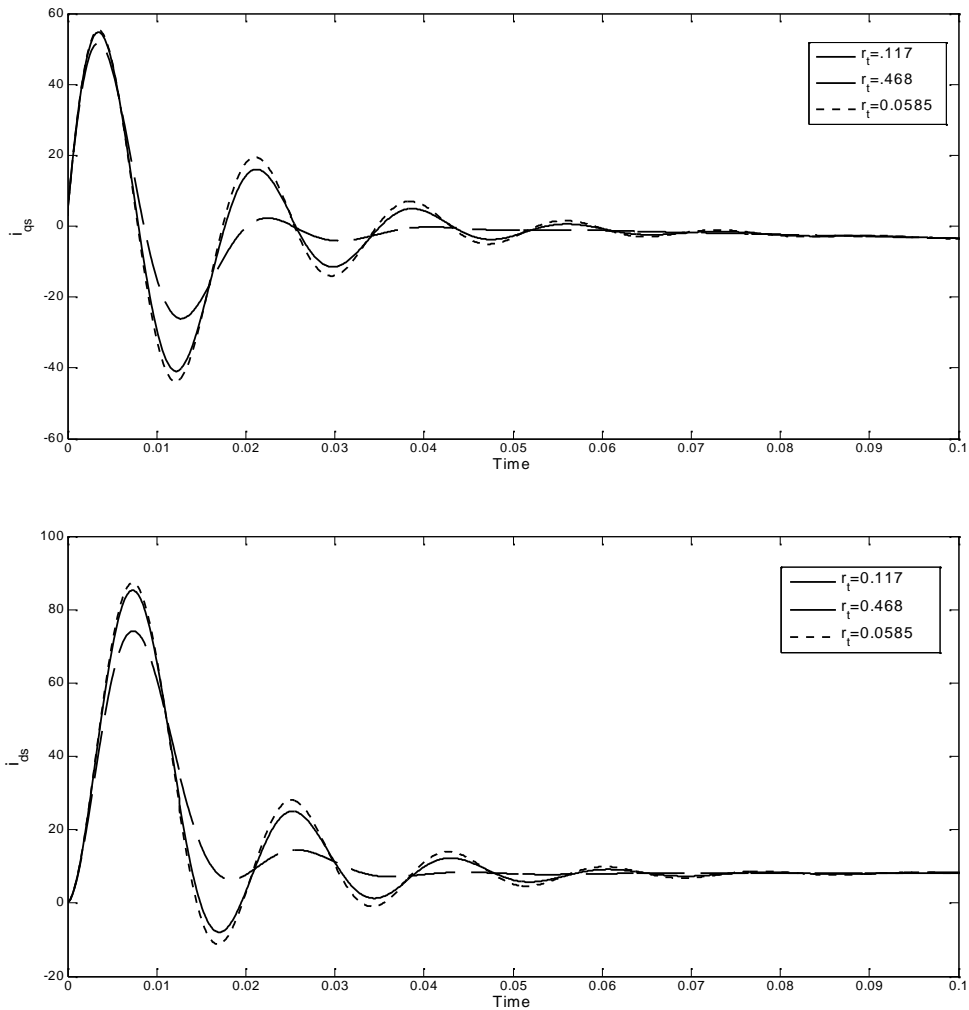


Figure 4.10 Stator currents of grid connected IG with different line resistance

The stator current of grid connected generator with different values of line resistance is shown in Fig. 4.10. There are fewer transients in currents when resistance of transmission line is high. With the increase in transmission line resistance the steady speed of generator is slightly less as compared to low resistance as shown in Fig.4.11. When generator is operated with low resistance, the steady speed is slightly high speed as compared with high resistance.

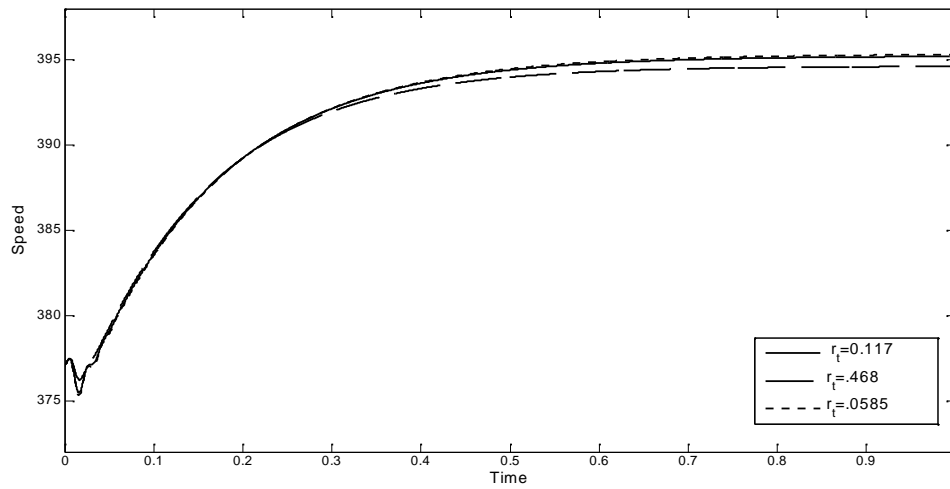


Figure 4.11 Speed-Time characteristics of IG with different transmission line resistance

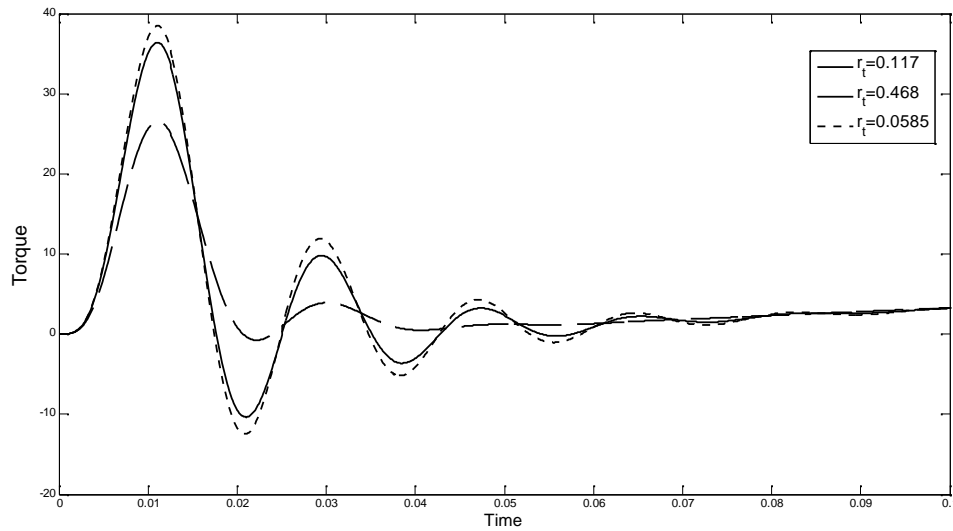


Figure 4.12 Torque-Time characteristics of IG with different transmission line resistance

Torque variation with time for different line resistance is shown in Fig. 4.12. A damping in torque transients has been experienced with increase in line resistance.

(b) EFFECT OF CHANGE IN TRANSMISSION LINE REACTACE

To study the effect of transmission line reactance (X_T) on the performance of induction generator is connected to grid with different value of transmission line reactance. Variations of machine variables with different line reactance are shown in Fig. 4.13 to Fig. 4.15. The stator d-q axis currents of IG are shown in Fig. 4.13. The peak value of transients in currents is reduced with high reactance but the transients are damped out early with low reactance.

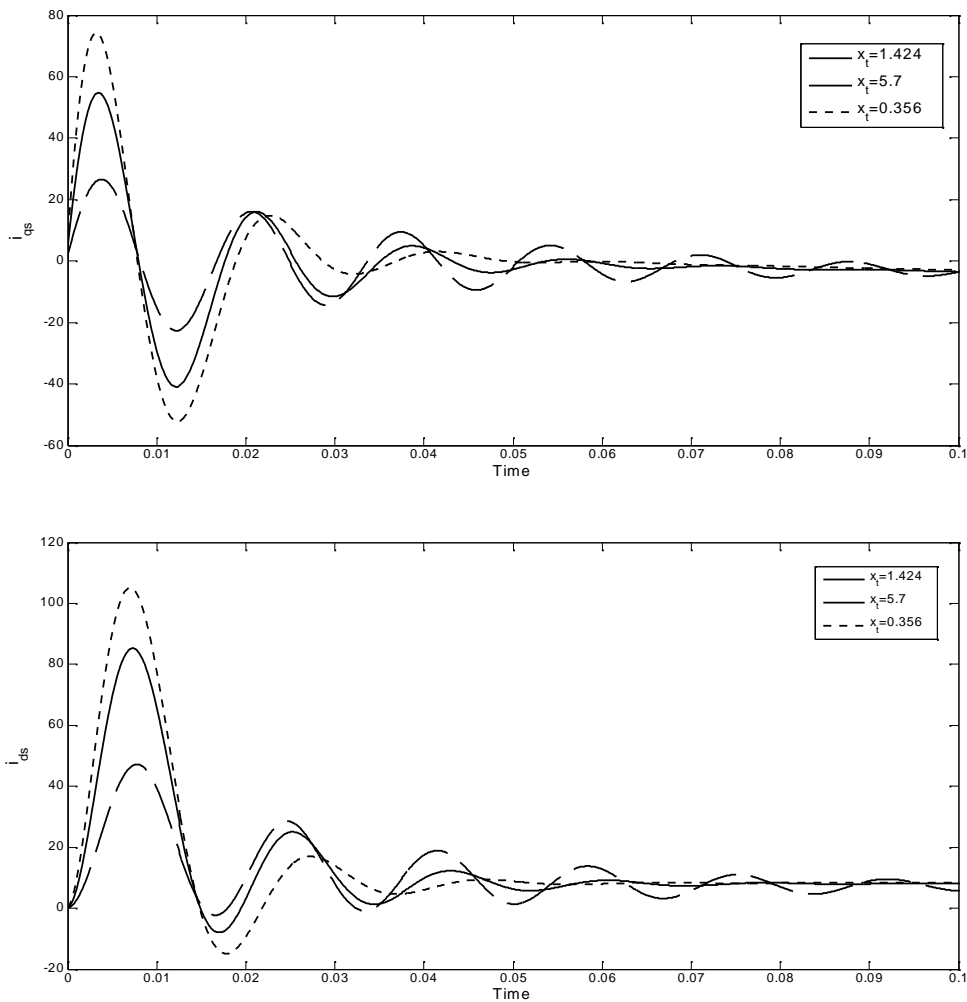


Figure 4.13 Stator currents of IG with different transmission line reactance

With increase in transmission line reactance steady generator speed is more as compared with low reactance. The comparison of speed with different values of reactance is shown in Fig. 4.14. The torque-time characteristics are shown in Fig. 4.15. The peak value of torque transient is reduced with increase in line reactance but with low reactance transients are damped out early.

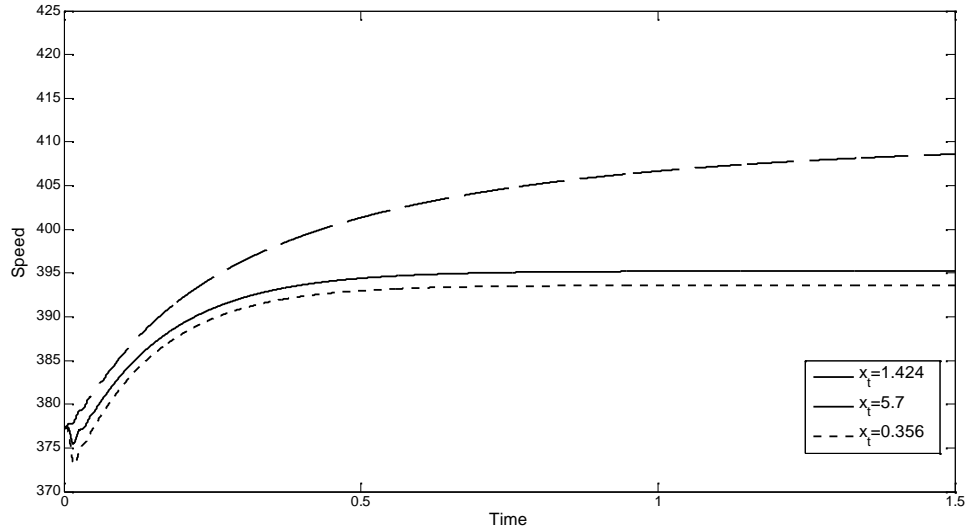


Figure 4.14 Speed-Time characteristics of IG for different transmission line reactance

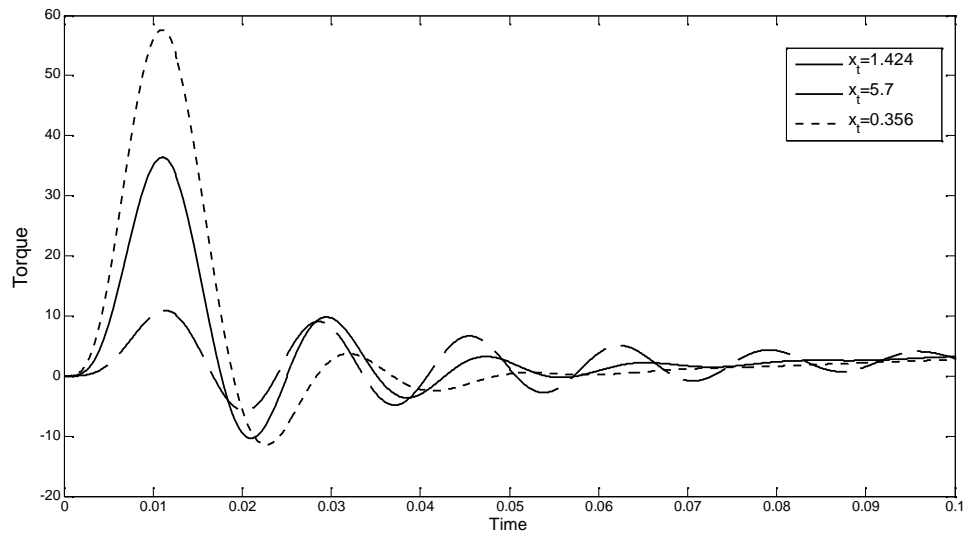


Figure 4.15 Torque-Time characteristics of IG for different transmission line reactance

4.1.2 INDUCTION GENERATOR DRIVEN BY WIND TURBINE

Before discussion on wind driven induction generator it is worth to give wind turbine characteristics model. Power from wind turbine depends on power coefficient (C_p) and cube of wind speed (v) as explained in sec 3.4. The C_p - characteristics are shown in figure 4.26.

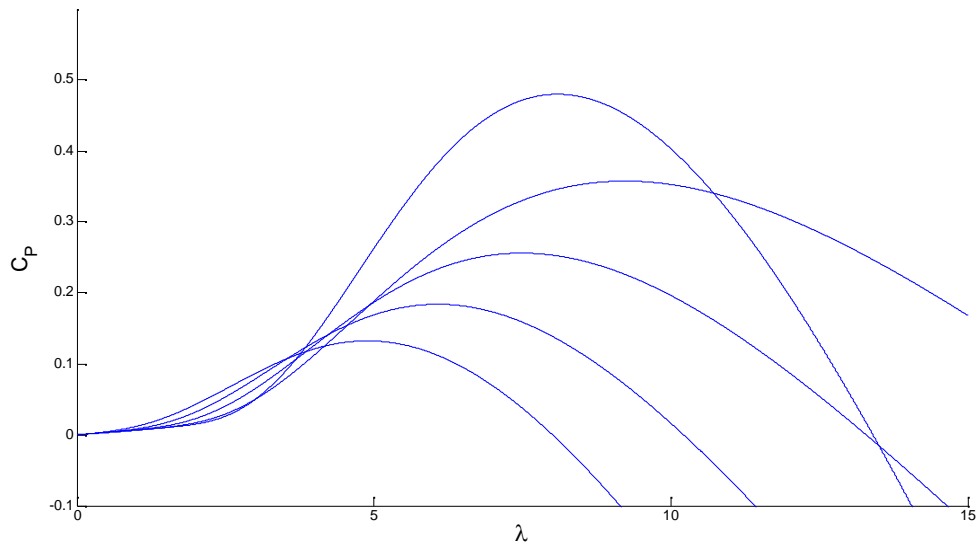


Figure 4.16 C_p - plot for a wind turbine

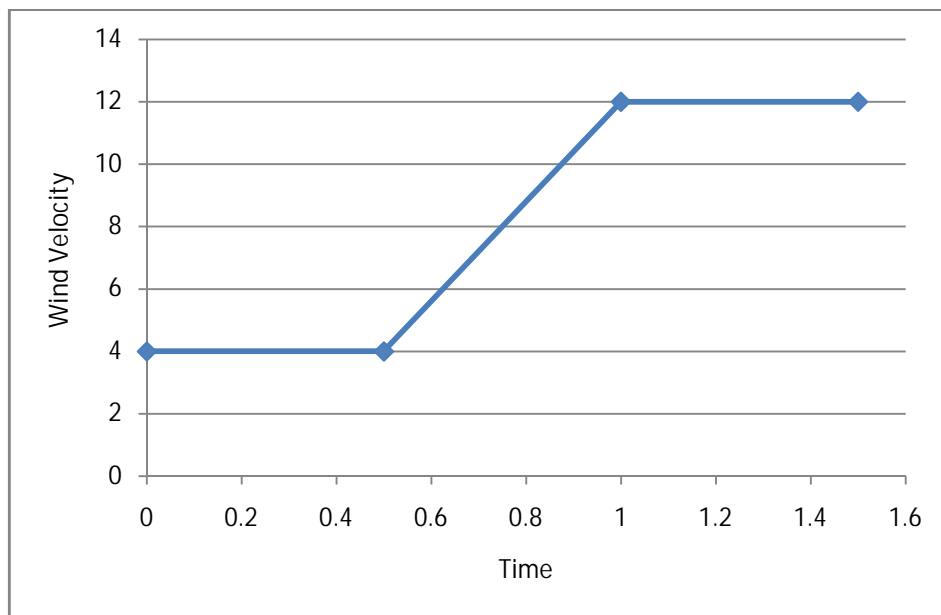


Figure 4.17 Wind speed function I

In sec 4.1.1 induction generator is driven with constant speed prime mover input but in this section generator is driven by wind turbine. In case of wind driven generator, prime mover input is function of wind speed which is variable. Because of the unavailability of continuous wind data we have taken two continuous wind functions. The wind turbine designed in this work, however, can be operated with any wind data. We have taken two wind functions and generator performance is checked with both of these functions. In Fig. 4.17 wind speed function (I) is shown. The generator currents corresponding to this wind speed function are shown in Fig. 4.18. The steady value of current is dependent on the speed of wind at that time. The variation of speed with time is given in Fig. 4.19. Speed does not become stable due to change in prime mover input which is dependent on the wind speed. Torque-time characteristics are shown in Fig. 4.20. The torque value changes continuously with the change in wind turbine outputs.

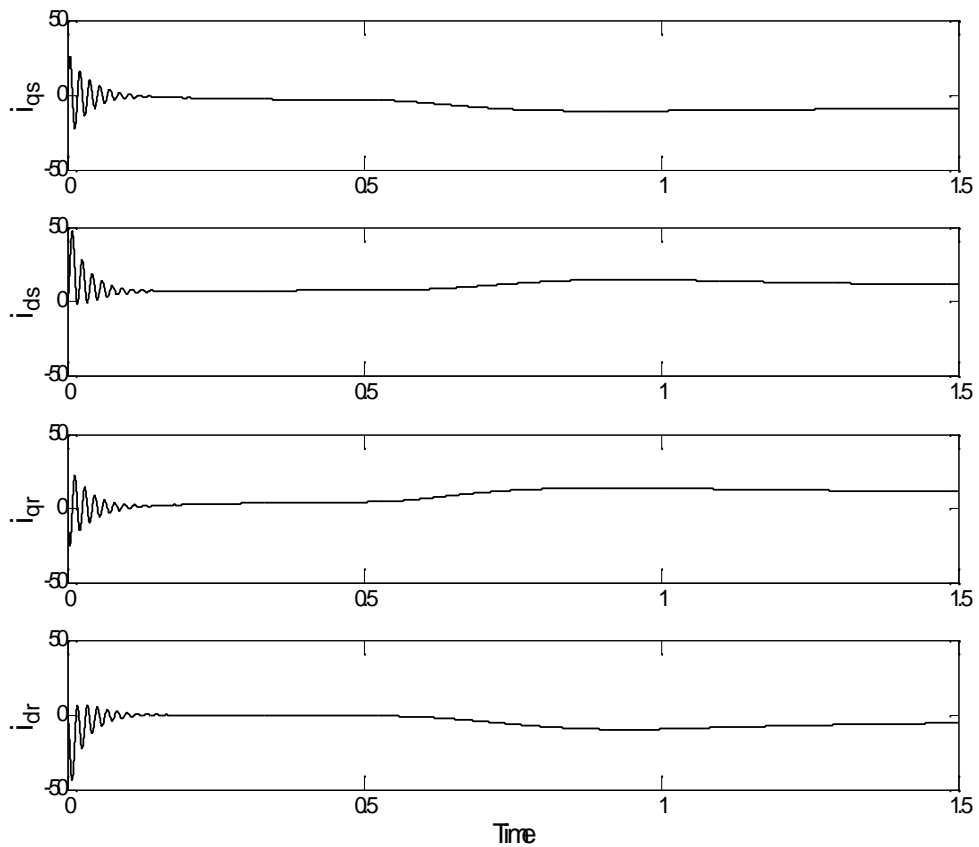


Figure 4.18 Stator and rotor Currents of wind driven IG with speed function I

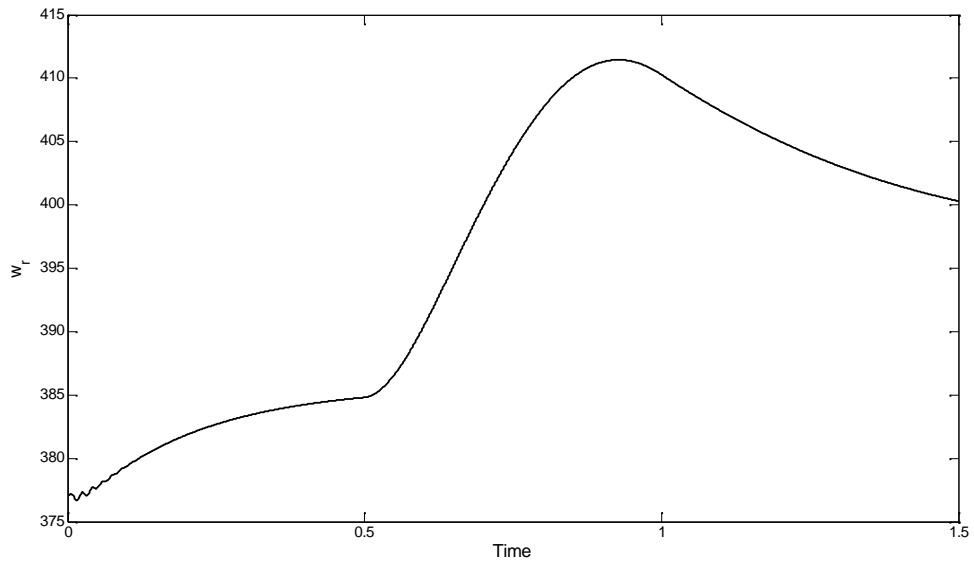


Figure 4.19 Speed-time characteristics of wind driven IG with wind speed function I

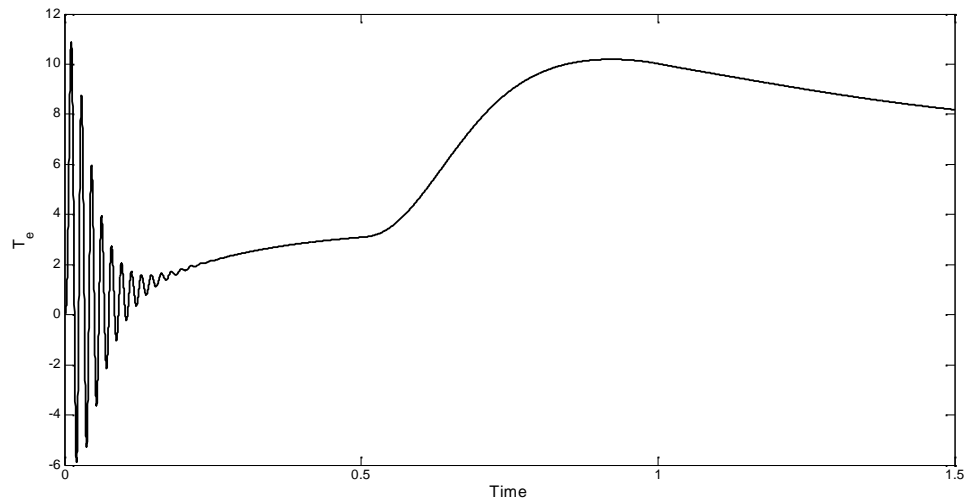


Figure 4.20 Torque-Time characteristics of wind driven IG with wind speed function I

The second wind speed function is shown in Fig. 4.21. The generator currents with this speed function are given in Fig. 4.22 and Fig. 4.23. During the starting, currents of very large peak are resulted. Due to continuous change in wind speed, the changes in currents and torque are resulted accordingly. The speed-time characteristics are shown in Fig.

4.24. The speed starts to build up from its initial synchronous speed but unlike in case of constant prime mover input the speed in this case fluctuates with the change in wind speed. These fluctuation remains for the whole operation of the generator operation.

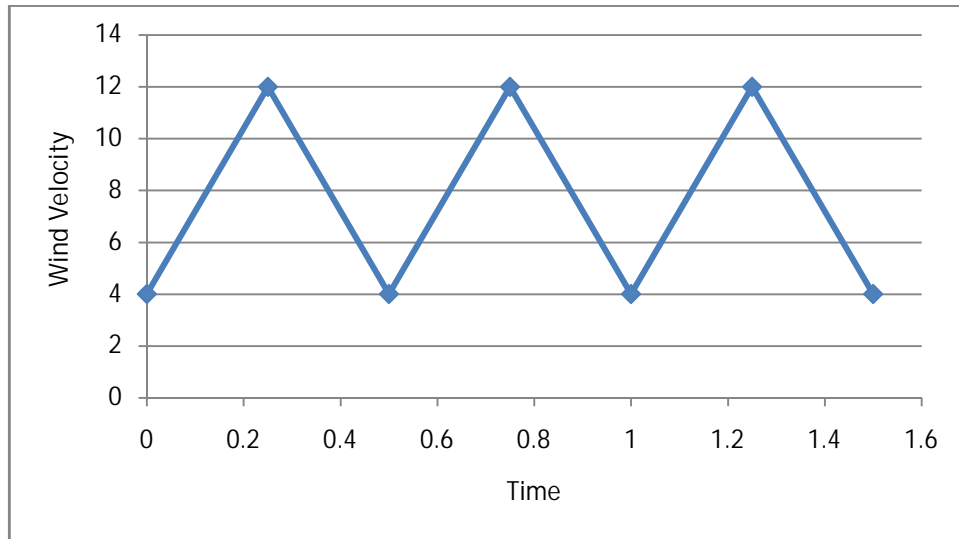


Figure 4.21 wind speed function II

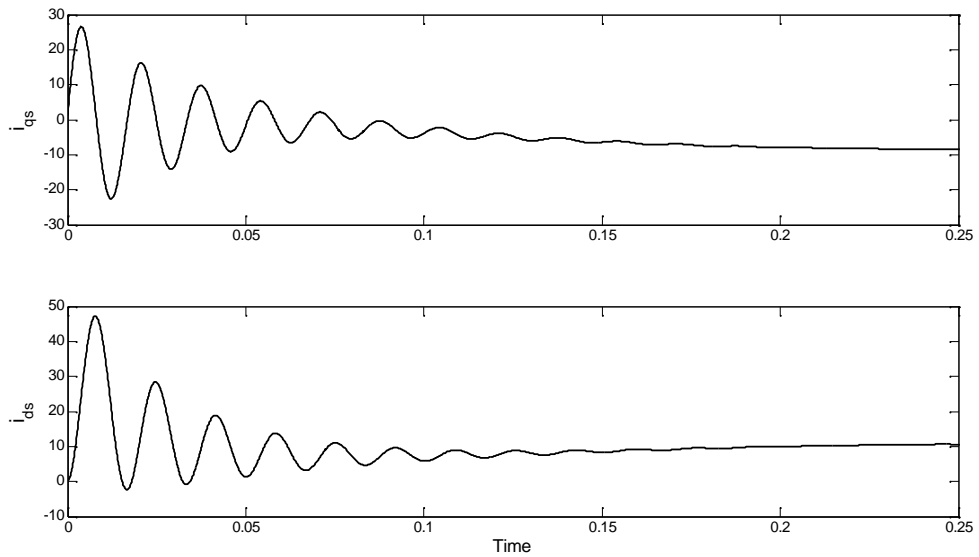


Figure 4.22 Stator Currents of wind driven IG with wind speed function II

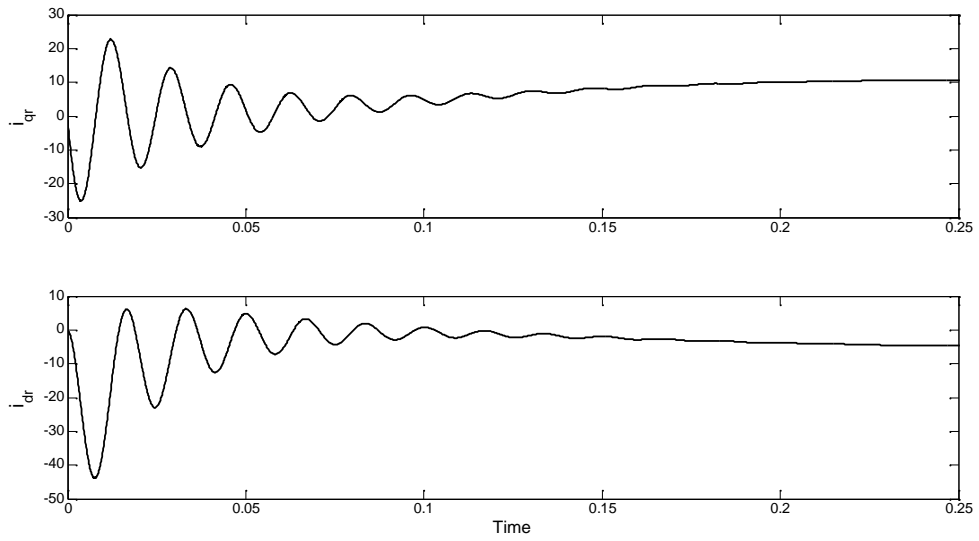


Figure 4.23 Rotor Currents of wind driven IG with wind speed function II

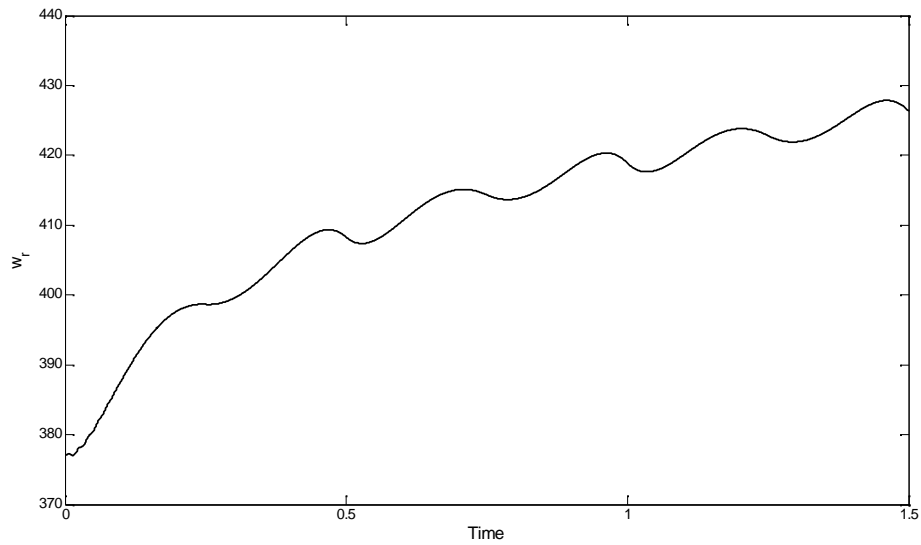


Figure 4.24 Speed-Time characteristics of wind driven IG with wind speed function II

The torque-time characteristics of wind driven generator is shown in Fig. 4.25. There are transients in generator torque during starting. After the transient period the torque vary continuously to match the applied wind turbine torque.

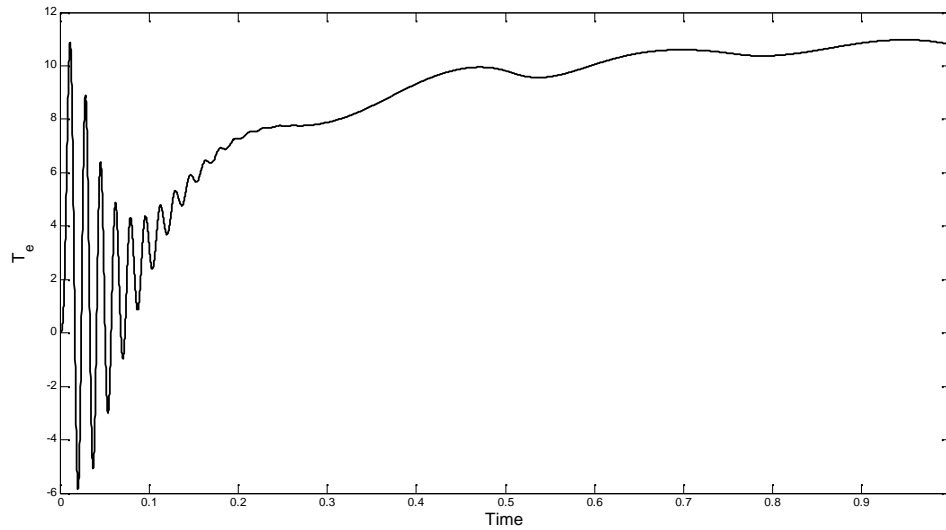


Figure 4.25 Torque-Time characteristics of wind driven IG with wind speed function II

(i) CHANGE IN INITIAL SPEED OF WIND DRIVEN INDUCTION GENERATOR

To compare the change in state variables of wind driven generator, the generator is started with three different speeds of 377, 396 and 358 radians/ sec. The effect of change in prime mover speed on wind driven induction generator variables is shown in Fig. 4.26 to Fig. 4.28.

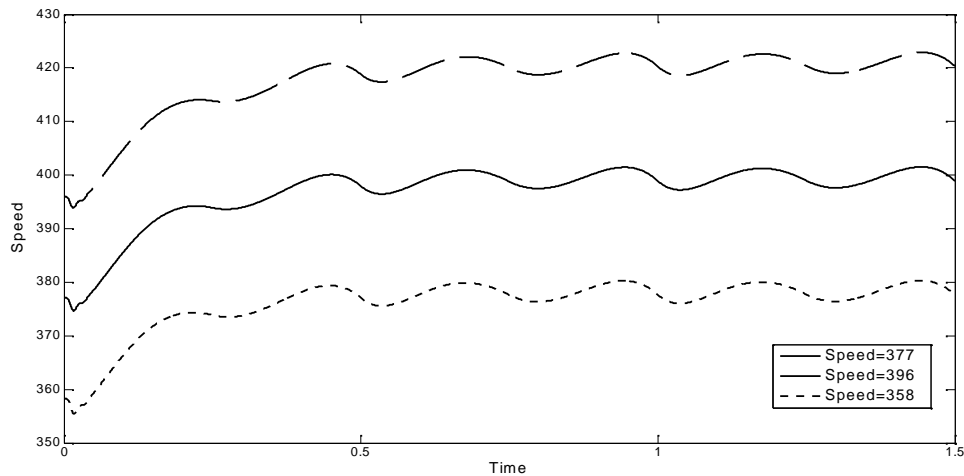


Figure 4.26 Speed-Time characteristics of wind driven IG with different starting speeds

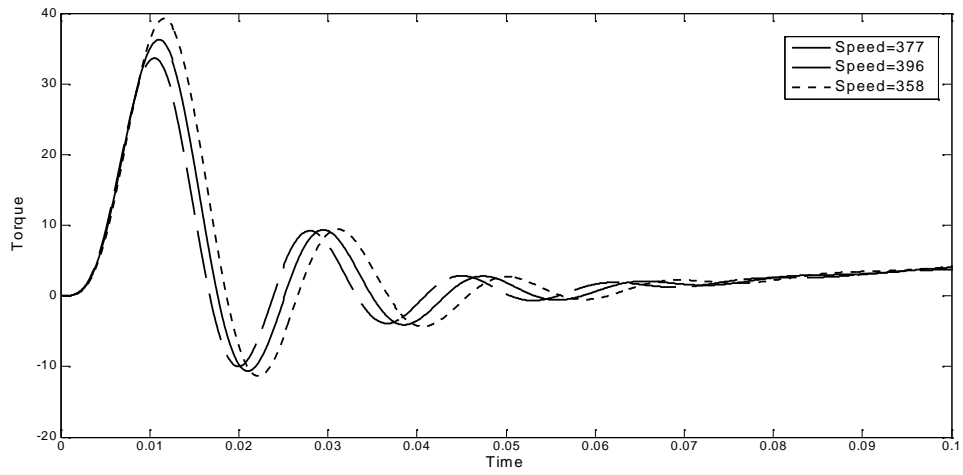


Figure 4.27 Torque-Time characteristics of wind driven IG with different starting speeds

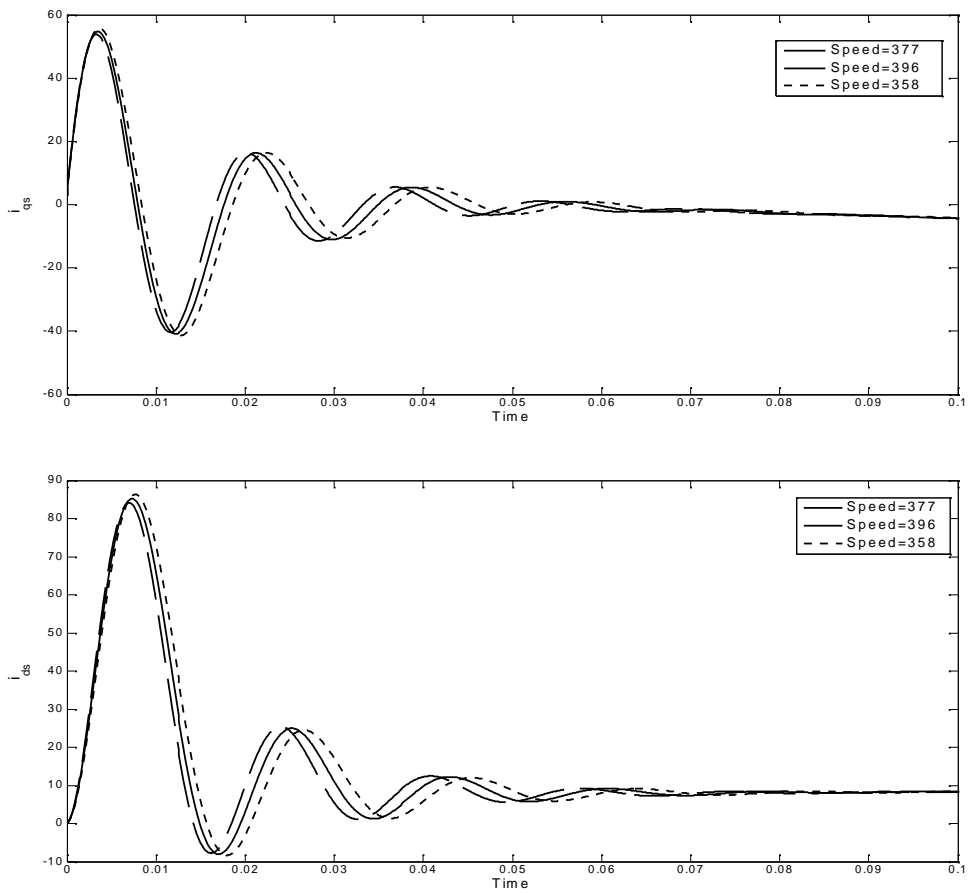


Figure 4.28 Stator currents of wind driven IG with different starting speeds

The variation of speed is shown in Fig. 4.26. In all three cases, after crossing the synchronous speed the speed tends to hover around the respective constant value. Since prime mover torque is not constant, speed varies continuously. Torque-time characteristics are shown in Fig. 4.27. Torque transients are more when generator is started with speed below the synchronous speed. The generator d-q axis stator currents of wind driven generator with different starting speed are shown in Fig. 4.28. When generator is started at speed below the synchronous speed the transients in current are more. The steady state value of currents in all cases is almost same.

(ii) CHANGE IN TRANSMISSION LINE PARAMETERS

To check the performance of wind driven induction generator with change in transmission line parameters the generator is operated with different values of resistance and reactance.

(a) CHANGE IN LINE RESISTANCE

The generator performance is observed with three values of 0.117 , 0.468 and 0.0585 and variations of state variables are compared with these three values of transmission line resistances.

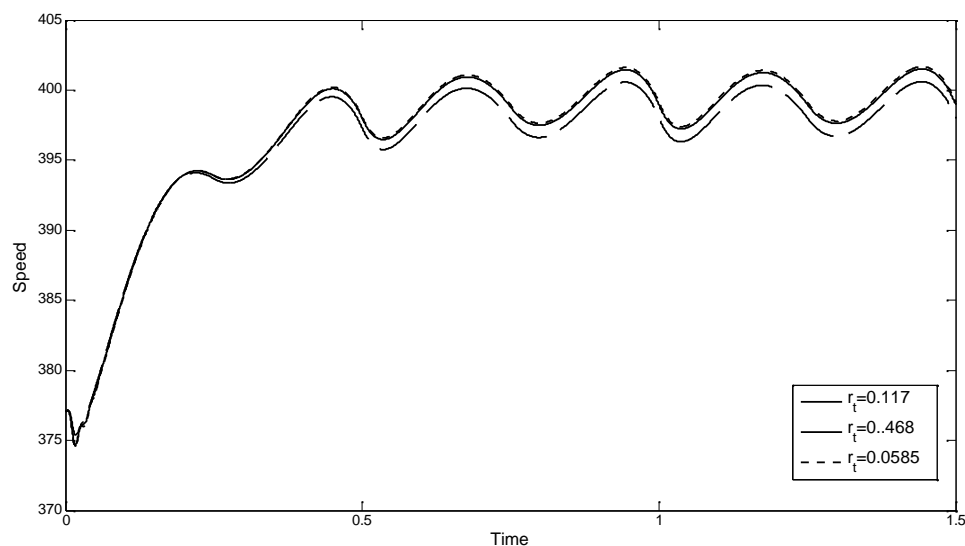


Figure 4.29 Speed-Time characteristics of wind driven IG with different line resistance

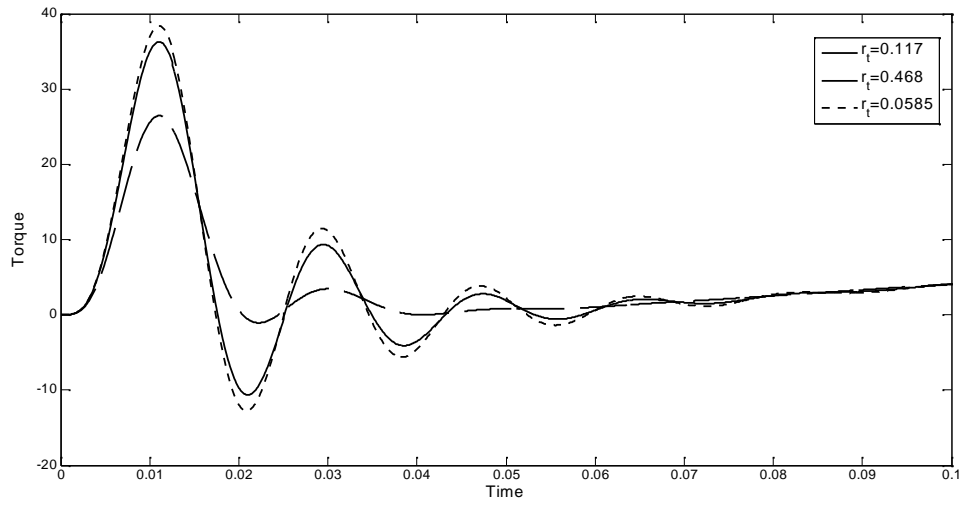


Figure 4.30 Torque-Time characteristics of wind driven IG with different line resistance

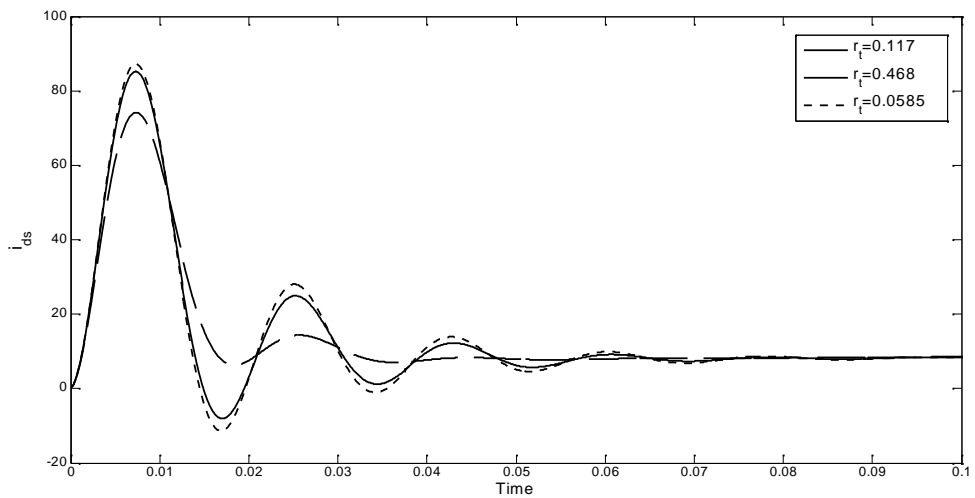
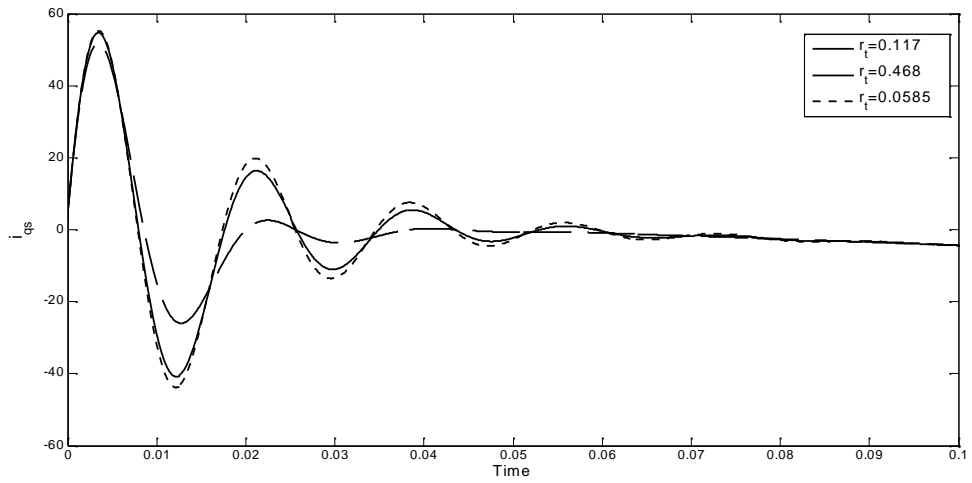


Figure 4.31 Stator currents of wind driven IG for different line resistance

The speed time characteristics are shown in Fig 4.29. When transmission line resistance is high then generator rotates at less speed as compared to speed with low resistance and due to continuous change in prime mover input speed do not settles to a steady value. The variation of torque with time for different values of line resistance is shown in Fig. 4.30. The transients in torque are reduced with increase in transmission line resistance. After this torque becomes steady and continuous small variations are due to change in prime mover input. With the increase in transmission line resistance, the current transients are reduced to large extent while with reduction in transmission line transients in currents are increased. After the transient period, the steady values of currents are almost same with all three different resistances considered in our study. The variation of stator currents is shown in Fig. 4.31.

(b) CHANGE IN LINE REACTANCE

The effect of reactance on wind driven induction generator is observed by comparing the responses of generator variables with different value of reactance. Three different values of reactance are chosen which are 1.424 , 5.7 and 0.356 . In Fig.4.32 the speed-time characteristics are given. With high reactance of transmission line, generator will run at speed higher as compared to speed with low reactance.

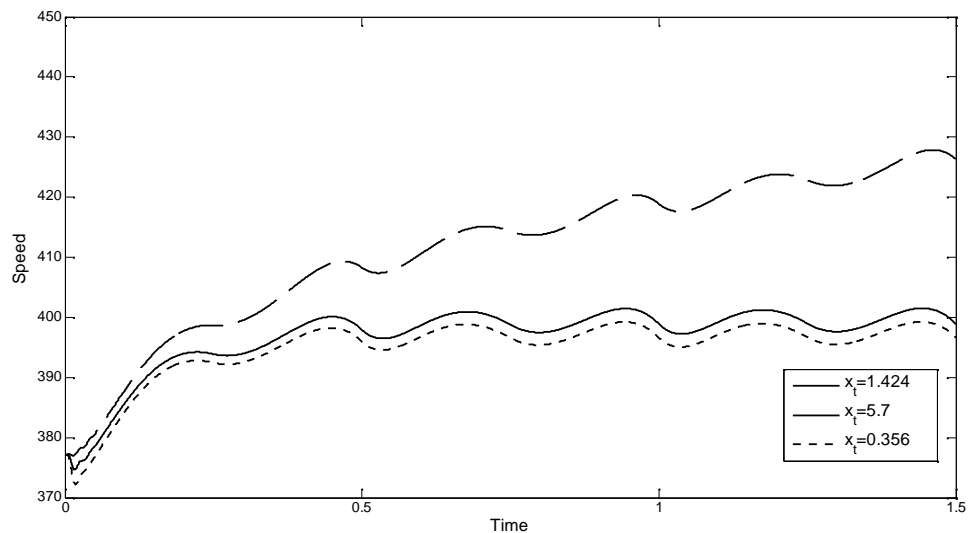


Figure 4.32 Speed-Time characteristics of wind driven IG with different line reactance

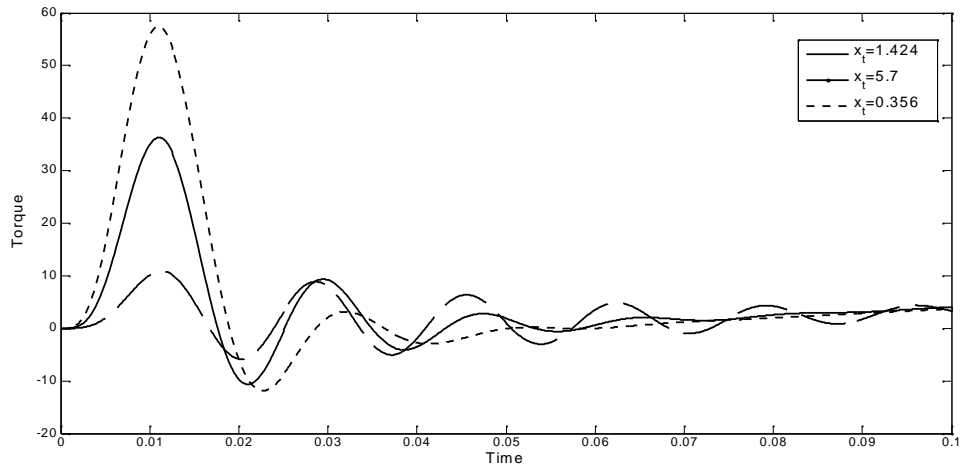


Figure 4.33 Torque-Time characteristics of wind driven IG with different line reactance

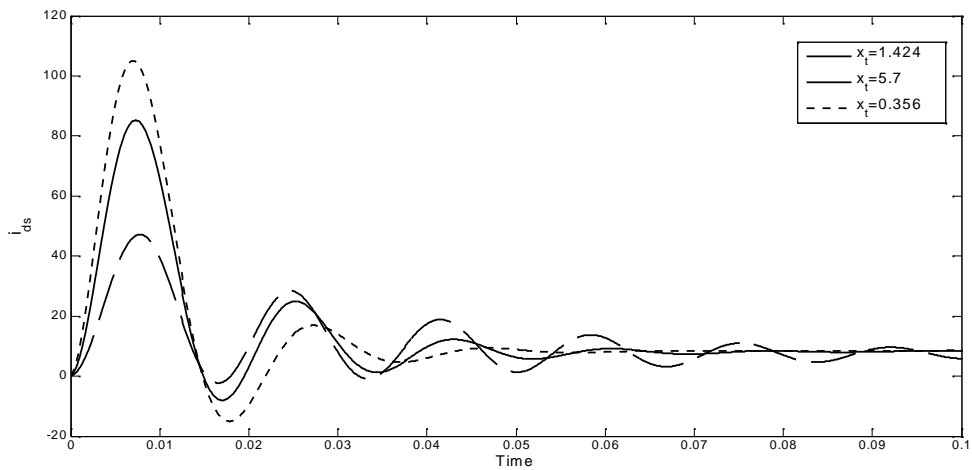
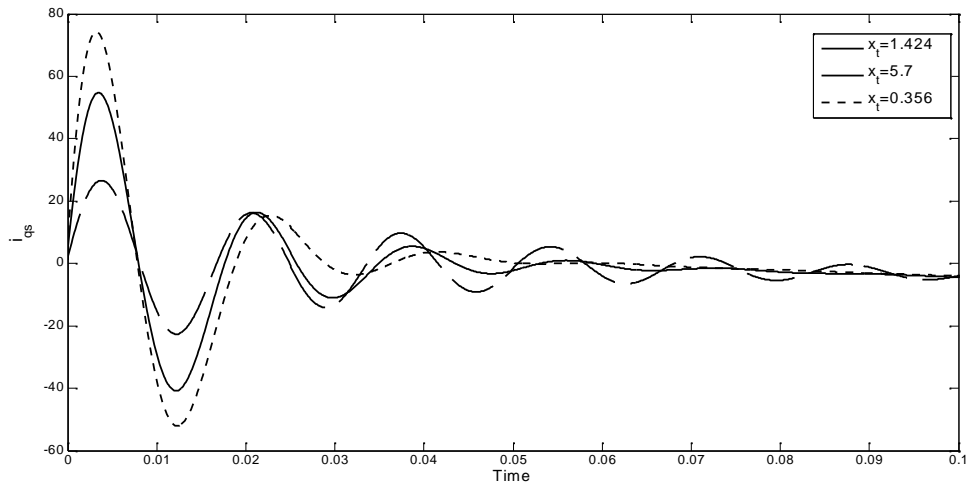


Figure 4.34 Stator currents of wind driven IG with different line reactance

The variation of torque is shown in Fig. 4.33. The transients in torque are more with low value of transmission line reactance. A large damping in torque transients is observed with high value of transmission line reactance. The Fig. 4.34 shows the d-q axis stator current characteristics. The peak values of transients are reduced with the increase in transmission line reactance but the transients damped out early in case of low reactance.

4.2 INDUCTION GENERATOR CONNECTED TO GRID WITH LOCAL LOAD AND CAPACITOR

In previous section generator performance has been studied with no load and no compensating capacitor. In this section induction a local load and compensating capacitor is connected to induction generator as shown in Fig. 3.8. Local load and capacitor is connected to generator at 0.7 sec. Generator in this case also can be driven either by constant speed prime mover or with wind turbine.

4.2.1 INDUCTION GENERATOR DRIVEN BY CONSTANT SPEED PRIME MOVER

When an induction generator with local load is driven by constant speed prime mover the variable are plotted against time and shown in Fig. 4.35 to Fig 4.40. The d-q axis stator currents are shown in Fig. 4.35. When load is connected sudden transients are present in d-q axis stator current. After that current reduces and attains a steady value.

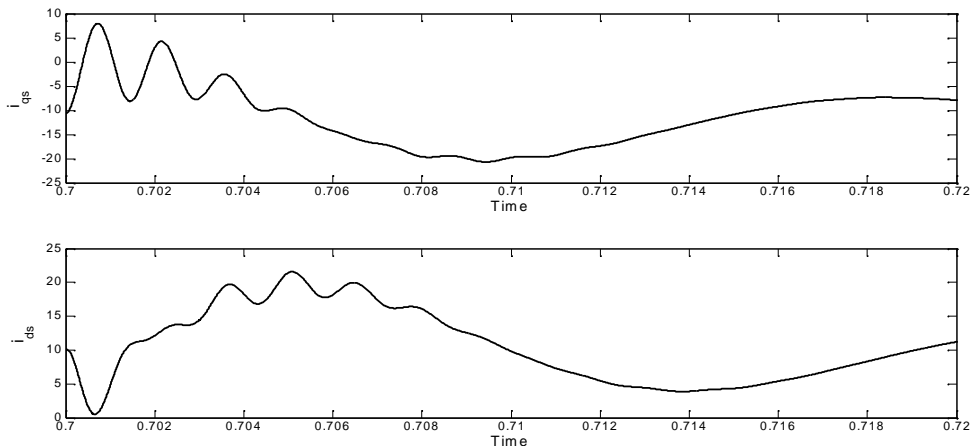


Figure 4.35 Stator currents of grid connected IG with local load and capacitor

The d-q axis rotor currents are shown in Fig. 4.36. Transients also present in rotor currents when load is connected at 0.7 sec. Steady value is attained after fraction of second. With the connection of load, transients are experienced in load current. The variation of the load current with time is shown in Fig. 4.37. The load current attains a steady value after short period of transients.

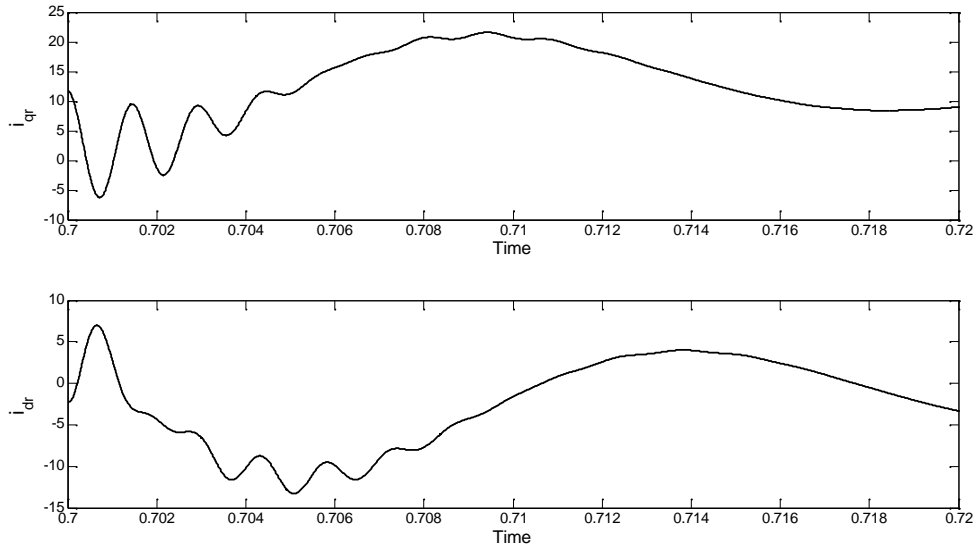


Figure 4.36 Rotor currents of grid connected IG with local load and capacitor

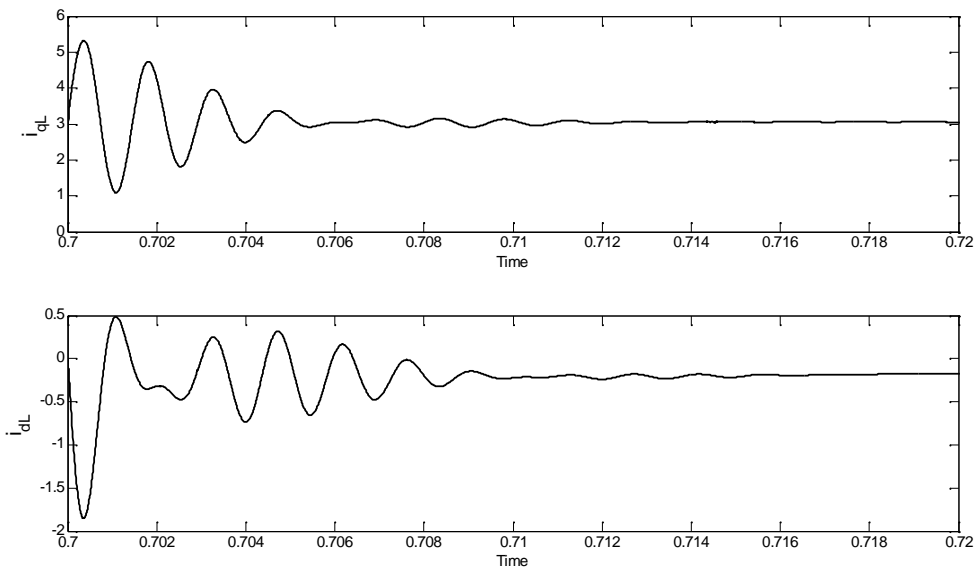


Figure 4.37 Load currents of grid connected IG with local load and capacitor

The transmission line currents are shown in Fig. 4.38. Voltage across compensating capacitor is shown in Fig. 4.39. There are transients in capacitor voltage when capacitor is connected across induction generator. The variation of speed with time is shown in Fig. 4.40. A small rise in speed is observed with the connection of load but this change last for small time and speed becomes steady.

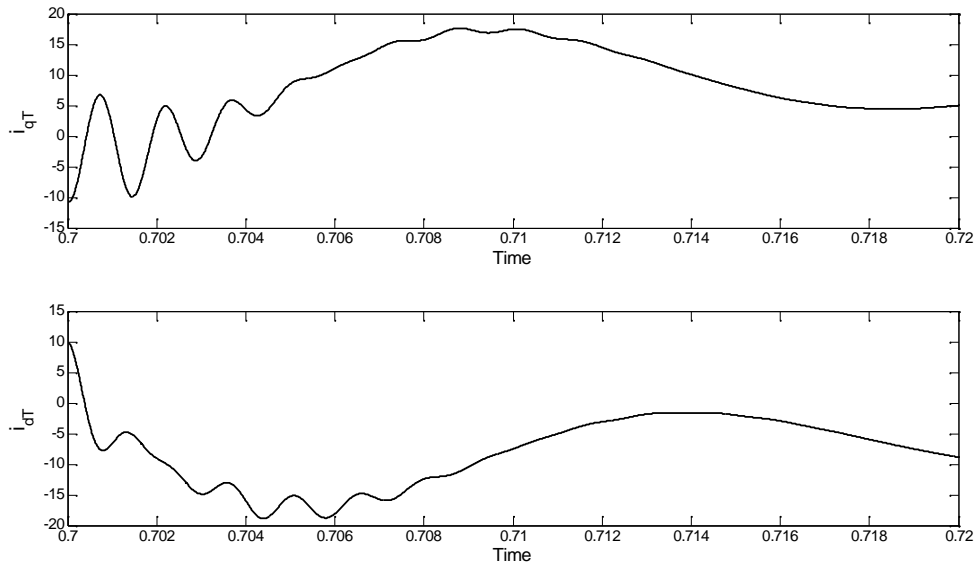


Figure 4.38 Transmission line currents of grid connected IG with local load and capacitor

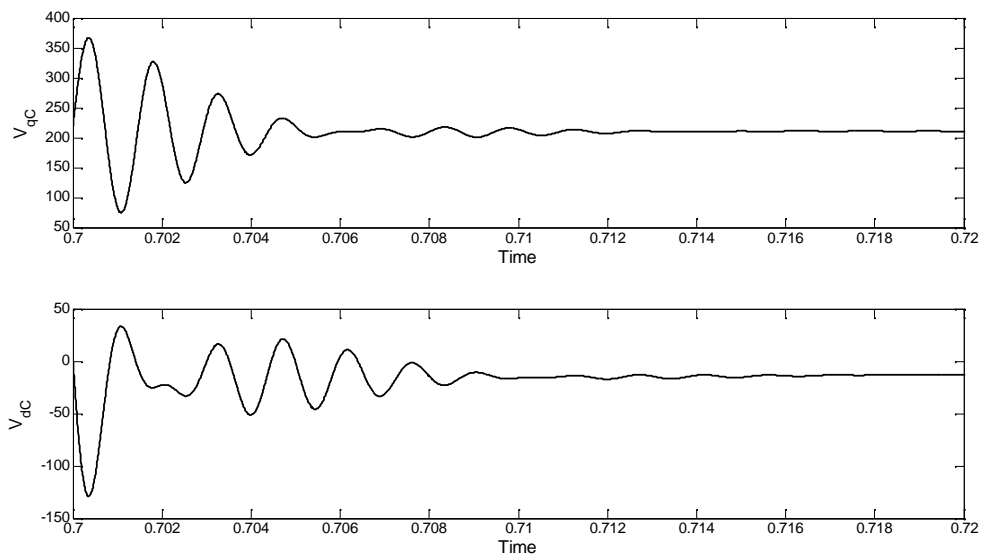


Figure 4.39 Voltage across capacitor of grid connected IG with local load and capacitor

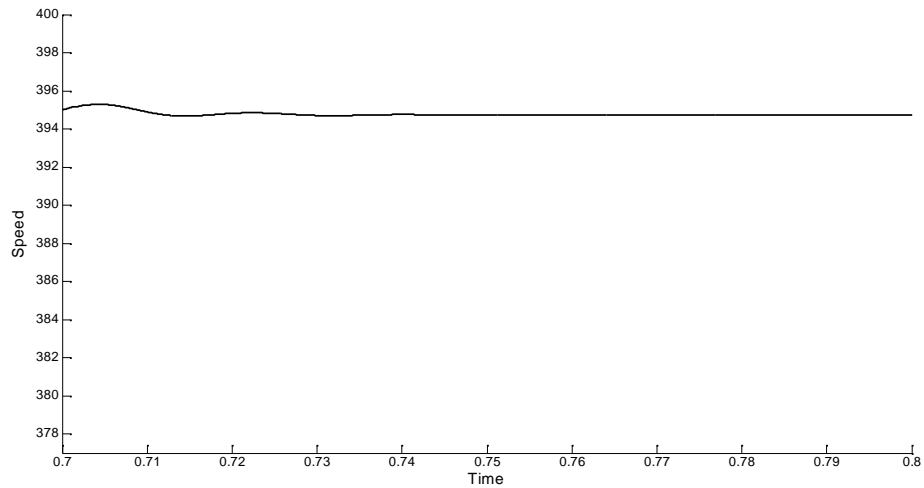


Figure 4.40 Speed-Time characteristics of grid connected IG with local load and capacitor

(i) CHANGE IN COMPENSATION

The performance of induction generator with local load is studied with different values of reactive power compensation. The variations of state variables of induction generator with 25%, 40% and 75% reactive power compensation are shown in Fig.4.41 to Fig 4.44. The performance is compared by comparing the variations with different values of reactive power compensation. The performance of generator with load is compared with different values of compensation.

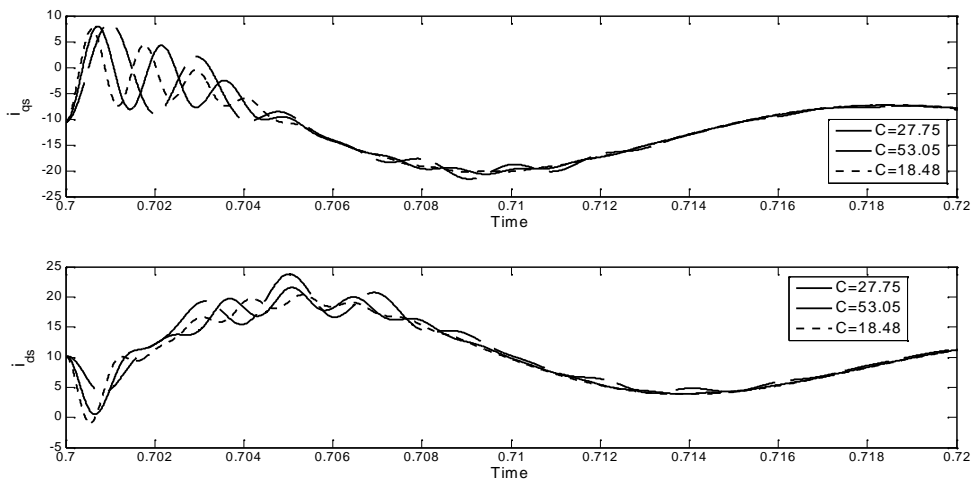


Figure 4.41 Stator currents of IG with local load with different compensation.

The d-q axis stator currents of generator for different values of compensation are shown in Fig. 4.41. With the connection of load, transients are observed in currents but the peak value of transients is different for different level of compensation. With the increased compensation the transients in generator currents are increased.

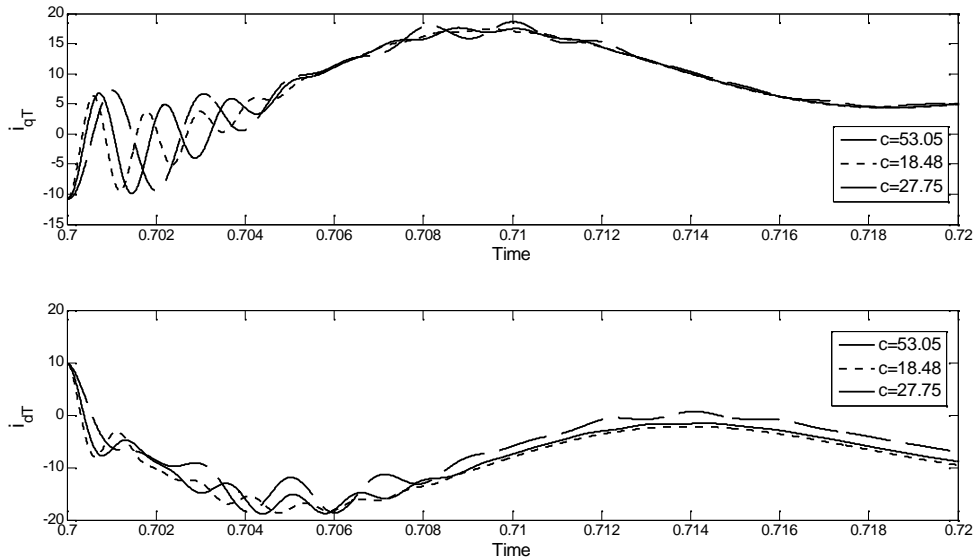


Figure 4.42 Transmission line currents of IG with local load with different compensation.

The variation in transmission line currents are shown in Fig. 4.42. With less compensation the peak value of transient in transmission line current is lower as compared to peak value with higher value of compensation. The steady value of transmission current is more when higher values of compensation is used. At the instant load is connected to generator the load currents starts to rise from zero. At starting transients are present in load current and after this current retains a almost steady value.the load current is shown in Fig. 4.43. It is clearly observed with the increase in reactive var compensation, transients in load current are reduced. The voltages across capacitors are shown in Fig. 4.44. Less transients in capacitor voltage are experienced with high compensation.

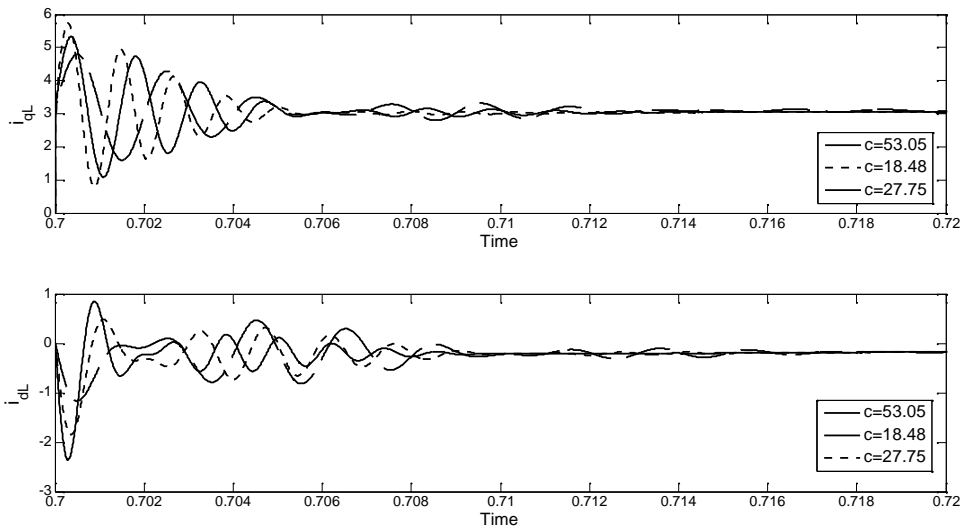


Figure 4.43 Load current of IG with local load with different compensation.

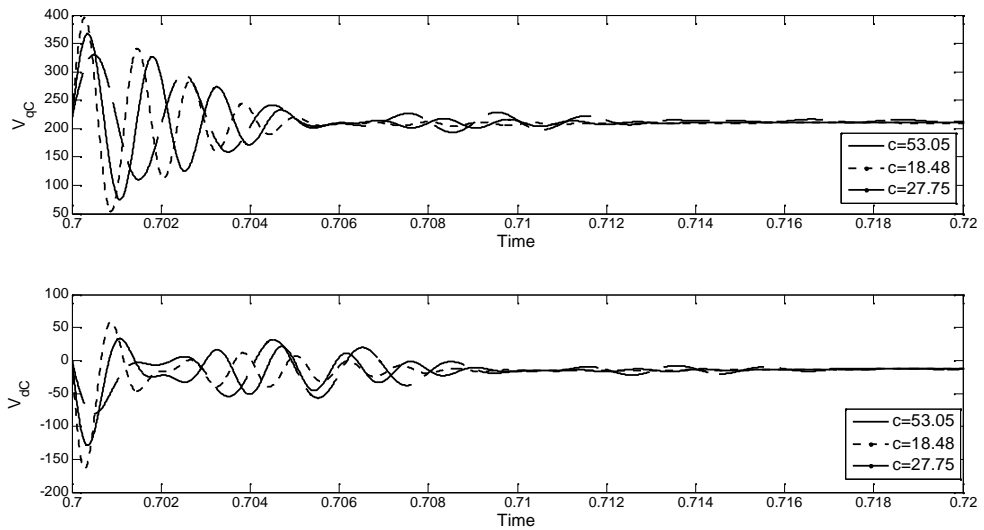


Figure 4.44 Capacitor voltages of IG with local load with different compensation.

4.2.2 INDUCTION GENERATOR DRIVEN BY WIND TURBINE

In this case IG with local load is driven by the wind turbine. The speed of wind turbine is not constant but varies with speed of wind. The wind speed function II is considered for this study and effect of change in local load and reactive power compensation is studied.

(i) CHANGE IN REACTIVE POWER COMPENSATION

The performance of wind driven induction generator to which a local load and compensating capacitor is connected is analyzed for different values of compensation. Variation in system variables for different compensation is shown in Fig. 4.45 to Fig. 4.49. The d-q stator currents are shown in Fig. 4.45. With increase in capacitive compensation the peak value of current transients is increase.

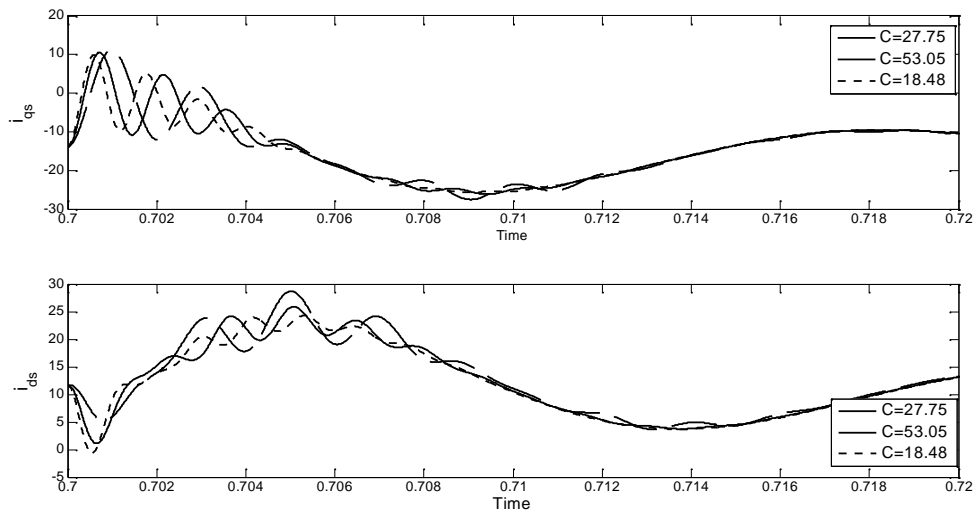


Figure 4.45 Stator current of wind driven IG with different compensation.

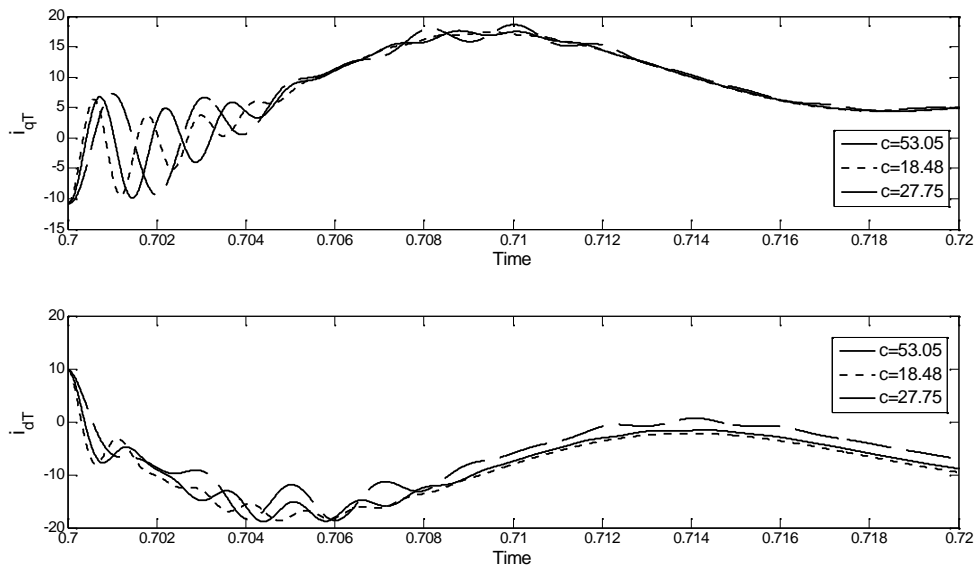


Figure 4.46 Transmission line currents of wind driven IG with different compensation.

The transmission line current of the system when driven by wind is shown in Fig. 4.46. with increase in compensation the The phase of currents with different value of compensation are different. The load current variation with time is shown in Fig. 4.47. The load current settles to a steady value after transient period.

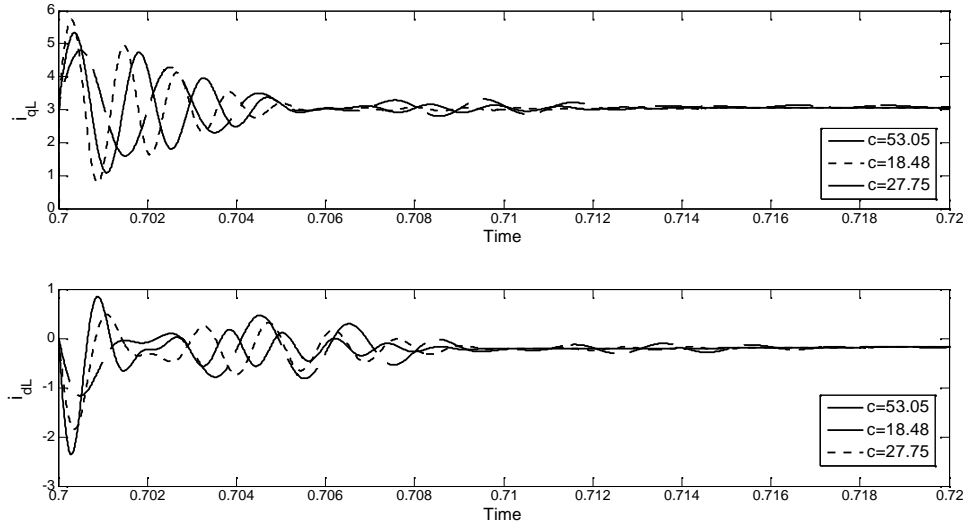


Figure 4.47 Load currents of wind driven IG with local load and different compensation.

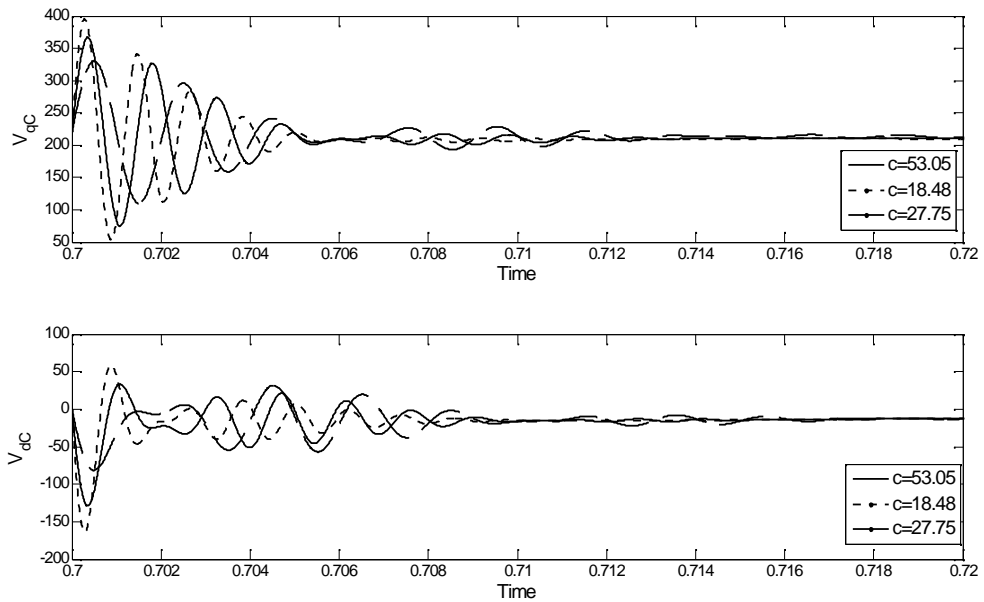


Figure 4.48 Capacitor voltages of wind driven IG with local load and different compensation

The voltage across capacitor is shown in Fig. 4.48. With the connection of load the voltage across compensating capacitor shows the transient behavior. With high compensation the transients in capacitor voltage is less. The speed variation with time is shown in Fig. 4.49. With the connection of load, speed falls slightly. With higher compensation the steady speed is slightly less as compared to low compensation.

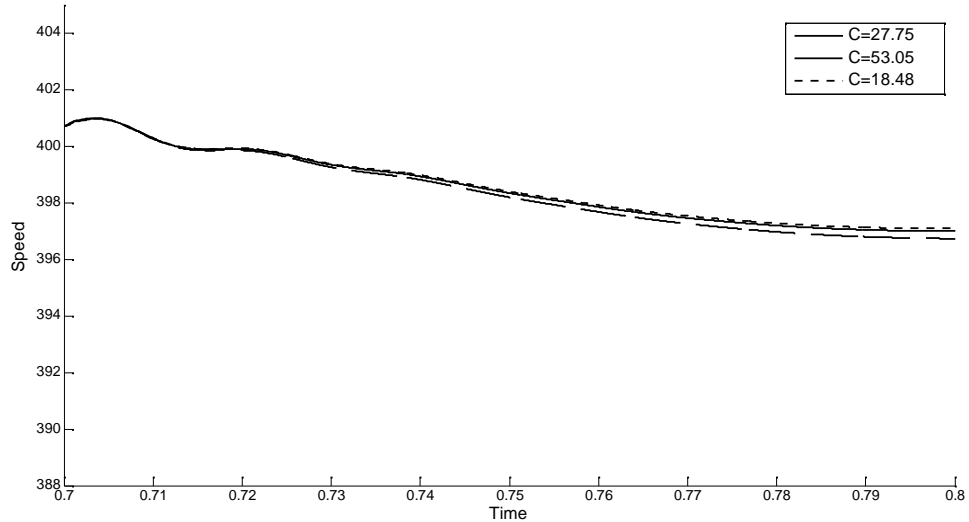


Figure 4.49 Speed-Time characteristics of wind driven IG with local load

(ii) CHANGE IN LOAD

To study the behavior of wind driven induction generator with change in load is studied by connecting different loads with induction generator. Three values of loads that are considered for study are 1 KW, 1.5 KW and 2.5 KW. The response of variables with these different loads is compared in Fig. 4.50 to Fig. 4.54. The d-q axis stator currents are shown in Fig. 4.50. The d-q axis transmission line currents are shown in Fig. 4.51. The transmission line current is decreased with increase in load. The peak value of transients in transmission line current is lower with higher value of load. The load current for different loads are shown in Fig. 4.52. The load current increases with increase in load. The transient in load current remains for short duration and after that steady value is attained.

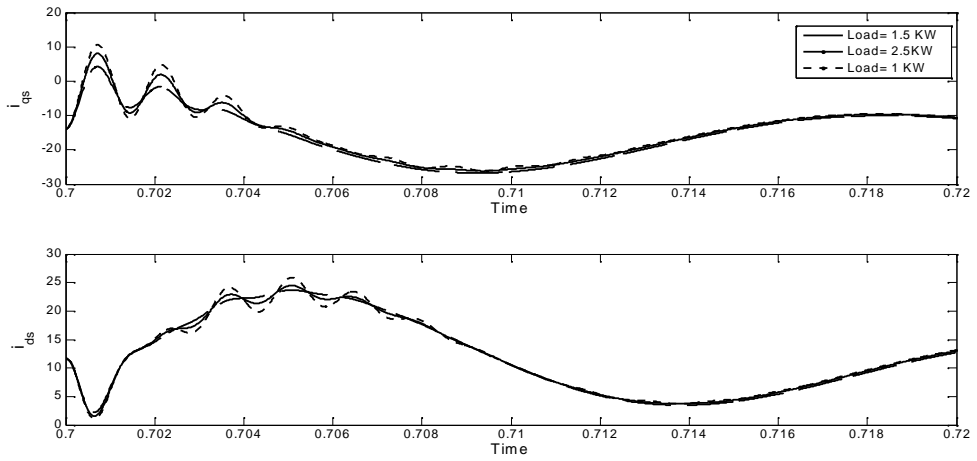


Figure 4.50 Stator current of wind driven IG with different load

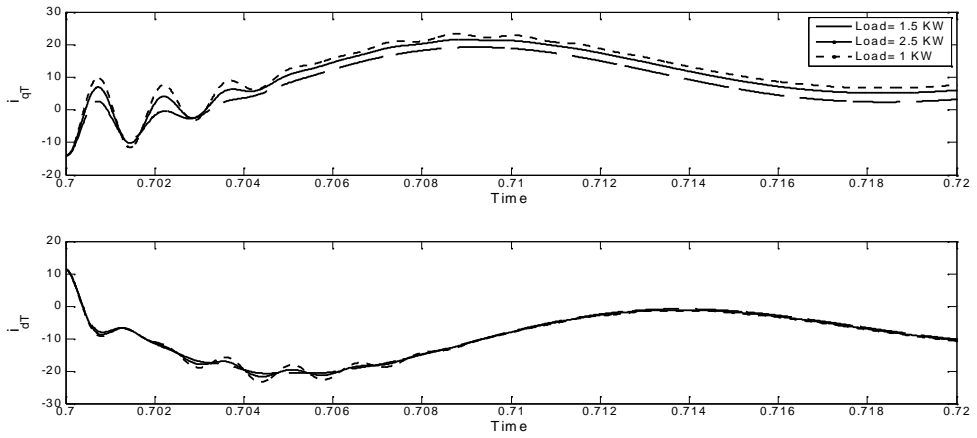


Figure 4.51 Transmission line currents of wind driven IG with different load.

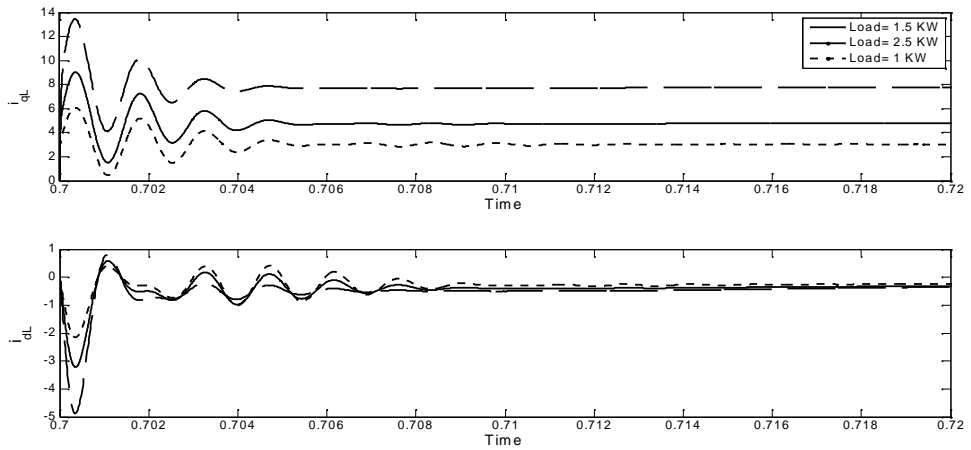


Figure 4.52 Load currents of wind driven IG with different load

The voltage across the compensating capacitor for different values of load is compared in Fig. 4.52. As the load increased the transients in capacitor voltage is increased. The capacitor voltage attains a steady value after these transients.

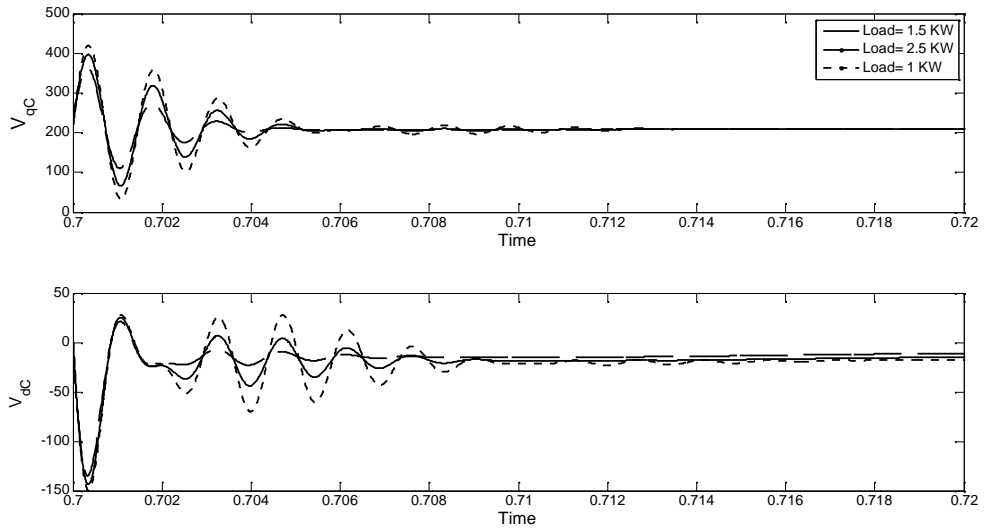


Figure 4.53 Voltage across capacitor of wind driven IG with different load

CONCLUSIONS AND SCOPE OF FUTURE WORK

5.1 CONCLUSIONS

The dynamic performance of wind driven cage induction generator has been studied through direct grid connected induction generator, and grid connected induction generator with local load and capacitor. The dynamic models of these systems are derived in synchronous reference frame and performance is simulated by fourth order Runge-Kutta integration method. The performance has been studied for change in various parameters. The following conclusions are drawn from the study -

- Transients in currents are increased when induction generator is started with speed different from synchronous speed. The steady value obtained by generator is same irrespective of initial value of speed.
- With increase in transmission line resistance, transients in currents and torques are reduced. The steady speed with higher resistance is comparatively less than obtained with lower line resistance.
- With increase in transmission line reactance, lower magnitudes of transients are experienced but transients last for longer duration. With higher reactance, the induction generator has to be driven at higher speed at steady state
- The initial transients are not affected significantly in generator driven by constant speed or wind turbine. This is because the magnetization of generator is having a dominating effect.
- With the increase in compensation, the peak value of transients in stator current and transmission line current are increased. Whereas transients in load current and capacitor voltage are reduced with increase in reactive power compensation.
- With increase in local load at generator, steady value of load current is increased and transmission line currents are decreased.

5.2 SCOPE OF FUTURE WORK

- The work can be extended to include the use of power electronics converters with the wind driven generator using cage or wound rotor induction generator.
- The wind generator performance in a local system instead of direct grid connection can be analyzed.

REFERENCES

1. "World wind energy report 2008," World Wind Energy Association, Feb. 2009. Available at: <http://www.wwindea.org/home/images/stories/worldwindenergyreport2008s.pdf>.
2. "Global Wind Energy Outlook 2008," Global Wind Energy Council, Oct 2008. Available at: <http://www.gwec.net/index.php?id=92>.
3. P.J. Musgrove, "Wind energy conversion an introduction," IEE Proceedings on Physical Science, Measurement and Instrumentation, Management and Education, Reviews, vol. 130, no.9, pp. 506-516, 1983.
4. B. K. Bose, "Power Electronics and Motor Drives Recent Progress and Perspective," *IEEE Transactions on Industrial Electronics*, vol. 56, no. 2 pp. 581-588, 2009.
5. T. H. Yeh, L. Wang, "A Study on Generator Capacity for Wind Turbines Under Various Tower Heights and Rated Wind Speeds Using Weibull Distribution", *IEEE Transactions on energy conversion*, vol. 23, no.2 pp. 592-602, 2008.
6. C. G. Anderson, J. B. Richon, T. J. Campbell, "An Aerodynamic Moment-Controlled Surface for Gust Load Alleviation on Wind Turbine Rotors," *IEEE Transactions on control systems technology*, vol. 6, no.5, pp.577-595, 1998.
7. E. Muljadi, C.P. Butterfield, "Pitch-controlled Variable-speed Wind Turbine Generation," *IEEE Transactions on Industry Applications*, vol. 37, no.1, pp. 240-246, 2001.
8. T. Thiringer, J. Linders, "Control by Variable Rotor Speed of a Fixed-Pitch Wind Turbine Operating in a Wide Speed Range", *IEEE Transactions on Energy Conversion*, vol. 8, no. 3, pp. 520-526, 1993.
9. Y. Xingjia, L. Yingming, X. Zuoxia, Z. Chunming, "Active Vibration Control Strategy Based on Expert PID Pitch Control of Variable Speed Wind Turbine," *IEEE International Conference on Electrical Machines and Systems*, pp. 635-639, 17-20 Oct. 2008.
10. S. Muller *et al.*, "Doubly Fed Induction Generator Systems For Wind Turbines," *IEEE Industry Applications Magazine*, vol. 8, pp. 26-33, 2002.

11. R. Datta, V.T. Ranganathan, "Variable Speed Wind Power Generation Using Doubly Fed Wound Rotor Induction Machine-A Comparison with Alternative Schemes," *IEEE Transaction on Energy Conversion*, vol. 17, no.3, pp. 414-421, 2002.
12. R. Takahashi, J. Tamura, "Frequency Control of Isolated Power System with Wind Farm by Using Flywheel Energy Storage System" *IEEE Proceedings on Electrical Machines*, pp.1-6, 6-9 Sep. 2008.
13. P.S. Bimbhra, 'Generalized Theory of Electric Machines', Khanna Publishers, 2002.
14. R.H. Park, "Two Reaction Theory of Synchronous Machines- Generalized Method of Analysis – Part 1," *AIEE Transactions*, vol. 48, no.3, pp. 716-727, 1929.
15. D.S. Brereton, D.G. Lewis, C. G. Young, "Representation of Induction Motor Loads during Power System stability studies," *AIEE Transactions on Power Apparatus and Systems*, vol. 76, no.3, pp. 451-461, 1957.
16. H. C. Stanley, "An Analysis of the Induction Motor," *AIEE Transactions*, vol. 57, no.12, pp.751-755, 1938.
17. T.J. Hammons, "Voltage Dips Due to Direct Connection of Induction Generators in Low Head Hydro Electric schemes", *IEEE Transactions on Energy Conversion*, vol. 9, no.3, pp. 460-465, 1994.
18. P. Kundur, 'Power System Stability and Control' New York: McGraw- Hill, 1994.
19. C. S. Demoulias, P. S. Dokopoulos, "Electrical Transients of wind Turbines In a Small Power Grid", *IEEE Transactions on Energy Conversion*, vol. 11, no. 3, pp. 636-642, 1996.
20. C. S. Demoulias, P. S. Dokopoulos, "Transient Behavior and Self-Excitation of Wind-Driven Induction Generator after its Disconnection from the Power Grid", *IEEE Transactions on Energy Conversion*, vol. 5, no. 2, pp. 272-278, 1999.
21. P. C. Krause, "Analysis of Electric Machinery," New York: McGraw-Hill, 1986.

22. L. Tang, R. Zavadil, "Shunt Capacitor Failures Due to Wind Farm Induction Generator Self-excitation Phenomenon" *IEEE Transactions on Energy Conversion*, vol. 8, no. 3, pp. 513-519, 1993.
23. T. Petru, T. Thiringer, "Modeling of Wind Turbines for Power System Studies", *IEEE Transactions on Energy Conversion*, vol. 17, no. 4, pp. 1132-1139, 2002.
24. L. M. Popa, F. Blaabjerg and I. Boldea, "Wind Turbine Generator Modeling and Simulation Where Rotational Speed is the Controlled Variable," *IEEE Transactions on Industry Applications*, vol. 40, no.1 pp. 3-10, 2004.
25. K. L. Shi *et al.*, "Modeling and Simulation of The Three-Phase Induction Motor Using Simulink," *International Journal on Electrical Engg. Education*, vol. 36, pp. 163–172, 1999.
26. J. G. Slootweg, S. W. H. de Hann and H. Polinder "General Model for Representing Variable Speed Wind Turbines in Power System Dynamics Simulations", *IEEE Transactions on Power Systems*, vol. 18, no. 1, pp. 144-151, 2003.
27. T.J. Hammons. "Analysis of Torques in Large Steam Turbine Driven Induction Generator Shafts Following Disturbances on The System Supply", *IEEE Transactions on Energy Conversion*, vol. 11, no.4, pp. 693-700, 1996.

APPENDIX A

RUNGA KUTTA METHOD OF ORDER FOUR

At each step, the Runge-Kutta method of order four uses four slopes, one calculated at the left-hand endpoint of the step, one calculated at the right-hand endpoint of the step and two calculated at the midpoint of the step. The two slopes calculated at the midpoint of each step are given twice as much weight as the slopes at the endpoints.

The solution of the initial value problem

$$\frac{dy}{dx} = f(x, y), y(x_0) = y_0 \quad (\text{A.1})$$

is approximated at the sequence of points (x_n, y_n) ($n=1,2,3,\dots$), where y_n is the approximate value of $y(x_n)$ by computing at each step

$$y_{n+1} = y_n + \frac{h}{6}(k_1 + 2k_2 + 2k_3 + k_4) \quad (\text{A.2})$$

$$k_1 = f(x_n, y_n) \quad (\text{A.3})$$

$$k_2 = f\left(x_n + \frac{h}{2}, y_n + \frac{hk_1}{2}\right) \quad (\text{A.4})$$

$$k_3 = f\left(x_n + \frac{h}{2}, y_n + \frac{hk_2}{2}\right) \quad (\text{A.5})$$

$$k_4 = f\left(x_n + h, y_n + hk_3\right) \quad (\text{A.6})$$

The maximum cumulative error on a bounded interval $[a, b]$ with $a=x_0$ is

$$|y(x_n) - y_n| \leq Ch^4 \quad (\text{A.7})$$

where C depends on the function $f(x, y)$, and on the interval $[a, b]$ but not on h . Thus decreasing h greatly decreases the error.

APPENDIX B

FREE ACCELERATING CHARACTERISTICS

To observe the free accelerating characteristics of induction machine the non linear differential equations which describes the dynamic model of induction machine has to simulate. To check the free accelerating characteristics we have taken a machine of 3 hp rating. Machine is 4 pole, 60 Hz, 3 phase induction motor [21]. The variation of machine variables has been checked in synchronous reference frame.

The 3 hp motor considered for study is relative high slip machine than motors of high power ratings. The rated torque is developed at speed considerably less than synchronous machine. The torque-speed and toque-time characteristics of motor are shown in Fig. B.1 and Fig. B.2 respectively.

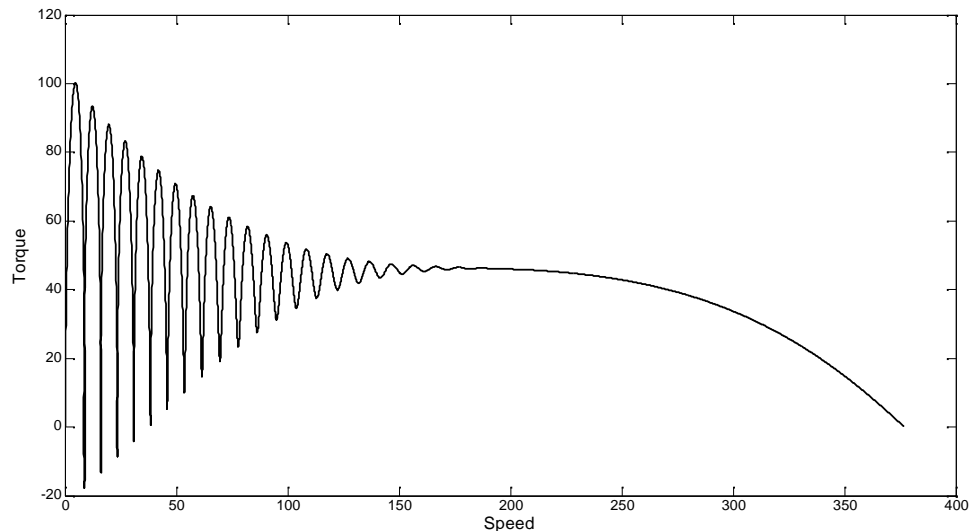


Figure B.1 Free accelerating torque-speed characteristics.

When an induction motor is started from standstill with no load then it will attain speed very near to synchronous speed in very short time because friction and windage losses are not considered. The variation of speed with time is shown in Fig. B.3

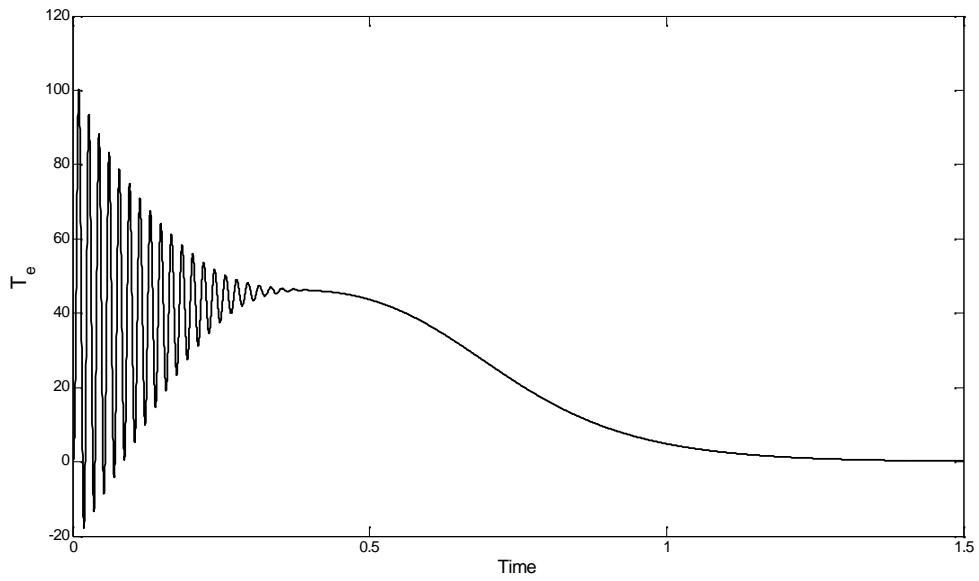


Figure B.2 Free accelerating torque-time characteristics.

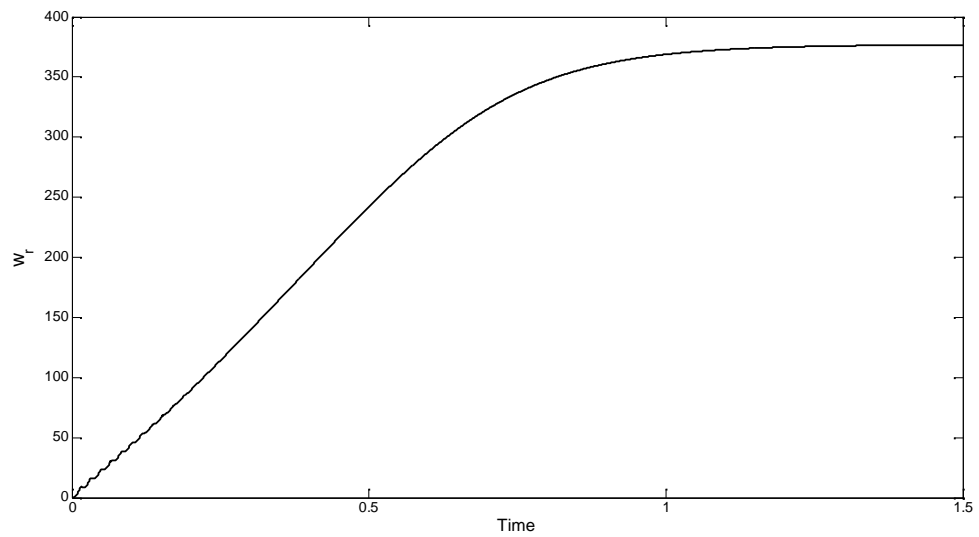


Figure B.3 Free accelerating speed-time characteristics

When induction motor is started from standstill with rated voltage applied, the starting current is high, in some cases it may be 8-10 times the rated current. The d-q AXIS currents are shown in Fig. B.4.

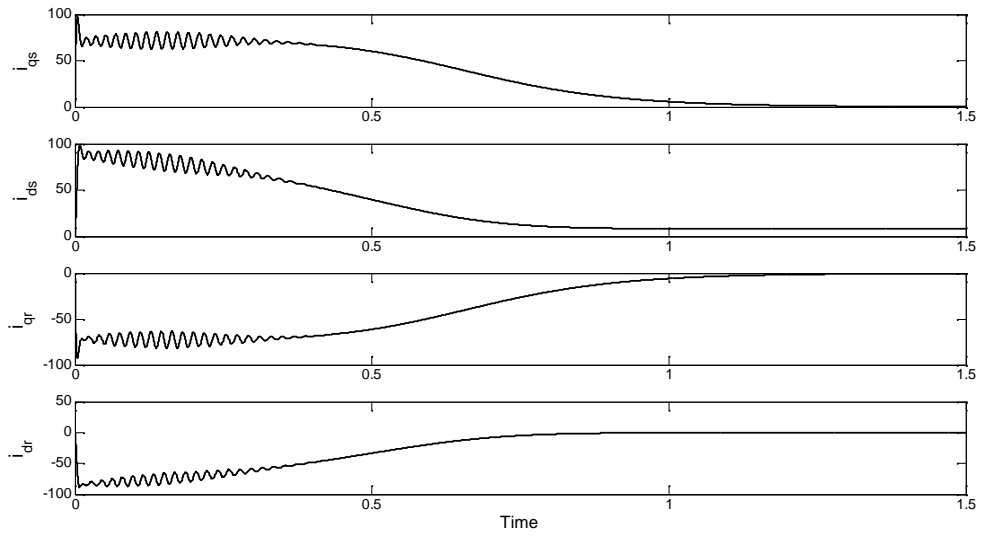


Figure B.4 Free accelerating d-q axis currents